

©Copyright 2019
Mark Ernest Madsen

MEASURING CULTURAL TRANSMISSION AT ARCHAEOLOGICAL SCALES:
MACHINE LEARNING AND AGENT-BASED SIMULATION METHODS

Mark Ernest Madsen

A DISSERTATION SUBMITTED IN PARTIAL FULFILLMENT OF THE REQUIREMENTS FOR
THE DEGREE OF DOCTOR OF PHILOSOPHY

UNIVERSITY OF WASHINGTON
2019

READING COMMITTEE:
James K. Feathers, co-Chair
Benjamin Marwick, co-Chair
Carl P. Lipo, Binghamton University

PROGRAM AUTHORIZED TO OFFER DEGREE:
Anthropology

University of Washington

Abstract

Measuring Cultural Transmission at Archaeological Scales: Machine Learning and
Agent-Based Simulation Methods

Mark Ernest Madsen

Chair of the Supervisory Committee:
Research Associate Professor, James K. Feathers, co-Chair
Associate Professor, Benjamin Marwick, co-Chair
Anthropology

Lorem ipsum dolor sit amet, consectetur adipiscing elit. Vestibulum viverra est est. Proin eget tellus metus. Aenean ac tortor pharetra libero ultricies sagittis. Nulla facilisi. Cras tincidunt interdum tellus, quis consectetur nunc facilisis nec. Sed fermentum erat a ligula posuere quis semper risus ullamcorper. Morbi vel tincidunt augue. Nam dolor ipsum, sagittis quis dignissim eu, pulvinar sed magna. In interdum magna eu orci facilisis congue. Cras a tellus et lorem sagittis viverra. Donec risus lectus, mollis at dignissim viverra, dapibus a nulla. Vivamus porttitor scelerisque turpis, eget lobortis orci auctor eget. Donec ultricies enim ac augue porttitor convallis. Pellentesque nisl lorem, consequat a facilisis in, ornare sed lorem. In luctus, elit ac mattis dapibus, lacus elit varius tortor, vel sollicitudin massa nisl id massa. Ut sit amet nibh a sem egestas sollicitudin. Vestibulum scelerisque, dui at tincidunt accumsan, ipsum enim feugiat neque, vel interdum turpis lectus sed nisi. Nullam ultrices sodales sem, et placerat nunc euismod eu. Duis leo lacus, semper quis eleifend vitae, viverra ut nisl. Vestibulum ante ipsum primis in faucibus orci luctus et ultrices posuere cubilia Curae; Proin rutrum eleifend est, id tempor velit viverra sed. Nam pharetra nunc a dui egestas semper. Nam venenatis velit pulvinar magna vulputate id varius leo ornare. Aliquam vel leo et orci elementum interdum. Morbi ut est eget mauris bibendum imperdiet. Nulla sed odio dui. Phasellus commodo est nec diam vulputate vitae rutrum libero elementum. Aliquam iaculis, turpis ac vulputate sollicitudin, sapien ligula aliquam dui, vel tincidunt mi quam vel tortor. Aliquam ut lectus non orci iaculis dapibus. Mauris nec orci sed sapien congue mollis quis at orci. Vivamus varius, leo ut condimentum hendrerit, elit libero elementum quam, quis mattis urna mauris a lectus. Vestibulum condimentum arcu nulla. Suspendisse potenti. Ut nunc leo, gravida tincidunt convallis non, pretium eu libero. Suspendisse neque quam, blandit ac tincidunt vitae, tincidunt sit amet lacus. Nunc feugiat feugiat leo sit amet dictum. Maecenas id tempus augue. Ut aliquam viverra velit, sit amet tincidunt erat accumsan at. Morbi non mi id nisi placerat pulvinar et nec purus. Etiam eget viverra lectus. Lorem ipsum dolor sit amet.

Contents

List of Figures	v
List of Tables	ix
Acknowledgements	xi
 Part I Introduction and Research Methods	 1
<hr/>	
1 Introduction	3
2 Research Methods	7
 Part II Research Papers	 9
<hr/>	
3 Neutral Cultural Transmission in Time Averaged Archaeological Assemblages	11
3.1 Introduction	12
3.2 Conceptual Structure of Neutral Cultural Transmission	14
3.3 Unbiased Transmission: The Wright-Fisher Infinite-Alleles Model	18
3.3.1 Statistical Tests for Neutrality	20
3.3.2 Estimation of Innovation Rates	22
3.3.3 Diversity Measures	23
3.4 Methods	24
3.4.1 Model Verification	25
3.4.2 Time-Averaging and Simulation Parameter Space	27
3.5 Results	29
3.5.1 Time Scales and Time averaging	30
3.5.2 Neutrality Testing	33
3.5.3 Theta Estimation and Innovation Rates	36
3.5.4 Diversity Measures	39
3.6 Discussion and Conclusions	43
3.7 Acknowledgements	46

4	Can We Identify Transmission Bias in the Archaeological Record: An Investigation Using Boosted Classifier Models	47
4.1	Introduction	48
4.2	Analysis	50
4.2.1	Reducible and Irreducible Equifinality Among Transmission Models	50
4.2.2	Equifinality As Classification Error	52
4.2.3	Study Design	54
4.2.4	Methods	55
4.2.4.1	Simulated Samples of Cultural Transmission Models	55
4.2.4.2	Variable Selection	57
4.2.4.3	Data Collection Treatments	59
4.2.4.4	Classifier Selection and Training	61
4.2.4.5	Classification Error and Equifinality Assessment	63
4.3	Results	64
4.3.1	Unbiased Versus Biased Cultural Transmission	65
4.3.2	Unbiased Versus Balanced Conformist/Anti conformist Bias	67
4.3.3	Conformist Dominated Versus Anti conformist Dominated Populations	68
4.4	Discussion	69
5	Combinatorial Structure of the Deterministic Seriation Method with Multiple Subset Solutions	77
5.1	Single Seriation Combinatorics	78
5.2	Deterministic Seriation with Multiple Solution Groups	79
5.3	Discussion	83
6	Measuring Cultural Relatedness Using Multiple Seriation Ordering Algorithms	85
6.1	Introduction	86
6.2	Seriation and the Frequency Principle	89
6.2.1	Unimodality and Cultural Transmission Processes	91
6.2.2	Continuity: An Alternative to Unimodality	93
6.2.3	Statistical Seriation Methods	95
6.2.4	Exact Distance Minimization Ordering: “Continuity” Seriation	97
6.3	Comparing Frequency and Continuity Seriation	98
6.3.1	Examining a Solution Which Differs	104
6.3.2	Multiple Seriations for Phillips, Ford and Griffin (1951) data	106
6.4	Discussion	106
7	Behavioral Modernity and the Cultural Transmission of Structured Information: The Semantic Axelrod Model	113
7.1	Introduction	114
7.2	The Semantic Axelrod Model for Trait Prerequisites	118
7.2.1	Representation of Traits And Their Prerequisites	121
7.2.2	The Axelrod Model of Social Learning and Differentiation	124
7.2.2.1	Axelrod’s Original Model	124
7.2.2.2	Semantic Extensions to the Axelrod Model	126
7.3	Measuring Cultural Diversity and the Results of Structured Learning	129

7.4	Experiments	132
7.5	Results	134
7.5.1	Cultural Diversity	134
7.5.2	Trait Richness and Knowledge Depth	136
7.5.3	Population Size	137
7.5.4	Trait Tree Symmetries	138
7.6	Discussion	140
7.7	Acknowledgements	142
7.8	Appendices	142
7.8.1	Algorithm Description	142
7.8.2	Availability of Software and Analysis Code	144
Part III Discussion and Conclusions		145
<hr/>		
8	Directions for Future Research	147
9	Conclusion	149
	Bibliography	151

List of Figures

3.1	Mean value of K_n for time averaged samples, plotted against assemblage duration in simulation steps, for each level of θ in the study. Note that the “onset” of time averaging effects (as measured by increased K_n), is quite gradual at low θ , while high innovation rates display increased richness with very minor amounts of time averaging.	32
3.2	Slatkin Exact test failure rate (above the expected 10% given two-tailed test with $\alpha = 0.10$, plotted against time averaging duration scaled by mean trait lifetime, for each level of θ in the simulation study. The red vertical line indicates the mean trait lifetime for that θ value, and the shaded region encompasses the standard error of the estimates for mean failure rates at each duration.	35
3.3	Estimates of mean population innovation rate ($\mathbb{E}(\hat{\theta})$) from samples ($n = 100$) taken for neutrality tests, using the approximation by Watterson (1975). Plotted against assemblage duration, for each level of actual innovation rate used in simulation runs.	38
3.4	Estimates of mean population innovation rate ($\mathbb{E}(\hat{\theta})$) from samples ($n = 100$) taken for neutrality tests, using results from Montgomery Slatkin’s neutrality test software. Plotted against assemblage duration, for each level of actual innovation rate used in simulation runs.	40
3.5	IQV diversity index, derived from samples of size 100, plotted against time averaging duration scaled by mean trait lifetime, for each level of θ in the simulation study. The red vertical line indicates the mean trait lifetime for that θ value.	42
4.1	Simple example of the effect of variable choice in distinguishing models. The variable on the X axis displays quite a bit of overlap between models, while the variable on the Y axis distinguishes the models with fairly high accuracy.	51
4.2	Simple example of model outcomes with different degrees of distinguishability: (A) simulated data point from two fully separate models, (B) two models with a limited overlap region, (C) and two models whose outcomes are highly overlapping.	52
4.3	Schematic of how sampling is implemented in this study. Time runs from the start of the simulation run at the top, to the end at the bottom. The interval of time over which we calculate the Kandler-Shennan trait survival is given as a simulation parameter, and represents the gap in the middle of the diagram. Before and after that gap are windows of successive duration, representing aggregation over 10, 25, 50, and 100 “generations” of the simulation.	60
4.4	Cohen’s kappa for correctly predicting whether simulated data points originate from unbiased copying or any of 3 other biased transmission models. High values of kappa correspond to high accuracy in correctly distinguishing between transmission models, while values well below 0.5 indicate great difficult and low classifier accuracy. Each line in the dotchart represents a different data collection treatment, and overall the results indicate that significant equifinality exists except when time averaging is absent and a population census (or near equivalent) is available.	65

4.5	Cohen's kappa for correctly predicting whether simulated data points originate from unbiased copying or a balanced mixture of pro- and anti-conformist individuals. Each line in the dotchart represents a different data collection treatment, and overall the results indicate that significant equifinality exists except when time averaging is absent and a population census (or near equivalent) is available.	67
4.6	Cohen's kappa for correctly predicting whether simulated data points originate from a conformist-dominated mixed population versus a mixed population dominated by anti-conformists. Each line in the dotchart represents a different data collection treatment, and overall the results indicate that strong equifinality exists regardless of the data collection treatment.	69
4.1	Simple example of the effect of variable choice in distinguishing models. The variable on the X axis displays quite a bit of overlap between models, while the variable on the Y axis distinguishes the models with fairly high accuracy.	73
4.2	Simple example of model outcomes with different degrees of distinguishability: (A) simulated data point from two fully separate models, (B) two models with a limited overlap region, (C) and two models whose outcomes are highly overlapping.	74
4.3	Schematic of how trait survival as described by Kandler and Shennan Kandler and Shennan (2013) is extended to time averaged samples of transmission events. Time runs from the start of the simulation run at the top, to the end at the bottom. The interval of time over which we calculate the Kandler-Shennan trait survival is given as a simulation parameter, and represents the gap in the middle of the diagram. Before and after that gap are sampling windows during which transmission events are accumulated over some number of simulated "generations" (values of 10, 25, 50, and 100 are used in this paper). Trait survival is then calculated as the number of traits present in the starting time averaged sample of transmission events, which are still present in the ending time averaged sample of events.	75
5.1	Example of a deterministic frequency seriation with assemblages partitioned into multiple subsets or solution groups. From Lipo (2001b), Figure 4.4.	80
5.2	Number of Unique Solution Sets for 40 Assemblages When Partitioned Into	82
6.1	Dunnell (1981) defines seriation to be a set of methods which use historical classes to chronologically order otherwise unordered archaeological assemblages and/or objects. Historical classes are those which display more variability through time than through space. Occurrence seriation uses presence/absence data for each historical class from each assemblage (Kroeber, 1916; Petrie, 1899). Frequency seriation uses ratio level abundance information for historical classes (Spier, 1917; Ford, 1935, 1962). Frequency and occurrence seriation techniques can take the form of deterministic algorithms that require an exact match with the unimodal model or probabilistic algorithms that accept departures from an exact fit. Identity approaches employ raw data (whether frequency or occurrence) to perform the ordering. Similarity approaches transform the raw data into a non-unique coefficient (e.g., Brainerd Robinson, squared Euclidean distance); the coefficients then form the basis for ordering.	88
6.2	Neiman's simulation of drift in cultural variant frequencies under unbiased cultural transmission (reproduction of Figure 2a from Neiman 1995.)	92
6.3	Example of an interval temporal network interpreted as a regional metapopulation model, with vertices representing communities, weighted edges representing intensity of interaction and migration, and changes in each representing their respective evolution over time.	101

6.4	Processing steps in simulating cultural transmission on a regional metapopulation model of lineage splitting, to compare seriation ordering algorithms.	102
6.5	Frequency seriation solution for simulation run f8a6f378 on the "lineage splitting" regional interaction model.	104
6.6	Continuity seriation solution for simulation run f8a6f378 on the "lineage splitting" regional interaction model.	105
6.7	Centered bar chart representation of the relative frequencies of type for simulation run f8a6f378 built with the IDSS frequency seriation algorithm. The groups correspond to the branches of the solution graph.	108
6.8	Centered bar chart representation of the relative frequencies of type for simulation run f8a6f378 built with the IDSS continuity seriation algorithm. The groups correspond to the branches of the solution graph.	109
6.9	Seriation solution with frequency and continuity seriation for PFG (1951) ceramic assemblages in the Lower Mississippi River Valley, as analyzed by Lipo (2001a) and re-analyzed by Lipo et al. (2015). There are no differences between frequency and continuity ordering algorithms in analyzing this set of assemblages, and thus only one graph is shown.	110
7.1	A single trait tree, represented by a balanced tree with branching factor 3 and depth factor 3, order 40. In our model, nodes higher in the tree represent prerequisites for nodes lower down the tree. Each instance of the model will have several or many of these trees in the design space.	122
7.2	A design space composed of 4 independent trees, each tree with branching factor 3 and depth factor 3, order 40. We also studied larger design spaces with 16 independent trees, and with larger branching and depth factors.	122
7.3	Illustration of a design space composed of a single trait tree, along with a random initial trait chosen from the design space, and a final sample from a simulation run, showing the evolution of traits within the design space. Also shown in the top panel are the "prerequisites" for a cultural trait (35), as an example.	127
7.4	An example set of traits at the conclusion of a simulation run, extracted from a simulation with branching factor 3 and depth factor 3, and a single trait tree as the trait space. The remaining density of vertices, mean vertex degree, and radius of the tree are noted. Vertex colors denote "structural equivalence" classes or "orbit structure," as measured by adjacency patterns, and is one measure of the symmetries present in the tree.	130
7.5	Number of cultural configurations in simulations with the smallest trait space (160 total traits in 4 trees), and a high individual innovation rate (10^{-4}).	135
7.6	Number of cultural configurations in simulations with an intermediate learning rate (0.4), across different sizes of trait space.	136
7.7	Mean depth of trait sets, by prerequisite learning rate and global innovation rate, for population size 100.	137
7.8	Mean depth of trait sets, by prerequisite learning rate and population sizes of 100, 225 and 400.	138
7.9	Number of symmetries in trait tree samples, measured as the log of the order of the automorphism group of the trait graphs, broken down by prerequisite learning rate (rows) and global innovation rate (columns).	139

List of Tables

3.1	Comparison of expected K_n from (3.8) with simulated values from WF-IA model, for θ values from 2 to 40. Total sample size across θ values is 408,478 samples of size 30.	27
3.2	Breakdown of sample sizes for analysis of trait richness (K_n), by size of time-averaging “window.” Some values of θ required larger numbers of simulation runs to achieve stable result, thus the difference between samples sizes at the same TA duration.	29
3.3	Mean lifetime (in model generations) of traits, by θ , along with analytical approximation from Equation 3.10.	31
3.4	Mean Estimated Theta ($\mathbb{E}(\hat{\theta})$) from Samples ($n=100$) compared to actual values employed in simulation models (θ_0), without any time-averaging.	37
4.1	Parameters for simulation runs across the four models studied. Intervals are treated as prior distributions, and each simulation run is assigned values derived from a uniform random sample on the interval indicated. Lists of values are all applied to every simulation run (e.g., there is both a 10% and a 20% sample from each simulation run. Single values are applied to every simulation run, and represent a point prior.)	56
4.2	Variables measured from each transmission model simulation sample. The parenthetical expression records whether the variable was calculated for cross-tabulations of all 4 loci (Class) or represent the order statistics from individual loci (Min/Mean/Max). The right column records the variable name used within R statistical models, for examining the relative importance of each variable in classifying observations.	57
4.3	Data collection strategies, applied to every simulation run. Time averaging duration is given in units of “generations,” which are units of 100 time steps (given the population size). 100 generations thus represents 10,000 elemental time steps in the Moran simulation dynamics.	60
4.4	Example confusion matrix. Columns correspond to the actual model for data points, rows correspond to predictions from a classification model. Bold numbers on the diagonal correspond to correct predictions, the off diagonal elements correspond to classification errors.	63
4.5	Relative importance of predictor variables for population census data, in the comparison between unbiased transmission and all biased models. The most important variable is (by convention) scaled to 100, and the values indicate the ratio of variable importance to the variable which is most effective at classifying data points. Only values greater than 10 are shown. The remainder of the predictor variables are 1/100th as effective as class richness or less.	66

4.6	Relative importance of predictor variables for population census data, in the comparison between unbiased transmission and a balanced mixture of pro- and anti-conformists. The most important variable is (by convention) scaled to 100, and the values indicate the ratio of variable importance to the variable which is most effective at classifying data points. Only values greater than 10 are shown. The remainder of the predictor variables are 1/100th as effective as class richness or less.	68
4.7	Two confusion matrices arising from the first model comparison, between unbiased and all biased models.	70
4.8	REDO!!! omPercentage of data points from the unbiased transmission model that are falsely identified as arising from a biased model.	71
5.1	Number of unique seriation solutions and parallel processing time for sets of assemblages $4 < n < 100$, testing solutions across 64 cores, assuming 5ms per trial	79
5.2	Number of ways to form m subsets (seriation solutions) from 20, 40, and 60 assemblages	81
5.3	Number of total solutions with multiple seriation groups and processing time for sets of assemblages $4 < n < 100$, testing solutions across 64 cores	83
6.1	Raw data for frequency seriation for simulation run f8a6f378, grouped into blocks corresponding to the branches of the solution graph	106
6.2	Raw data for continuity seriation for simulation run f8a6f378, grouped into blocks corresponding to the branches of the solution graph	107
7.1	Size of design space for different trait tree configurations	133
7.2	Parameter space for simulations described in this chapter	133

Acknowledgements

RCD

Lipo

Feathers

Grayson

Peter Ward

Nicole, Scott, K&K, Hamilton

My mother, Joy Colleen Berkey Madsen (1944-2005), encouraged me from the earliest age in a love of learning, not merely because it would lead to opportunity, but because knowledge and learning were important values in and of themselves. Her own opportunities for higher education were limited by the need to support herself from a young age, and then by the need to work and support her family, but she supported my education in every way possible.

This dissertation is both dedicated to her, and many ways a joint accomplishment.

Part I

Introduction and Research Methods

Introduction

From our vantage point in 2019, it seems as if the study of cultural transmission is a formalized, model-driven, highly interdisciplinary field, encompassing the “hard science” side of most of the traditional social sciences including psychology, economics, and anthropology. The field is growing and maturing, creating bridges between the social sciences, cognitive science, and the behavioral side of evolutionary biology, leading to a deeper conception of “cultural evolution” than past attempts to import Darwinian ideas into the social sciences. Anthropology can rightly claim a central place in introducing and elaborating the idea of the “transmission” of culture, and it is the only discipline among those listed here for which cultural transmission is—and has been, for more than a century—a *central organizing concept* for the discipline (Lyman, 2008). And within anthropology itself, archaeology has been central to the framing of cultural transmission as one of our discipline’s central pillars both in terms of theory and by providing evidence for the spatio-temporal structure of the products of transmission.

And yet, despite our long history with the concept, and despite a plethora of recent works which provide formalized models and tools, we struggle to use our models to explain the archaeological record we observe in convincing, testable ways. Kandler and Shennan (2015) note that even the most studied case—ceramic type frequencies from the Merzbach *Linearbandkeramik* in Germany—has

produced conflicting results, with some studies consistent with neutral models, and others rejecting neutrality in favor of anti-conformist transmission models. This failure to achieve clarity is not due to lack of theoretical sophistication; the methods involved having evolved well beyond simple tests of neutrality borrowed from population genetics in favor of non-equilibrium and generative models combined with sophisticated Bayesian methods and large amounts of computational resources.

Some of our issue with empirical sufficiency and connecting models to data arises because of our choice of models and hypotheses, if we are being honest with ourselves. The shadow of Boyd and Richerson's (1985a) pioneering book is understandably quite long, since it (along with neutral theory from theoretical population genetics) gave us a quantitative framework within which to pose, and potentially answer, questions about cultural transmission. We have been content in most cases to assume that cultural transmission models written in the language of social psychology should also directly speak the language of class frequencies in artifact assemblages. In most cases, this is an unreasonable expectation.

The phenomena we seek to explain in archaeology are always aggregated in various ways; at a minimum the typical archaeological deposit is a time averaged record of many events of occupation and activity. It may be unreasonable to expect that a highly aggregated and time averaged record should be cleanly informative about the average psychological and cognitive biases of past populations. A great deal of recent work has focused on the issue of *equifinality* between different models of cognitive bias, attempting to quantify the degree to which we may be able to distinguish theoretical models given varying amounts of aggregation. My own early work in this area forms the first case study presented in this dissertation.

Equifinality can occur for many reasons beyond simply time averaging, and it is a phenomenon which we cannot fully eliminate. When it occurs, however, we must understand why, and what it is telling us about our models, the observational units we're measuring to create data with which we confront models (in addition to issues such as sample size). Equifinality arises for several principal reasons, which are linked respectively, to the ideas of *dynamic sufficiency* and *empirical sufficiency* of

our theories (Lewontin, 1974).

Equifinality may be *structural* and a feature of our models and the way they represent the phenomena we are analyzing. It is simply the case that two models may make the same distributional predictions about the same observable variables. In such cases, we cannot tell the two models apart from observations of that variable or set of variables. In this case, our set of models is dynamically insufficient in a very fundamental way.

(EXAMPLE from archy models – different things that lead to power law frequency distributions - Rorabaugh?)

A second major source of equifinality is that our models might make distinguishable predictions given various “pure” states and parameter values, but converge strongly given more realistic population states. We often make simplifying assumptions when we formulate models, often to gain analytic tractability or apply a simple model which has already been studied in another field, but has the same mathematical structure (this is extremely prevalent in theoretical population genetics, and thus in the borrowings made into cultural transmission theory). Such simplifications have been critical to both population genetics and cultural transmission theory. Without them, Neiman’s (1995) seminal contribution would not have been possible, giving rise to a rich lineage of work applying the implications of neutral theory to artifact class frequency distributions (including some of my own early work, e.g., Lipo et al., 1997a). But nobody really believes that real populations are composed of individuals who are all “conformists” or essentially unbiased in their adoption of traits, or any other “mode” we have collectively modeled in the cultural transmission literature. Real populations are always mixtures of people with varying cognitive biases (and, of course, our deployment of various cognitive biases changes situationally, and our tendency to have specific biases changes over the course of one’s lifetime). The second case study in this dissertation begins the study of such issues, using machine learning methods to determine what the limits of our ability to discriminate among data generating processes may be given realistic mixtures and issues such as sample size.

** what this means for choice of variables - since that’s a key conclusion in the classifier paper

** third cause of equifinality is in the choice of variables or observational units. This leads to two main threads of research, designed to get away from the sole fixation on trait frequency distributions.

** seriation

** structured information models

so long as we do not examine the observational units we use, and expand our toolkit for generating the data we need to test our models ([Tostevin, 2019](#)).

My own recent work is aimed at evaluating the potential for "coarse graining" cultural transmission models to archaeological scales, which means first and foremost, forming a new set of "observable" units which are appropriate to the diachronic, aggregated, and time averaged empirical record we study. This dissertation is a progress report on forming such observables and examining how to use them to study the kind of data we *actually have*, not the data that would make our task easier—or in other words, the data we *wish* we had.

Research Methods

OVERVIEW Lorem ipsum dolor sit amet, consectetur adipiscing elit. Ut purus elit, vestibulum ut, placerat ac, adipiscing vitae, felis. Curabitur dictum gravida mauris. Nam arcu libero, nonummy eget, consectetur id, vulputate a, magna. Donec vehicula augue eu neque. Pellentesque habitant morbi tristique senectus et netus et malesuada fames ac turpis egestas. Mauris ut leo. Cras viverra metus rhoncus sem. Nulla et lectus vestibulum urna fringilla ultrices. Phasellus eu tellus sit amet tortor gravida placerat. Integer sapien est, iaculis in, pretium quis, viverra ac, nunc. Praesent eget sem vel leo ultrices bibendum. Aenean faucibus. Morbi dolor nulla, malesuada eu, pulvinar at, mollis ac, nulla. Curabitur auctor semper nulla. Donec varius orci eget risus. Duis nibh mi, congue eu, accumsan eleifend, sagittis quis, diam. Duis eget orci sit amet orci dignissim rutrum.

CONTENTS Nam dui ligula, fringilla a, euismod sodales, sollicitudin vel, wisi. Morbi auctor lorem non justo. Nam lacus libero, pretium at, lobortis vitae, ultricies et, tellus. Donec aliquet, tortor sed accumsan bibendum, erat ligula aliquet magna, vitae ornare odio metus a mi. Morbi ac orci et nisl hendrerit mollis. Suspendisse ut massa. Cras nec ante. Pellentesque a nulla. Cum sociis natoque penatibus et magnis dis parturient montes, nascetur ridiculus mus. Aliquam tincidunt urna. Nulla ullamcorper vestibulum turpis. Pellentesque cursus luctus mauris.

Part II

Research Papers

Neutral Cultural Transmission in Time Averaged Archaeological Assemblages

OVERVIEW Neutral models are foundational in the archaeological study of cultural transmission. Applications have assumed that archaeological data represent synchronic samples, despite the accretional nature of the archaeological record. Using numerical simulations, I document the circumstances under which time-averaging alters the distribution of model predictions. Richness is inflated in long-duration assemblages, and evenness is “flattened” compared to unaveraged samples. Tests of neutrality, employed to differentiate between biased and unbiased models, suffer serious problems with Type I error under time-averaging. Estimation of population-level innovation rates, which feature in many archaeological applications, are biased even without time averaging, but have sharply increased bias given longer assemblage durations. Finally, the time scale over which time averaging alters predictions is determined by the mean trait lifetime, providing a way to evaluate the impact of these effects upon archaeological samples.

3.1 Introduction

The evolutionary study of culture today crosses many disciplines and employs a variety of experimental and observational methods to study its subject matter. What makes the archaeological record unique as a source of data concerning the evolution of culture is time depth, creating the possibility of studying both the unique histories of human groups and the evolutionary processes that shape those histories. Archaeology is not unique in studying temporal data on human activity, but like our colleagues in paleobiology, we study an empirical record that is unlike the time-series data available to disciplines such as economics or epidemiology (e.g., [Arrow, 2009](#); [Keeling, 2005](#); [Keeling and Rohani, 2007](#); [Kendall and Hill, 1953](#); [Rothman et al., 2008](#)). The archaeological record is not a sample of measurements from individual moments in time stacked together into a sequence. Instead, archaeological deposits are almost always accretional palimpsests, representing cumulative artifact discard over durations of varying length ([Bailey, 2007, 1981](#); [Binford, 1981](#); [Schiffer, 1987](#); [Stein, 1987](#)). Thus, when archaeologists count the richness of faunal taxa in an assemblage, or measure the relative frequencies of ceramic types, the data obtained summarize the bulk properties of artifact discard and deposition over significant spans of time, often with nonconstant rates of accumulation.¹ We refer to assemblages which are accretional in this manner as “time averaged.”

A growing number of studies apply cultural transmission models to artifact assemblages by comparing the predictions such models make for the richness, diversity, or frequency distribution of cultural traits, to counts or frequencies of artifact classes (e.g., [Bentley and Shennan, 2003](#); [Bettinger and Eerkens, 1999](#); [Eerkens and Lipo, 2007](#); [Jordan and Shennan, 2003](#); [Lipo and Madsen, 2000](#); [Perreault and Brantingham, 2011](#); [Premo and Scholnick, 2011](#); [Scholnick, 2010](#); [Shennan and Wilkinson, 2001](#); [Shennan, 2011](#); [Steele et al., 2010](#)). The question is, are model predictions comparable to archaeological measurements? Given the time averaged structure of most archaeological deposits, I suspect the answer is no. Transmission models developed outside archaeology are typically constructed to make predictions concerning variables observed at a point in time. To date, almost none of the archaeo-

¹As well as the action of various post-depositional and taphonomic processes, of course.

logical literature employing cultural transmission models has taken this “time averaging” effect into account and modified the way predictions are made to match the nature of the phenomena we measure (cf. [Bentley et al., 2004](#)). Evaluating the effects of temporal aggregation upon the predictions made by cultural transmission models is the first step in understanding how to rewrite and adapt transmission models to understand their dynamics given time averaged observations.

In his dissertation, [Neiman \(1990\)](#) considered a potential source of time averaging effects in diachronic assemblages: variation in discard rates across traits. With respect to this particular effect within accretional deposits, Neiman’s results suggested that the predictions made by a neutral model of cultural transmission were directly applicable to the relative frequencies of traits as we would measure them in a time averaged assemblage. Nevertheless, there is good reason to consider the effects of aggregation directly, outside of variation in discard rates. Paleobiologists, for example, have documented systematic differences between living and fossil assemblages, including increased species richness, reduced spatiotemporal variance in taxonomic composition, and flatter species abundance curves in time averaged assemblages ([Olszewski, 2011](#); [Tomašových and Kidwell, 2010a,b](#)). [Lyman \(2003\)](#) extended these results to zooarchaeology, noting that time averaging can be a significant problem when the process one is applying or studying occurs over a shorter time scale than the empirical record available to study its properties (see also [Grayson and Delpech, 1998](#)). This relation between time scales is applicable to cultural transmission modeling as well.

Archaeologists now employ a variety of cultural transmission models, which differ in the kind of variation and traits they describe and the copying rules and evolutionary processes they incorporate. Discrete models describe individual variants or traits by their count or frequency in a population and are foundational for the study of stylistic variation in many artifact categories (e.g., pottery). The simplest discrete model is random copying in a well-mixed population with innovation, representing neutral variation with the stochastic effects of drift. We frequently construct more complex models of transmission bias by adding additional terms or frequency-dependent copying rates to the basic unbiased copying model ([Cavalli-Sforza and Feldman, 1973a,b, 1981a](#); [Boyd and Richerson, 1985a](#)).

Thus, an understanding of the effects of time averaging upon neutral transmission will be informative about many (if not all) of the discrete transmission models in use by archaeologists today, and forms the focus of the present study.

I report the results of numerical simulations designed to observe neutral transmission using variables employed in the archaeological literature, aggregated over time at a variety of intervals designed to mimic a wide range of “assemblage durations.” In Section 3.2 I describe the relationship between neutrality, unbiased copying, and the separate but related concept of “drift,” followed by a review of the quantitative properties of the well-mixed neutral Wright-Fisher infinite-alleles model in Section 3.3. Section 3.4 outlines the simulation model employed to study time averaging in this paper, including model verification and testing, and the algorithm used to effect temporal aggregation within the simulations. Section 3.5 presents the results of simulating unbiased cultural transmission for a variety of innovation rates and assemblage durations, and Section 5.3 summarizes the effects seen and points to next steps in reformulating our cultural transmission models for archaeological contexts.

3.2 Conceptual Structure of Neutral Cultural Transmission

In his classic article “Style and Function: A Fundamental Dichotomy,” Dunnell (1978a) proposed that many aspects of an artifact would play little or no role in its engineering performance, and thus have no impact on the fitness of individuals employing it. In other words, some attributes of artifacts are neutral with respect to selection. This has been widely misinterpreted as a claim that the artifacts themselves are neutral or have no fitness value, which is not the case. Dunnell was saying that if one describes an artifact solely using attributes which have equal cost or performance, the resulting classes meet the definition of neutral variation.

Fraser Neiman (1990) first connected Dunnell’s identification of style as selectively neutral variation, to population genetic models designed to describe genetic drift. His dissertation considers a wide range of cultural transmission models, especially those described by Cavalli-Sforza and Feld-

man (1973a,b, 1981a) and Boyd and Richerson (1985a). Neiman employed simulation to calculate the consequences of both individual processes as well as processes combined with various archaeological factors such as variable rates of artifact discard. In this work, Neiman pioneered virtually every technique used by archaeologists today to model and study cultural transmission. The discipline as a whole was introduced to this work in his now classic 1995 article (Neiman, 1995), in which the dynamics of Woodland ceramic variation were explicitly modeled as a random copying process.

Despite the fact that there are multiple ways that neutrality can arise as a population level effect, there is a tendency today to equate neutrality with “drift” in the archaeological literature on cultural transmission. For example, Bentley et al. (2004, p.1443) offer a fairly typical description of unbiased cultural transmission as “random genetic drift, which describes how the diversity of variants evolve when the dominant process is one of random copying.” In fact, drift and the copying rules that create population-level trait distributions are different and independent aspects of a transmission system. Before we turn to the details of a formal model for unbiased, neutral transmission, it is worth reviewing the conceptual elements that make up such models.

Drift is a feature of any stochastic transmission model in a finite population, regardless of whether selection or bias is also present in the model. Sewall Wright gave the name “genetic drift” to the random fluctuations in gene frequency that occurred because some individuals might be the source of many genes in the next generation, and others none at all. Translated into a cultural model, drift occurs when some individuals, by random chance, are imitated or copied and others are not. In an infinite population, by contrast, the variants held by individuals would be sampled at their exact frequencies in the population, and thus there would be no stochastic “wobble” in trait frequencies. This is reflected in population genetics by the famous “Hardy-Weinberg” equilibrium, where in the absence of selection or other forces, gene frequencies stay the same from generation to generation. This means that we can easily have *neutrality without drift*, in an infinite population. In a large but still finite population, we can expect drift to have very tiny, potentially even unmeasurable effects upon the trajectory of trait frequencies.

Drift, moreover, occurs in combination with a variety of inheritance rules, mutation models, and in combination with natural selection. In small populations, we can expect drift to be a factor when examining the engineering properties of ceramics and the relative fitness of firing technologies, or the fitness of foraging strategies. Whenever such traits are learned and passed on within small, finite populations, the stochastic aspect of who learns from whom will create fluctuations in variant frequencies that have nothing to do with the performance or survival value of traits, or the prestige of those we choose to learn from or imitate. In other words, we can have *drift without neutrality*. In small enough populations or during bottlenecks, even adaptive technologies and knowledge can be lost to drift (Henrich and Boyd, 2004; Henrich, 2006). We should always be on the lookout for the effects of drift, especially as population sizes get smaller as we go back in time. Drift is not a model of human social learning; it is a consequence of finite populations, injecting stochastic noise into the dynamics of a system that affects our ability to cleanly fit models and test hypotheses.

Neutrality, by contrast, is a population level phenomenon, arising when there is no net force systematically favoring certain variants over others for a particular dimension of variation. Most commonly, of course, we mean that there is no natural selection that favors some alleles over others, but from a mathematical perspective, the transmission bias rules of Cavalli-Sforza and Feldman (1981a) and Boyd and Richerson (1985a) are equivalent to selection models.² The simplest way for neutrality to arise is for individual social learning to be “unbiased.” Unbiased transmission models always yield population-level neutrality for the traits being passed, because the probability of imitating any specific trait is simply proportional to its frequency among individuals in the population. The Wright-Fisher model is one of the earliest stochastic models in population genetics (Provine, 1989, 2001; Wright, 1931), and was originally created to describe the process of genetic drift and its effects in combination with other evolutionary processes. Following Kimura’s theory of neutral alleles, Wright-Fisher is also used to describe the evolution of populations in which variants are selectively neutral. Elaborations

²In this paper I leave aside the relationship between “natural” and “cultural” selection, and transmission biases, since such issues are largely philosophical and theoretical and do not affect the nature of the models we employ for quantitative analysis of cultural variation.

of the basic Wright-Fisher model add mutation, selection, loci with multiple alleles, and multiple loci with interactions between loci (see esp. [Crow and Kimura, 1970](#); [Ewens, 2004](#)).³

But unbiased copying is not the only source of neutrality among variants, and it is important to keep this in mind when selecting models to test as explanations for archaeological phenomena. In any realistic human population, there will be heterogeneity in social learning rules, with individuals using different rules for different traits, or kinds of traits, and perhaps having individual propensities for conformism (all other things being equal) or pro-novelty bias ([Mesoudi and Lycett, 2009](#)). A population which is heterogeneous for such rules may display the characteristic frequency distributions of conformity or pro-novelty biased if we are able to observe small numbers of transmission events or individual transmission chains, while simultaneously cancelling each other out at the level of the population. In other words, heterogeneity is a major source of equifinality between different models of social learning, when observed through population-level trait frequencies. No archaeological applications of cultural transmission models today have employed heterogeneous models, probably because the theory behind such models is not well-studied. But this is clearly a frontier for future research since homogenous models poorly reflect what occurs in real human populations.

Returning to unbiased models of transmission, we face a further choice in selecting a specific model to employ or study. In addition to the copying rules, we must specify an innovation rule. Such a rule answers questions like: how do new variants enter the population, can variants be invented multiple times independently, and is there a constrained range of variation for a particular dimension of an artifact? For example, painted design elements on a ceramic pot offer a “design space” of possibilities that is potentially unbounded, even if only a tiny fraction of possible designs occur in any archaeological context. Such attributes are best modeled by the “infinite alleles” innovation model. In contrast, stylistic aspects of lithic tools may be sharply constrained by the technology and materials themselves, and may be best modeled by innovation among a small set of variants, with the

³And, the Moran family of models mirrors the Wright-Fisher models, with overlapping generations, by representing dynamics as continuous-time stochastic processes. Moran models are likely the best framework for modeling cultural transmission when the exact temporal dynamics matters. In this paper I follow archaeological convention by employing the more familiar Wright-Fisher discrete generation framework.

material constraints causing frequent “reinvention” of the same shapes over and over. Such attributes are best modeled by constraining the design space, and employing a finite or “k-alleles” version of the unbiased model. Since Neiman’s pioneering work, most archaeological applications of neutral models have employed the “infinite alleles” variant of the Wright Fisher model (WF-IA)([Kimura and Crow, 1964](#)). Therefore, in the remainder of this paper, I focus on the unbounded model of neutral evolution with innovation, since it is relevant to a large number of archaeological contexts and artifact categories, but the reader should be aware that the models with a constrained number of variants may be hugely important in specific archaeological contexts, and are underexplored in the archaeological literature.

3.3 Unbiased Transmission: The Wright-Fisher Infinite-Alleles Model

WF-IA is a stochastic process that models unbiased transmission within a fixed-size population as multinomial sampling with replacement, with a mutation process that adds new variants to the population at a known rate. After describing the model, I review the sampling theory of [Ewens \(1972\)](#), which gives the distribution of variants expected in small samples taken from the population as a whole. The sampling theory, rather than the distribution of variants in the full population, is both well-understood, and most relevant to archaeologists, who are always sampling an empirical record of past artifact variation.

The well-mixed neutral Wright-Fisher infinite-alleles model ([Kimura and Crow, 1964](#)) considers a single dimension of variation (“locus”) at which an unlimited number of variants (“alleles”) can occur, in a population of N individuals.⁴ The state of the population in any generation is given in several ways: a vector representing the trait possessed by each individual (census), a vector giving the abundance of each trait in the population (occupation numbers), or by the number of traits represented

⁴Conventionally, the model treats a diploid population, in which N individuals each have two chromosomes and thus there are always $2N$ genes tracked in the population. The haploid version is more appropriate for modeling cultural phenomena, and thus formulas given in this paper may differ from those given by [Ewens \(2004\)](#) and other sources by a factor of two. For example, the key parameter θ is defined as $2N\mu$ rather than the common genetic definition $4N\mu$.

in a population by a specific count (spectrum).

In each generation, each of N individuals selects an individual at random in the population (without respect to spatial or social structure, hence “well-mixed”), and adopts the trait that individual possessed in the previous generation.⁵ Equivalently, a new set of N individuals are formed by sampling the previous generation with replacement. At rate μ for each individual, a new variant is added to the population instead of copying a random individual, leading to a population rate of innovations $\theta = 2N\mu$ (Ewens, 2004), with no “back-mutation” to existing traits.⁶ An important consequence of this innovation model is that each variant is eventually lost from the population given enough time, and replaced with new variants. Thus, there is no strict stationary distribution for the Markov chain describing WF-IA, although there is a quasi-stationary equilibrium in which the population displays a characteristic number of variants, with a stable frequency distribution governed by the value of θ (Ewens, 2004; Watterson, 1976).

Beginning with a now-classic paper Ewens (1972) constructed a sampling theory for the neutral WF-IA model, allowing the calculation of expected moments and frequency distributions for small samples (compared to overall population size) (see Ewens, 2004, for a complete summary of results on the sampling theory). In what follows, we assume that a neutral WF-IA process is running within a population of size N . At some moment in time after the population has reached its quasi-stationary equilibrium, we take a sample of n individuals, where the sample is small compared to the population size ($n \ll N$). We then identify the variants held by each individual. The total number of variants seen in the sample will be denoted by k , or k_{obs} depending upon context.

Given such a sample, Ewens (1972) found that the joint distribution of the variant spectrum (a_i represents the number of variants represented i times in a sample), given the population innovation rate (θ), is given by the following formula (now known as the Ewens Sampling Distribution):

⁵An individual can select themselves at random since sampling is with replacement, and this would be equivalent to “keeping” one’s existing trait for that generation.

⁶It is important to note that θ is not a measure of the “diversity” of traits in the population, as it has been employed in several archaeological studies, but is instead a *rate* parameter of the model.

$$\mathbb{P}_{\theta,n}(a_1, \dots, a_n) = \frac{n!}{\theta^{(n)}} \prod_{j=1}^n \frac{(\theta/j)^{a_j}}{a_j!} \quad (3.1)$$

where $\theta^{(n)}$ is the Pochhammer symbol or “rising factorial” $\theta(\theta + 1)(\theta + 2) \cdots (\theta + n - 1)$. In most empirical cases, we cannot measure (or do not set through experiment) the value of θ , so a more useful relation is the distribution of individuals across variants (i.e., the occupation numbers), conditional upon the number of variants k_{obs} observed in a sample of size n :

$$\mathbb{P}(n_1, n_2, \dots, n_k | k_{\text{obs}}) = \frac{n!}{|S_n^k| k! n_1 n_2 \cdots n_k} \quad (3.2)$$

where $|S_n^k|$ denote the *Stirling numbers of the first kind*, which give the number of permutations of n elements into k non-empty subsets (Abramowitz and Stegun, 1965). The latter serves here as the normalization factor, giving us a proper probability distribution.

From Ewens’s sampling theory, and in particular Equation 3.2, a number of useful measures can be derived, relevant to archaeological applications. In this study, I focus upon the most commonly used: statistical tests of neutrality, estimation of innovation rates (θ), and the evenness with which variants are represented in the population (as revealed by several diversity measures).

3.3.1 Statistical Tests for Neutrality

Because Equation (3.2) requires no unobservable parameters, it serves as the basis for goodness-of-fit tests between empirical samples and the neutral WF-IA. The two most important such tests are the Ewens-Watterson test using the sample homozygosity and Slatkin’s “exact” test (Durrett, 2008; Ewens, 2004; Slatkin, 1994, 1996, 1994, 1996).⁷ Both have been adopted for use by archaeologists, beginning with Neiman (1995) and Lipo (2001b), who described Watterson’s work in detail, and more recently, applications of Slatkin’s exact test by Steele et al. (2010) and Premo and Scholnick (2011).

⁷There are several other important tests of neutrality when dealing with DNA sequence data, including Tajima’s D, the HKA test, and the McDonald-Kreitman test (Durrett, 2008). Because their assumptions are highly specific to the structure of sequence data, I omit consideration of them here.

The Slatkin test makes no assumptions concerning the process underlying an alternative hypothesis to neutrality, whereas the Ewens-Watterson test examines the observed heterozygosity at a locus versus the expected heterozygosity predicted by Ewens sampling theory. Slatkin's test does not employ the concept of heterozygosity, and relies only upon the “shape” of the Ewens Sampling Distribution given a specific innovation rate. As a result, archaeologists should prefer Slatkin's test for examining the fit of a synchronic sample of variants to the null hypothesis of neutrality. Slatkin's test is modeled upon the Fisher exact test for contingency tables. Where the Fisher exact test determines the probability of an unordered configuration from the hypergeometric distribution, Slatkin's test determines the probability of a sample of traits (characterized by occupation numbers) with respect to Equation 3.2.

There are two methods for determining how probable a given sample is, with respect to the ESD. For relatively small n and k , it is possible to enumerate all possible combinations (\mathbf{C}) of the n individuals among k variants. Each configuration ($c_j \in \mathbf{C}$) then has a probability given Equation 3.2, as does the observed configuration (c_{obs}). With larger sample sizes and values of K_{obs} , it becomes impractical or simply time consuming to enumerate all possible configurations and thus determine the likelihood of an observed sample. In such cases, Monte Carlo sampling of configurations from the Ewens Sampling Distribution is used. We then determine the total probability mass of all configurations (enumerated or sampled) whose probability are less than or equal to the observed configuration:

$$\mathbb{P}_e = \sum_{c_j \in \{\mathbf{C} : P(c_j | k) \leq P(c_o | k)\}} \mathbb{P}(c_j | k) \quad (3.3)$$

\mathbb{P}_e then represents the Fisherian p-value of the sample with respect to the Ewens Sampling Formula, and thus can be interpreted as a test of the hypothesis that the sample was drawn from a neutral dimension of variation which followed the WF-IA copying model. The \mathbb{P}_e value for a given sample gives the tail probability of its occurrence given the ESD. Thus, if we take a sample of size 100 in a population with innovation rate $\theta = 0.1$, and identify two variants with counts 51 and 49, we might not be surprised to see a \mathbb{P}_e value of 0.01181, indicating that such a sample is highly unusual for a

WF-IA process. On the other hand, in the same sample of size 100, if we identify four variants, with counts 55, 38, 6, and 1, this seems a much more typical result of an unbiased copying process. Indeed, the \mathbb{P}_e value of 0.48544 confirms that we should expect to see such samples quite often.

3.3.2 Estimation of Innovation Rates

The behavior of the WF-IA neutral model is governed by the innovation rate (θ). Recall that $\theta = 2N\mu$, and thus represents the population-level rate at which new variants enter the population. In general, for low values of the innovation rate ($\theta < 1.0$), the process is “drift-dominated,” and one or a small number of variants dominate the population. At innovation rates above 1.0, which implies that every single “generation” incorporates one or more new variants, the process is “mutation-dominated,” and more variants are maintained at intermediate frequencies in the population.

Thus, estimation of the innovation rate from empirical data is of great interest when investigating empirical cases. If we measure the number of variants (K_n) in a sample of artifacts of size n , the sampling theory gives the following probability distribution (Ewens, 2004, Eq. 3.84):

$$\mathbb{P}_\theta(K_n = k) = \frac{|S_n^k| \theta^k}{\theta^{(n)}} \quad (3.4)$$

This is a somewhat inconvenient distribution to work with directly, since calculating the Stirling numbers and rising factorials is both analytically difficult and computationally expensive, but the expected value of K_n has a simple form:

$$\mathbb{E}(K_n) = \frac{\theta}{\theta} + \frac{\theta}{\theta + 1} + \frac{\theta}{\theta + 2} + \cdots + \frac{\theta}{\theta + n - 1} \quad (3.5)$$

K_n is the sufficient statistic for θ , containing all of the information required to calculate the maximum likelihood estimate of the innovation rate ($\hat{\theta}$) from an empirical sample. This is done numerically by finding the value of θ that maximizes the likelihood function of Equation 3.4, or equivalently, finding the value of θ for which the expected value of K_n given Equation 3.8 is equal to the observed

number of variants in a sample (since the full distribution may not have a closed-form likelihood function). In the archaeological literature, [Neiman \(1995\)](#) introduced this estimator of θ and called it t_e . With larger samples, [Watterson \(1975\)](#) showed that $k / \log n$ is a good approximation for the MLE estimator ([Durrett, 2008](#)).

Despite the fact that this estimator (and its approximations) are the best that can be achieved from samples, [Ewens \(1972\)](#) showed that all such estimates of θ are biased. Simulations demonstrate, furthermore, that $\hat{\theta}$ (or t_e) is an overestimate of the actual value, and that the amount of bias increases with θ itself ([Ewens and Gillespie, 1974](#)). In addition, the variance of the estimator is quite large, and decreases very slowly with increased sample size ([Durrett, 2008](#)). The situation is quite different using the “infinite sites” model of neutral evolution and DNA sequence data, where there are excellent and nearly unbiased estimators of θ .

But with the WF-IA and no additional structure to “traits” or alleles, it is very difficult to estimate the innovation rate with any accuracy, or determine whether two samples come from populations with the same innovation rate, or different rates. This fact calls into serious question the degree to which t_e is useful in archaeological analysis, either for estimating innovation rates in past populations, or as a measure of richness or diversity across assemblages or samples. These caveats apply to estimates of innovation rates and t_e given synchronic samples; the effects of time averaging on θ estimation have not been previously documented, and are addressed in [Section 3.5.3](#).

3.3.3 Diversity Measures

The amount of variation expected in a sample is an important quantity, given that we would clearly expect transmission models incorporating bias terms to differ from unbiased or neutral models (e.g. [Kohler et al., 2004a](#)). Conformist transmission should result in smaller numbers of variants than expected under unbiased transmission, and of course anti-conformist, or “pro-novelty”, biases should result in larger numbers of variants being maintained, on average. But beyond helping us assess goodness-of-fit to an unbiased copying model, comparing the number of variants in a sample (K_n)

either to a model, or between assemblages, is difficult without reliable estimates of the population-level innovation rate (θ). Since this is inherently difficult and inaccurate, we might ask instead what the evenness of variants is across our samples, since both innovation rates and different models of cultural transmission have clear implications for the diversity of traits we observe.

In the archaeological literature on cultural transmission, the most important evenness measure is t_f , which is a summed estimate of dispersion given trait frequencies [Neiman \(1995\)](#):

$$t_f = \frac{1}{\sum_{i=1}^k p_i^2} - 1 \quad (3.6)$$

To make this measure easier to compare across different innovation rates, it is convenient to normalize. Wilcox’s “index of quantitative variation,” does so, and varies between 0 (when all cases belong to a single category), and 1 (when all cases are evenly divided across categories) ([Wilcox, 1973](#)):

$$IQV = \left(\frac{k}{k-1}\right)\left(1 - \sum_{i=1}^k p_i^2\right) \quad (3.7)$$

Paleobiologists have found that fossil assemblages have considerably “flatter” species diversity curves compared to living communities, and I expect that time averaging will have the effect here of pushing IQV towards 1.0 compared to its value in unaveraged samples.

3.4 Methods

In this research, I employ a “forward-time” approach to computational modeling of unbiased cultural transmission, by contrast to most modeling in theoretical population genetics today, which employs the coalescent or “backward-time” approach ([Kingman, 1977](#); [Durrett, 2008](#); [Wakeley, 2008](#)). In archaeological research, we are interested in the entire distribution of variants which transmitted through the population, samples of which may be deposited and become part of the archaeological record regardless of which variants ultimately leave descendants in later generations. Forward-time

approaches evolve a population in steps, applying rules for the generation of variation, copying between individuals, innovation, and sometimes population dynamics.⁸ Several well-tested forward-time population genetic frameworks exist, including a very flexible framework called **simuPOP** (Peng et al., 2012; Peng and Kimmel, 2005).

In this research, I employ a framework written by the author specifically for cultural transmission simulations. This project calls for integrating computation models of archaeological classification and seriation, which require code beyond that supplied by population genetics frameworks. My simulation codebase is called **TransmissionFramework**, and is available as open-source software.⁹ **TransmissionFramework** runs on any platform capable of supporting a Java 1.6+ runtime, with optional scripts requiring Ruby 1.9+.

3.4.1 Model Verification

Simulation modeling plays an increasingly important role in scientific inquiry, to the extent that computational science is now recognized as a third branch of physics, along with the pre-existing theoretical and experimental branches (Landau and Binder, 2005). Indeed, as theory becomes more complex and realistic, we often cannot directly solve theoretical models and derive predictions that should be measurable by experiment. Computational science sits between theory and experiment, allowing us to understand the behavior and dynamics of complex theoretical models, and calculate predictions that can be used for experiment or hypothesis testing.

The problem of assessing simulation model quality is important enough that the Department of Energy and the Air Force Office of Scientific Research requested that the National Research Council study the foundations of verification, validation, and uncertainty quantification (VVUQ) activities for computational models in science and engineering. Their draft report forms the basis of my approach

⁸Forward-time approaches are not necessarily equivalent to “agent-based models,” but ABM techniques are useful in implementing forward-time models.

⁹**TransmissionFramework** can be downloaded or the code examined at <http://github.com/mmadsen/TransmissionFramework>.

to verification and uncertainty analysis in this research ([Committee on Mathematical Foundations of Verification Validation and Uncertainty Quantification, National Research Council, 2012](#)).

Verification answers the question, “how accurately does a computational model solve the underlying equations of a theory for the observable quantities of interest.” Given that we know the true value of θ which drives our simulation runs, it is possible to calculate the expected number of variants at stationarity, and use this to verify that **TransmissionFramework** is correctly implementing the WF-IA. The expected number of traits is a good validation estimate because the number of variants present in a sample will be sensitive to the relative rates of copying and innovation events being handed correctly in the simulation code. Errors in handling these events in software will be magnified across many individuals over many simulation steps.

Since θ is known, the mean value of K_n is well approximated by:

$$\mathbb{E}_\theta(K_n) = \int_0^1 (1 - (1 - x)^n) \frac{\theta}{x} (1 - x)^{\theta-1} dx \quad (3.8)$$

Using Equation (3.8), I compared expected K_n to the average of k_n for a large sample of simulation runs. To ensure that behavior is correct across a range of useful θ values, I performed multiple simulation runs at θ values ranging from 2 to 40, for 5000 generations in a simulated population of 2000 individuals. Each parameter combination was represented by 3 simulation runs. The initial transient behavior of the model is discarded from data analysis by skipping the first 750 generations, given the mixing time analysis by [Watkins \(2010\)](#). At each time step in a simulation run, the simulator took a sample of 30 individuals and tabulated the traits held by those individuals, and recorded the value of K_n . This yielded 408,478 samples across validation runs.

Using Mathematica 8.0 with MathStatica 2.5 installed, I calculated expected values for each θ level used in simulation, employing Equation (3.8). Table 3.1 compares the expected and observed values. In all cases, the analytical results are extremely close to the observed mean K_n values from simulation, and certainly well within 1 standard deviation. Thus, I conclude that the **TransmissionFramework** implementation of WF-IA employed in this study accurately represents the desired theoretical model.

Theta	$\mathbb{E}(K_n)$	Simulated \bar{K}_n	Sim. Stdev K_n
2	6.054	6.511	1.838
4	9.022	8.991	2.269
8	12.869	12.616	2.464
12	15.397	15.306	2.571
16	17.228	17.187	2.569
20	18.629	18.737	2.486
40	22.601	22.693	2.253

Table 3.1: Comparison of expected K_n from (3.8) with simulated values from WF-IA model, for θ values from 2 to 40. Total sample size across θ values is 408,478 samples of size 30.

3.4.2 Time-Averaging and Simulation Parameter Space

Time-averaging was modeled in `TransmissionFramework` by implementing a series of statistical “windows” within which trait counts were accumulated between time steps. At the end of each temporal window, a sample of appropriate size is taken from the accumulation of trait occurrences, trait counts within that sample tabulated, and K_n values recorded. The simulator architecture allows an arbitrary number of temporal windows to be employed simultaneously (albeit with a small performance penalty for each window). As a consequence, during a single simulation run, the simulator tracks both unaveraged statistics and the same statistics averaged over any number of “assemblage durations.” All trait samples taken in the simulator, whether unaveraged or for a specific assemblage duration, were also recorded to allow calculation of Slatkin’s Exact test. Additionally, to facilitate analysis of time scales within the simulation model, for each trait the interval between entry and loss through drift was recorded. In the simulation results reported here, trait samples were of uniform size 100. Constant sample size removes the effect of different sample sizes on the reported results, although the interaction of the fixed sample size and the innovation rate will lead to cutoff behavior at very high θ values. This is acceptable since the very highest θ values employed here are unrealistic for almost any prehistoric phenomena, and may be approached only for “viral” behavior on modern social networks.

All simulations reported here were performed with a population size (N) of 2000 individuals, and

simulation runs were conducted for the following values of θ : 0.1, 0.25, 0.5, 1.0, 2.0, 5.0, and 10-100 at intervals of 10. This range encompasses innovation rates that are very small, through populations in which a full 5% of the population has a never-before-seen variant each generation. Simulations were performed in several batches, with a core set of runs performed for 40,000 steps in order to determine the effects of long-duration time averaging, yielding simulated assemblages at a variety of windows ranging from 3 steps to 8000 steps (the exact durations sampled are given in the first column of Table 3.2). In order to increase the sample size of long-duration assemblages, a second set of simulation runs using the same parameters were done with only the five largest windows recorded (the short duration window sizes were discarded to avoid a flood of raw data beyond that needed for stable statistical analysis). Finally, since the statistical behavior of the process at very small values of θ is highly variable, a third set of runs was performed to increase the number of samples for θ values between 0.1 and 1.0.

Trait samples were post-processed outside the simulator environment, since calculation of Slatkin Exact tests within the simulator itself would slow down the primary simulation model by a large factor. Montgomery Slatkin's original C language program was used in Monte Carlo mode to produce an estimate of $\mathbb{P}(E)$ for each sample of individuals. I modified Slatkin's original `montecarlo.c` program to not require the data to be embedded in the source code, instead taking data as a command line parameter, and outputting only the $\mathbb{P}(E)$ value and θ estimate, to allow easy post-processing of the simulation output.¹⁰

The simulation results reported here, once post-processed, comprise 3,024,085 sample values for K_n , across the θ values listed above, and broken down across assemblage durations as in Table 3.2, and 1,113,134 Slatkin Exact test results for the same combinations of θ and assemblage duration.

¹⁰These modifications are available, along with all other analysis scripts, in the Github repositories <http://github.com/mmadsen/saa2012>, and the **TransmissionFramework** source code.

TA Duration	Min Sample Size	Max Sample Size
1	130494	247491
3	4497	43494
7	1926	18639
15	897	8694
31	435	4209
62	216	2103
125	105	1038
250	516	981
500	255	486
1000	114	228
2000	57	114
4000	27	54
8000	12	16

Table 3.2: Breakdown of sample sizes for analysis of trait richness (K_n), by size of time-averaging “window.” Some values of θ required larger numbers of simulation runs to achieve stable result, thus the difference between samples sizes at the same TA duration.

3.5 Results

Simple inspection of the relationship between assemblage “duration” (i.e., accumulation interval) and the average number of variants (K_n) in a sample of size 100, shows a strong time averaging effect (Figure 3.1).¹¹ Temporal aggregation of the results of transmission inflates the number of variants we see in a sample, with greater effect as the population innovation rate (θ) increases. The effect is very small at low theta values (i.e., when the process is drift-dominated, $\theta < 1.0$) and requires long accumulation of copying events to have a measurable effect upon mean K_n . Conversely, inflated K_n appears at fairly short duration as theta increases.

Simulation steps (or “generations”) represent an arbitrary time scale with respect to the chronological time archaeologists can (with effort) measure. In order to understand the effects of time averaging on archaeologically-relevant time scales, it will be useful to rescale simulation time by some factor which is observable as a function of artifact class duration in the depositional record. I take

¹¹Here, the time axis represents raw simulation steps, each of which represents $N = 2000$ copying events within the population. This is the only figure in this paper which uses raw simulation time steps as the time variable.

up this issue further in Section 5.3, but the ideal time scale would be the mean duration of artifact classes in the classification system being used in a given empirical study. I do not explicitly model archaeological classification in the present results, but a related measure is the lifespan of the traits being transmitted within the simulated population.

3.5.1 Time Scales and Time averaging

The “mean trait lifetime” in WF-IA is a direct consequence of the balance between innovation and loss of traits to drift, in a fixed-size population. At the quasi-stationary state, the population will fluctuate around a mean number of traits, as individual traits enter and leave the population constantly. This implies that at stationarity, if we add traits at a higher rate due to migration or innovation, more traits must be lost to drift each generation. WF-IA thus satisfies a balance equation characterizing the average number of variants (\bar{n})(Ewens, 1964):

$$\frac{\bar{n}}{\bar{t}} = \theta \quad (3.9)$$

where \bar{t} represents the average number of generations that a new trait lasts in the population before its loss to drift (i.e., the mean trait lifetime).

An exact expression for mean trait lifetime has not been derived from the transition probabilities of the WF-IA Markov chain (Ewens, 1964), but it can be approximated by summing the average amount of time that a trait within a population spends at specific frequencies (i.e., mean sojourn times). Ewens (2004, Eq. 3.20) gives the following approximation:

$$\bar{t} \approx \mathbb{E}(t_i) = \sum_{j=1}^{\infty} \frac{2N}{j(j-1+\theta)} (1 - (1-p)^j) \quad (3.10)$$

Since θ is in the denominator of the summation, increasing the population rate of innovation reduces the mean trait lifetime by decreasing the amount of time any specific trait spends at a given frequency, and thus the total amount of time a trait spends in the population before being lost to drift.

Theta	Mean Trait Lifetime	$\mathbb{E}(t_i)$
0.10	36.54	36.89
0.25	25.61	24.05
0.50	21.10	19.97
1.00	17.31	17.21
2.00	14.57	15.21
5.00	12.43	13.05
10.00	10.83	11.57
20.00	9.50	10.16
30.00	8.68	9.36
40.00	8.12	8.79
50.00	7.72	8.36
60.00	7.36	8.01
70.00	7.08	7.72
80.00	6.83	7.46
90.00	6.60	7.42
100.00	6.40	7.05

Table 3.3: Mean lifetime (in model generations) of traits, by θ , along with analytical approximation from Equation 3.10.

Table 3.3 lists the observed mean lifetime of traits for each level of θ employed in this study, and the expected value as calculated using Equation 3.10. The observed values are systematically lower than the expected values, which reflects slightly faster loss of traits due to drift in a finite and small population compared to the large populations often studied in population genetics (Ewens, 1964; Kimura and Crow, 1964). Examination of Figure 3.1 appears to show that the onset of time averaging effects, however small, occurs around the time scale of the mean trait lifetime, for values of $\theta \geq 1.0$. This outcome is sensible given the enhanced probability of longer duration samples incorporating new variants in the sample due to innovation. In the analyses to follow, I scale the time variable by the mean trait lifetime, displaying assemblage duration as a multiple of this value. Thus, for the remainder of this paper, a scaled assemblage duration of 100 will indicate 100 times the mean trait lifetime at that specific θ value. For example, if we are examining results at $\theta = 5.0$, a scaled duration of 100 would indicate $12.43 * 100 = 1243$ simulation steps.

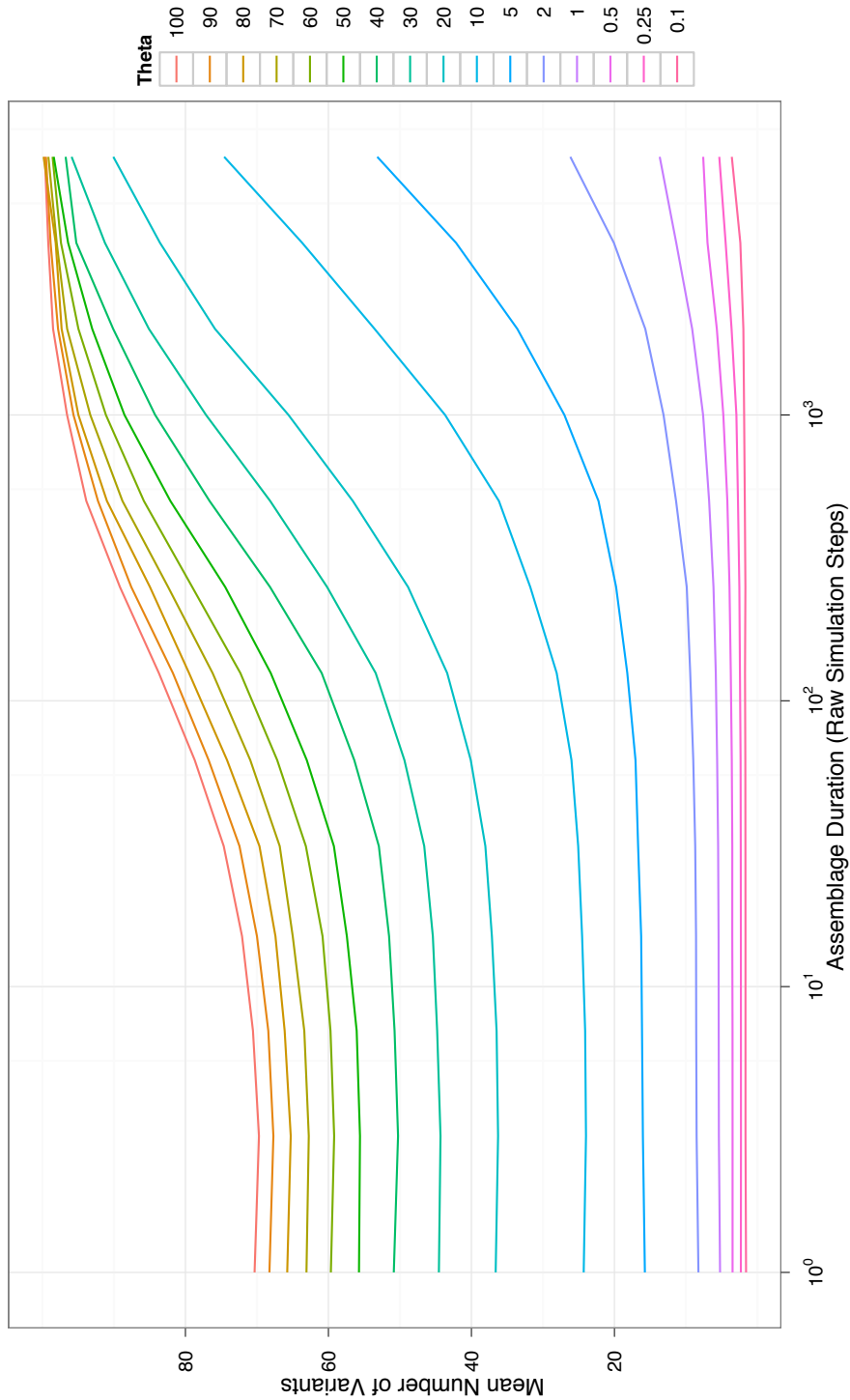


Figure 3.1: Mean value of K_n for time averaged samples, plotted against assemblage duration in simulation steps, for each level of θ in the study. Note that the “onset” of time averaging effects (as measured by increased K_n), is quite gradual at low θ , while high innovation rates display increased richness with very minor amounts of time averaging.

3.5.2 Neutrality Testing

The Slatkin Exact test for neutrality, discussed in Section 3.3.1, determines the “tail” probability for a sample of size n , with observed number of traits k , to be derived from the Ewens Sampling Formula (Equation 3.2). The test employed in this study is Slatkin’s Monte Carlo version, which allows the use of larger sample sizes, using random selection to create unlabeled configurations from the ESD to compare against the observed values. The resulting tail probability is converted into a standard hypothesis test by selecting an α value. For purposes of this study, I considered the upper and lower 5% of tail probabilities to indicate that a sample was probably not derived from a neutral transmission model, leading to $\alpha = 0.10$.

Given this α level, we should expect roughly 5% of the samples taken from a pure neutral copying process to fall into each of the the upper and lower tail regions, and thus for a Slatkin Exact test to reject the null hypothesis of neutrality. Roughly 90% of the samples we take from the neutral WF-IA process should fall between $0.05 < p < 0.95$ and thus lead to acceptance of the null hypothesis. This experimental setup also implies the limited utility of performing a single neutrality test on a single sample of class counts or frequencies, as has been archaeological practice by necessity. A single Slatkin exact test with P_e value of, say, 0.96, would constitute some, but relatively weak, evidence of non-neutrality. Better practice would be taking many samples from a large assemblage or multiple collections and calculating independent Slatkin tests for each sample, and examining their distribution.

If time averaging has no effect on the validity of the Slatkin Exact test employed against temporally aggregated samples, we would expect the fraction of samples in the two tails (upper and lower 5% in this case) to equal 10%. Anything over 10% would constitute evidence of extra Type I errors, since we know the samples to have been generated by a process meeting the definition of the null hypothesis. Therefore, after post-processing the simulation output to produce Slatkin tests as described in Section 3.4.2, I tabulated the fraction of Slatkin Exact tail probabilities that exceeded the expected 10% tail population. These are, in other words, “excess” failures of the Slatkin Exact test, beyond

those expected by the probability distribution itself. For each θ level, and for each time averaging duration, the mean “excess” failure rate was computed, from the 1,113,134 raw Slatkin Exact test results generated in the simulation study.

Figure 3.2 depicts the relationship between the excess failure rate, and time averaging duration scaled by the mean trait lifetime (as previously described). The mean trait lifetime is indicated by a vertical red bar in each graph. Three major results are apparent. First, at values of $\theta \geq 1.0$, the excess failure rate in non-time-averaged data is zero, as one would expect, and then begins to increase (albeit slowly) as the time averaging duration of samples exceeds the mean trait lifetime. In some cases, such as $\theta = 5.0$, the Slatkin Exact test continues to be accurate given the chosen α value through samples which are aggregated for 10 times the mean trait lifetime. But in all cases, with sufficient time averaging, the Slatkin Exact test begins to suffer from increased Type I error, reporting an ever increasing fraction of samples as not derived from a neutral transmission process. The extreme situation is seen at very high rates of innovation, where nearly every test fails, at high levels of time averaging. These failures are caused by saturation of a finite sample with singleton traits, causing the sample to display too much evenness in frequency to have been the result of sampling from the Ewens Sampling Formula. But unrelated to this saturation effect, there is considerable failure in employing the Slatkin Exact test to detect neutrality. For example, at $\theta = 5.0$, at 100 times the mean trait lifetime, approximately 70% of all samples appear in the tail region of the distribution, compared to the expected 10%. Clearly, the Slatkin Exact test is not robust for long-duration assemblages.

Second, at low θ values, the test results show excessive Type I error, even without time averaging. There are several potential causes. It is possible that the WF-IA process had not reached quasi-stationarity by 750 time steps, when sampling began. This would mean that the effects of initial trait assignment might still be present and skewing the frequency distribution of traits. Second, the Slatkin test is sensitive to the number of rare or singleton traits given the sample size, and in a small population (2000 individuals) with a low innovation rate (e.g., $\theta = 0.1$), counts of rare traits could be unstable. This would not typically be the case in samples from large populations or entire species.

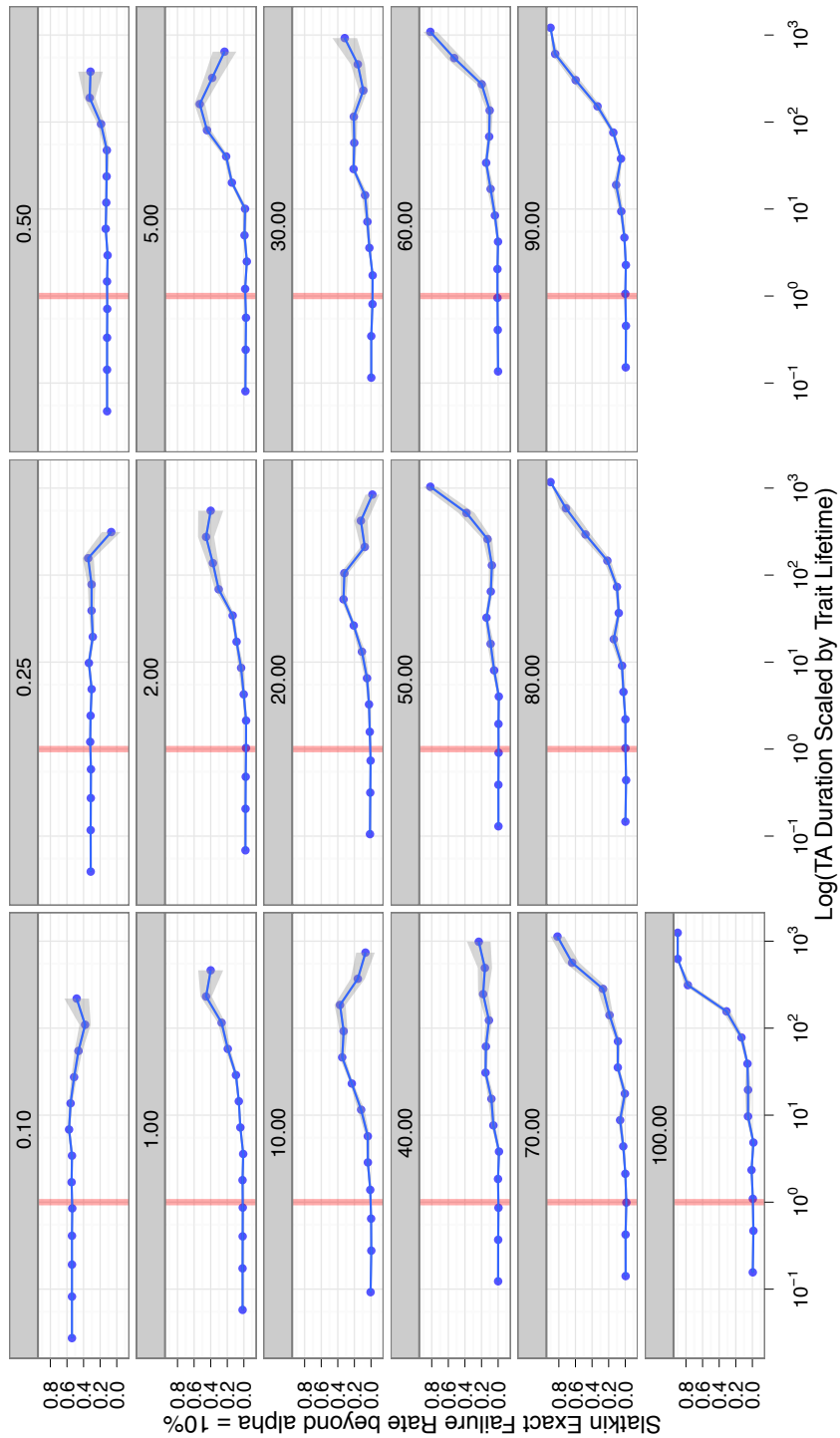


Figure 3.2: Slatkin Exact test failure rate (above the expected 10% given two-tailed test with $\alpha = 0.10$, plotted against time averaging duration scaled by mean trait lifetime, for each level of θ in the simulation study. The red vertical line indicates the mean trait lifetime for that θ value, and the shaded region encompasses the standard error of the estimates for mean failure rates at each duration.

I do not consider the cause of this anomaly further in this paper, but it warrants further simulation study.

In general, with long-duration assemblages, archaeologists should be careful interpreting the results of neutrality tests adopted from population genetics. The effect seen here can be summarized as: with significant time averaging, trait frequencies generated by unbiased cultural transmission can falsely appear to be non-neutral and thus driven by bias or selection (Type 1 error). The longer the duration of an assemblage with respect to the mean trait lifetime, the larger the probability of a Type 1 error. With sufficient duration, in fact, the probability of a Type 1 error becomes virtually certain, and the Slatkin Exact test loses any discriminatory power. In summary, if one were to employ Slatkin's test to examine the hypothesis of neutrality in long-duration archaeological deposits, one would overwhelmingly come away with the impression that most cultural transmission was biased, either towards conformity or a pro-novelty bias – regardless of the underlying process occurring during prehistory.

3.5.3 Theta Estimation and Innovation Rates

There would be considerable value in estimating the population-level innovation rate (θ) from sample data if it could be done accurately. As discussed in Section 3.3.2 above, such estimates are usually biased and have large variance. In this section, I examine the effects of time averaging upon theta estimates generated from the samples taken to perform neutrality tests in the previous section. For each of the 1.1 million samples of variants (distributed across actual theta values and assemblage durations), I calculated theta estimates given Watterson's approximation (Durrett, 2008):

$$\hat{\theta} \approx \frac{k_n}{\log n} \quad (3.11)$$

For each combination of actual theta and assemblage duration, theta estimates were averaged, to give a mean estimated theta value ($\mathbb{E}(\hat{\theta})$), and its standard deviation. The results are shown in Table 3.4. There are two regions of behavior apparent in the table, corresponding to drift- versus

innovation-dominated dynamics. At and below $\theta = 1.0$, estimated values are higher than the actual θ used to generate samples, and above 1.0, theta estimates begin to systematically lag below the actual theta value. Overestimation at $\theta \leq 1.0$ matches the simulation results by [Ewens \(1974\)](#), although the authors did not simulate innovation rates above 2.0 (a large value in most genetic situations). In addition to being biased, theta estimation appears to be even *approximately* accurate only within a narrow range of values around $\theta = 1.0$.

θ_0	$\mathbb{E}(\hat{\theta})$	$\sigma(\hat{\theta})$
0.10	0.36	0.21
0.25	0.50	0.26
0.50	0.76	0.33
1.00	1.17	0.42
2.00	1.85	0.51
5.00	3.49	0.67
10.00	5.23	0.87
20.00	7.93	0.95
30.00	9.70	0.99
40.00	10.99	0.99
50.00	12.19	1.00
60.00	12.94	1.01
70.00	13.76	0.97
80.00	14.32	0.98
90.00	14.85	0.94
100.00	15.27	0.95

Table 3.4: Mean Estimated Theta ($\mathbb{E}(\hat{\theta})$) from Samples ($n=100$) compared to actual values employed in simulation models (θ_0), without any time-averaging.

Figure 3.3 examines estimates of theta by time averaging duration scaled by the mean trait life-time, for each level of actual θ used in the simulation runs. The pattern evident in synchronic or unaveraged samples carries over to time averaged assemblages: below $\theta \leq 1.0$, theta estimates are larger than the actual values, and increase in a non-linear fashion with assemblage duration. Above 1.0 but below about 30.0, theta estimates begin below the actual value, cross the actual value, and continue to accumulate as assemblage duration increases. Finally, at the very highest innovation rates, in a sample size 100, theta estimates are always drastic underestimates of the actual value, even with

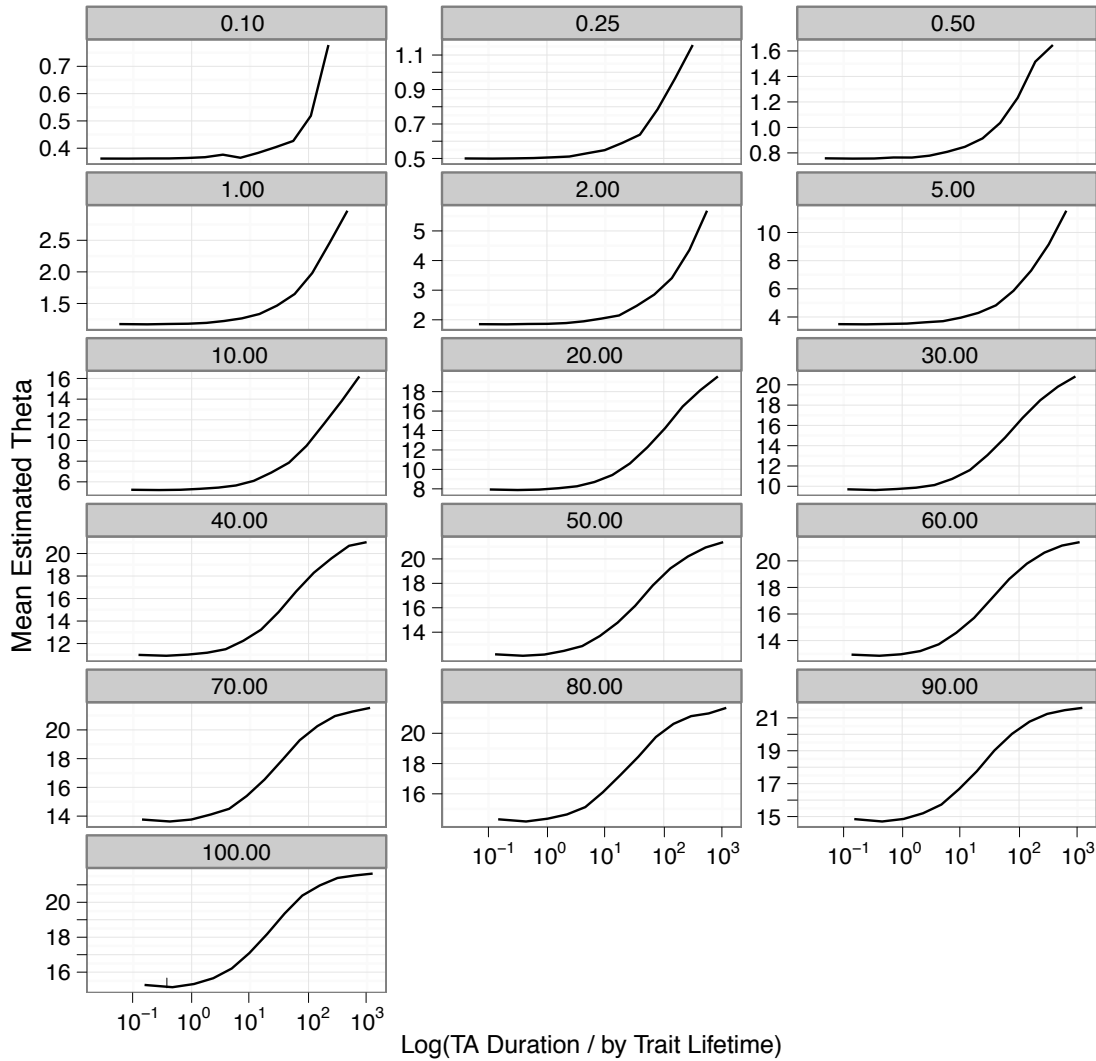


Figure 3.3: Estimates of mean population innovation rate ($\mathbb{E}(\hat{\theta})$) from samples ($n = 100$) taken for neutrality tests, using the approximation by [Watterson \(1975\)](#). Plotted against assemblage duration, for each level of actual innovation rate used in simulation runs.

long assemblage duration increasing the accumulation of traits.

The Slatkin Exact test software also provides an estimate of θ , finding the maximum likelihood value of theta when K_n is set in Equation 3.8 to equal the observed value (this is the t_e statistic introduced to archaeological usage in [Neiman, 1995](#)). Figure 3.4 depicts the Slatkin theta estimates by time averaging duration scaled by the mean trait lifetime, for each level of actual θ used in the

simulation runs. One interesting difference between Figure 3.3 and the Slatkin theta estimates is that the latter are more accurate for actual $\theta \geq 1.0$ than the Watterson approximation, in unaveraged assemblages. Unfortunately, with increased assemblage duration, estimates explode to much larger values than those calculated by the Watterson approximation (i.e., $\theta \approx 1500$ for true $\theta = 30$ at maximum assemblage duration of 1000 times the mean trait lifetime, compared to the *underestimate* of approximately 22 in Figure 3.3).

In short, estimation of population-level innovation rates from samples of artifacts using either estimation method are inaccurate, and the time averaging effect of accretional deposition renders such estimates even more inaccurate. Clearly, such values cannot be used as actual indications of innovation rate or to “work backward” towards past population sizes. And without fairly precise control over assemblage duration, the use of t_e as a relative diversity measure between assemblages (in the manner common to archaeological applications) is highly suspect. In the next section, I turn to t_f , the other common diversity measure in archaeological studies, which does not require an estimate of θ , employing instead the variant frequencies directly.

3.5.4 Diversity Measures

Much of the current effort in distinguishing biased and unbiased transmission models rely upon trait evenness and the shape of frequency distributions, given Alex Bentley’s application of power-law distributions to both ancient and contemporary data sets (Bentley and Shennan, 2003; Bentley et al., 2004; Bentley, 2007a,b; Bentley et al., 2009; Hahn and Bentley, 2003; Herzog et al., 2004). One of the ways that unbiased and “conformist” models of cultural transmission differ is in the expected amount of variation. Compared to unbiased transmission, conformism of even a mild degree tends to strongly concentrate adoption onto a very small number of traits (Mesoudi and Lycett, 2009).¹² It is difficult,

¹²This is especially the case when conformist transmission is implemented in simulations as a “global” rule where only the most common trait is copied during “conformist” copying events, rather than weighting all traits by their relative popularity. Very little work has been done to compare the results from different methods of simulating biased transmission models. This is a topic which would benefit greatly from additional research.

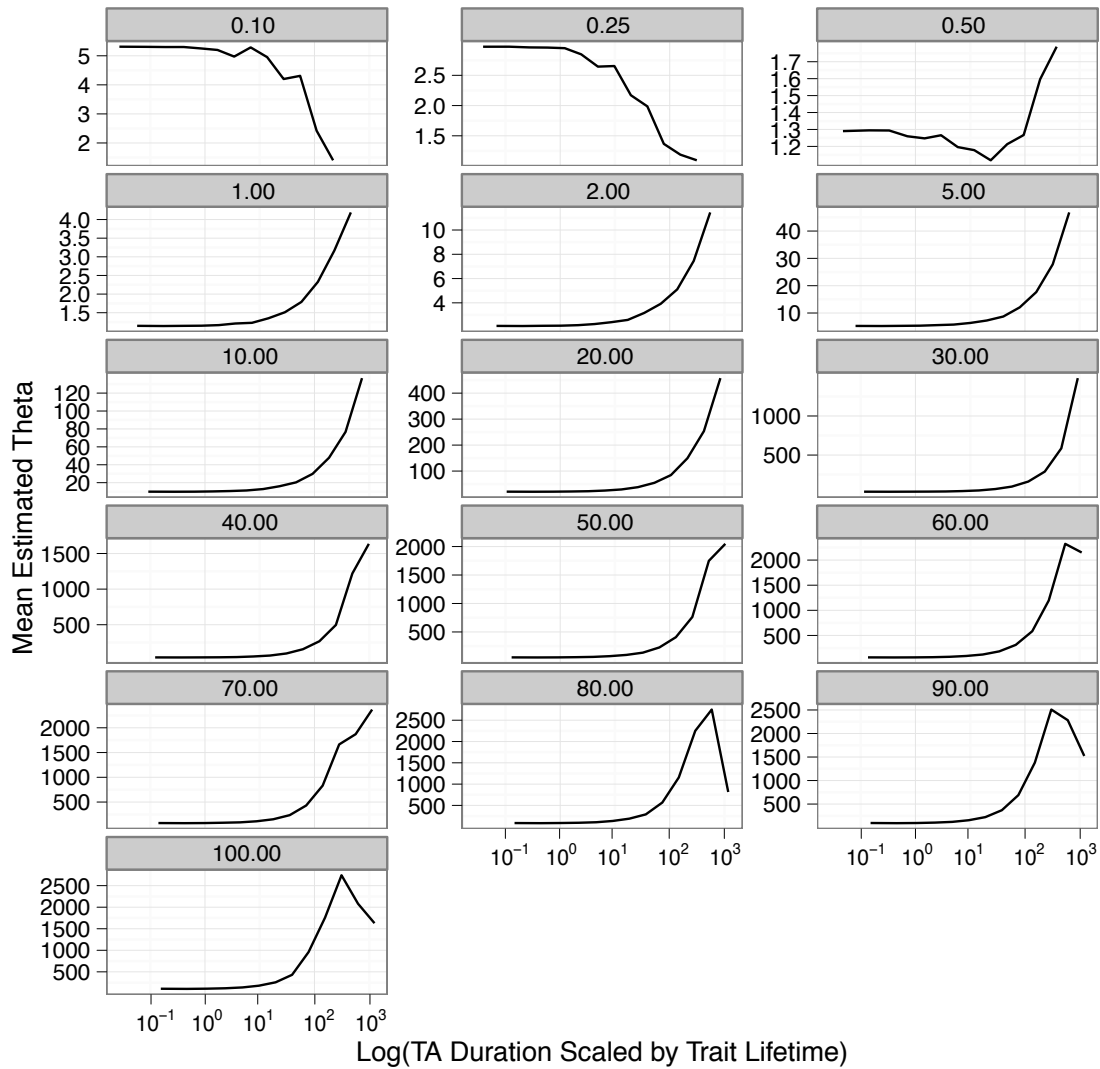


Figure 3.4: Estimates of mean population innovation rate ($\mathbb{E}(\hat{\theta})$) from samples ($n = 100$) taken for neutrality tests, using results from Montgomery Slatkin's neutrality test software. Plotted against assemblage duration, for each level of actual innovation rate used in simulation runs.

however, to interpret the absolute number of traits (K_n) without knowledge of the population size, so Kohler et al. (2004a) employed diversity measures instead in his classic examination of conformist transmission in Southwest pottery.

The most commonly used measure in the archaeological literature on cultural transmission is t_f (Equation 3.6), since it is related to Wright's original measures of heterozygosity and thus associated directly with the historical development of the Wright-Fisher model. But it is useful to normalize the results of t_f between 0 and 1 so that we can compare different levels of θ and assemblage durations easily, in the same way that statisticians occasionally employ coefficients of variation or normalize covariances into correlation coefficients. Equation 3.7 does exactly this, and is called the "index of qualitative variation" (IQV) (Wilcox, 1973).

Figure 3.5 displays the relationship between the IQV for samples of size 100, and time averaging duration scaled by mean trait lifetime, as before. IQV values range from 0.0, if only a single trait occurred within a sample (which happens in simulations with very low innovation rates), through 1.0, which indicates that traits are perfectly evenly distributed within a sample. Even at the highest innovation rate studied, values of 1.0 were not seen in *unaveraged* samples from the simulation runs. It is apparent that time averaging can yield greater evenness among trait frequencies, although the plateau in IQV values seen at high θ and high assemblage duration is a function of the saturation of K_n in a finite sample seen above. At very low innovation rates ($\theta \ll 1.0$), time averaging in contrast seems to have little effect on the dispersion of trait frequencies, with one or a very few traits always dominating a sample.

In between, when innovation rates are sufficient to guarantee at least one innovation on average per model generation ($\theta = 1.0$) but fewer than 10, there is non-monotonic behavior apparent in the IQV index. For example, at $\theta = 2.0$, time averaging has no effect on IQV until duration is 10 times the mean trait lifetime (\bar{t}), at which point assemblages begin to appear *less even* in frequency distribution, until about 100 times the mean trait lifetime, when evenness begins to steadily increase. This effect is interesting, since it suggests that we cannot easily compare diversity indices between assemblages

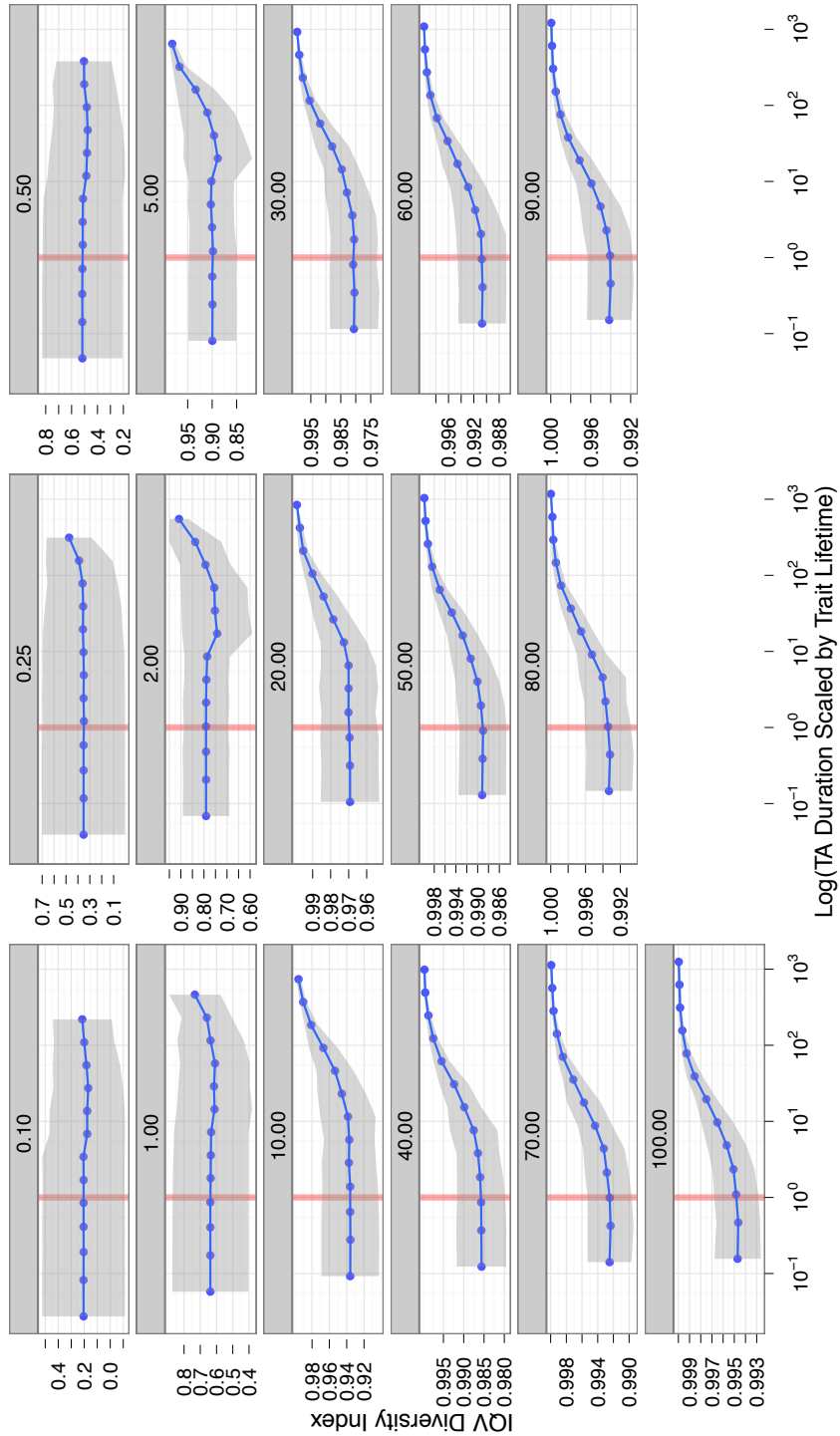


Figure 3.5: IQV diversity index, derived from samples of size 100, plotted against time averaging duration scaled by mean trait lifetime, for each level of θ in the simulation study. The red vertical line indicates the mean trait lifetime for that θ value.

unless we control for duration or have independent evidence concerning innovation rates.

3.6 Discussion and Conclusions

When we examine the effects of time averaging on the sample properties of unbiased transmission, using the mean lifetime of traits as our fundamental time scale, several lessons for practical applications emerge. First, it appears that assemblages with very small amounts of temporal aggregation display little of the distributional alterations that characterize long-duration assemblages. Statistical tests of neutrality and diversity measures, and thus arguments based on them, can probably be used with care. Second, estimates of population-level innovation rate derived from Ewens's sampling formula are biased (and therefore inaccurate), and become seriously inaccurate with increased assemblage duration. Archaeologists should strongly reconsider using t_e or other theta estimates even in relative comparisons, and should definitely not consider such estimates to reflect the innovation rate or population size present in the prehistoric population. Third, for assemblages that have a duration longer than the mean trait lifetime, it is important to measure and control for the relative duration of assemblages when comparing statistical results across samples. Without doing so, we cannot interpret relative differences of diversity indices or trait richness values as indicative of different modes of transmission.

One caveat to the above is that such effects refer specifically to *assemblage* level data, composed of many artifacts deposited over time. Artifact-scale analysis, where the attributes under analysis come together in a short period of time, and where single artifacts comprise the counting unit for transmission studies, will not necessarily suffer the quantitative effects described here, or would suffer no measurable time averaging effects if the assemblage durations were short compared to the lifetime of traits. A good example of this is Jonathan Scholnick's chapter in the present issue, expanding on his previous research into cultural transmission in Colonial America through gravestones ([Premo and Scholnick, 2011](#); [Scholnick, 2010](#)), where his samples cover 10 year periods based on the death dates

carved on each stone.

Furthermore, while the mean lifetime of transmitted information plays a central role in establishing a “natural” time scale over which time averaging affects unbiased transmission, this time scale is not an archaeological one. This discrepancy in time scales arises because the abstract “traits” of our models are not equivalent to the classification units employed by archaeologists. This is not a trivial difference, and is one that is rarely even discussed in archaeological applications of cultural transmission models. Instead, we frequently act as if “traits equal types,” despite occasional acknowledgement of the difference.

But we have no direct empirical access to the information prehistoric populations were learning, teaching, and imitating. We will never find “units of transmission” in any empirical sense for archaeological applications of cultural transmission models, and we have no warrant to equate our models of prehistoric information flow with the classes we use to observe it today. Long ago, [Osgood \(1951\)](#) recognized that when anthropologists study the ideas held within a social group under study, what is actually being studied are the ideas we *construct* about the ideas individuals in other cultures may have had. [Dunnell \(1971\)](#) systematized this distinction, pointing out that we always operate with analytic classes whose construction is done by archaeologists, for archaeological purposes. These classes serve as a “filter” by which we detect patterns in artifact assemblages, which reflect patterns in the information which flowed within past populations. There is no “natural” set of classes to employ in studying cultural transmission, but we often forget to incorporate this fact into our analyses. Linking the time scale over which variation entered and left a prehistoric population, and the time scale over which archaeological classes appear and then exit the archaeological record will involve further research on the relationship between transmission dynamics and complex, multi-dimensional archaeological classes. Such research is essential to connect the abstract quantities described by theoretical models, to observable aspects of the archaeological record.

These results paint a fairly gloomy picture of almost all of the standard variables archaeologists have used since Neiman’s ([1995](#)) pioneering work. One wonders why empirical studies using diver-

sity measures, innovation rate estimates, or neutrality tests appear to “work” and give sensible results? One possibility, of course, is that some studies don’t yield the expected results. We see this, possibly, in a fascinating analysis by [Steele et al. \(2010\)](#). The authors employed ceramic classes that appeared to be non-neutral and subject to selection or biased transmission. Yet Slatkin exact tests were unable to rule out the null hypothesis of neutrality. I do not present an analysis of conformist transmission under time averaging in this article, but using **TransmissionFramework** I see evidence that temporal aggregation has the opposite effect on Slatkin exact tests in populations with weak conformist biases: neutrality tests suffer increased Type II error, making it more likely that we will accept a null hypothesis of neutrality when the opposite is the case.

Another possibility is that certain variables may retain their distributional character, but have their values inflated by temporal aggregation. In such situations, there would be no reason to reject the neutral model, but inferences about the values of parameters would be inaccurate. Even if investigators did not rely upon the absolute value of parameters, frequently such inferences (e.g., diversity values) are employed as relative comparisons between assemblages. I suspect that this has occurred in a number of published studies, but few cultural transmission applications include detailed information concerning assemblage duration, so it is difficult to redo the researcher’s original hypothesis tests with temporal controls, without going back to original field information or reports. Clearly, both possibilities may also occur in some situations.

As archaeological usage of cultural transmission theory becomes more frequent and we move from proof-of-concept studies to demanding interpretive accuracy from our models, methodological research is essential to ensure that our applications are empirically and dynamically sufficient. The present study focused on a necessary first step in such method development, developing an understanding of the effect of time averaging in accretional assemblages upon the observable variables in neutral cultural transmission models. The results demonstrate that frequently employed statistics, such as t_e , are highly inaccurate and biased when measured in time averaged assemblages, and that neutrality tests are subject to enough additional Type I or Type II error that the results can be sys-

tematically misleading. Clearly, in order to apply cultural transmission models to diachronic data derived from time averaged assemblages, we need to develop observational tools and methods suited specifically to the archaeological record, instead of simply borrowing statistical methods and models from theoretical population biology.

3.7 Acknowledgements

This paper was originally presented in a symposium titled “*Recent Developments in Cultural Transmission Theory and its Applications*” at the 2012 Annual Meeting of the Society for American Archaeology, Memphis, TN. The author wishes to thank Kristen Safi, the organizer, for the opportunity to participate, and Carl P. Lipo, Fraser Neiman, James Feathers, Jonathan Scholnick, and Michael J. O’Brien for comments on drafts of this paper.

Can We Identify Transmission Bias in the Archaeological Record: An Investigation Using Boosted Classifier Models

ABSTRACT Lorem ipsum dolor sit amet, consectetur adipiscing elit. Ut purus elit, vestibulum ut, placerat ac, adipiscing vitae, felis. Curabitur dictum gravida mauris. Nam arcu libero, nonummy eget, consectetur id, vulputate a, magna. Donec vehicula augue eu neque. Pellentesque habitant morbi tristique senectus et netus et malesuada fames ac turpis egestas. Mauris ut leo. Cras viverra metus rhoncus sem. Nulla et lectus vestibulum urna fringilla ultrices. Phasellus eu tellus sit amet tortor gravida placerat. Integer sapien est, iaculis in, pretium quis, viverra ac, nunc. Praesent eget sem vel leo ultrices bibendum. Aenean faucibus. Morbi dolor nulla, malesuada eu, pulvinar at, mollis ac, nulla. Curabitur auctor semper nulla. Donec varius orci eget risus. Duis nibh mi, congue eu, accumsan eleifend, sagittis quis, diam. Duis eget orci sit amet orci dignissim rutrum.

SOURCE Posted to Arxiv.org (<https://arxiv.org/abs/TBD>), in July 2019.

4.1 Introduction

A major use of cultural transmission models in archaeology is inference regarding the mode of transmission operative within past populations. Identifying cognitive biases is central, for example, to several hypotheses for the origin of cumulative cultural transmission and complex culture [Boyd and Richerson \(1985a\)](#); [Cavalli-Sforza and Feldman \(1981a\)](#); [Henrich and Boyd \(1998\)](#); [Wakano and Aoki \(2007\)](#). In more recent archaeological contexts, the identification of frequency-biased social learning has been used to support inferences concerning sociopolitical structure in past societies [Kohler et al. \(2004b\)](#). Simulation and mathematical studies have yielded many insights into the empirical patterns we can expect from different transmission models [Bentley and Shennan \(2003\)](#); [Bentley et al. \(2007, 2004\)](#); [Evans and Giometto \(2011\)](#); [Mesoudi and Lycett \(2009\)](#), although much of this knowledge is derived from very simplified population models. In particular, theoretical analyses of transmission models have ignored until recently the effect of data collection methods and coarse-grained observations on the patterns we should expect in archaeological data. As a result, we simply do not know whether the mode of transmission can be reliably inferred from samples of the archaeological record, if it is possible at some time scales but not others, or how we might tailor data collection strategies to maximize the accuracy of such inferences.

We do know that the coarse graining of observable variables that occurs given time averaging reduces our ability to distinguish between unbiased and biased transmission models [Madsen \(2012a\)](#); [Porčić \(2014\)](#); [Premo \(2014a\)](#), that non stationary population sizes reduce our ability to infer transmission modes [Rorabaugh \(2014\)](#), and that diachronic statistics and non equilibrium models are better than synchronic measures and equilibrium models [Kandler and Shennan \(2013\)](#); [Wilder and Kandler \(2015\)](#). The effect of these factors is such that when deposits are highly time averaged, equifinality occurs, with different models yielding the same empirical distributions despite describing different underlying processes [von Bertalanffy \(1949\)](#). Equifinality between theoretical models is a serious concern whenever we study complex systems, and has been discussed in geomorphology, hy-

drology, climatology, and within archaeology itself [Aronica et al. \(1998\)](#); [Beven \(2006\)](#); [Bonham et al. \(2009\)](#); [Cicchetti and Rogosch \(1996\)](#); [Culling \(1987\)](#); [Marean et al. \(1992\)](#); [Rogers \(2000\)](#); [Savenije \(2001\)](#). If models which represent different modes of cultural transmission cannot be distinguished when we include aggregation, heterogeneity, or sampling in our models, then there may be questions concerning past cultural transmission that we cannot answer. As a result, there may be classes of models which are useful for contemporary or historical research, but not for the coarse grained scales of observation that archaeologists often confront.

Existing theoretical studies have almost exclusively focused upon distinguishing models based on the ability of a single statistic or variable to distinguish the distribution of outcomes from different social learning modes. Scores from the power law exponent in a log-log plot of trait frequencies have received the most attention along with more recent application of neutrality tests [Bentley and Shennan \(2003\)](#); [Bentley et al. \(2004\)](#); [Mesoudi and Lycett \(2009\)](#); [Slatkin \(1994, 1996\)](#). More recently, Kandler’s work has demonstrated that diachronic measures such as trait survival time, or the length of time the most common trait stays ranked the most common, can be robust predictors of different classes of transmission models [Kandler and Shennan \(2013\)](#); [Wilder and Kandler \(2015\)](#). But there is little reason to suspect that single statistics will be adequate in most cases to cleanly separate and identify different transmission models, given the strong convergence in distribution that characterize diffusion processes. Instead, we should expect that statistical models employing multiple predictors would be the best discrimination tools, if any exist for a set of transmission models. In this paper, I employ a robust machine learning classifier algorithm and multiple ways of measuring trait richness, diversity, and survival times to test whether equifinalities exist between various combinations of unbiased and biased transmission rules when measurements come from realistic data collection scenarios.¹

The results indicate that while neutral and biased transmission models can be distinguished very

¹Throughout this paper, I used “classification” in the statistical and machine-learning sense of a statistical model whose dependent variable is a binary or discrete value, such that the model predicts which value a data point takes from a labeled set. Archaeologists will be used to using the term in the sense of systematics and taxonomy, which is not the intent here.

accurately given measurements from entire populations taken when no temporal aggregation occurs, the introduction of sampling and the interaction between sampling and time averaging markedly degrades our ability to distinguish these transmission rules. Furthermore, the degradation is not symmetric. With sampled, time averaged data, we are extremely likely to conclude that samples represent biased transmission, even when this is not the case. Other mixtures of conformist and anti-conformist transmission rules are even less distinguishable given time averaging and limited samples. As a result, I conclude that it may be difficult or impossible to infer the details of cognitively biased transmission rules from frequency data alone, when we lack data from an entire population and when only coarse grained, aggregated data are available.

4.2 Analysis

4.2.1 Reducible and Irreducible Equifinality Among Transmission Models

Equifinality among cultural transmission models can arise from several sources. First, equifinality may occur because of our measurement and analysis procedures. There is growing evidence, for example, that assemblage duration affects our ability to distinguish biased from neutral transmission across a variety of statistical predictors [Madsen \(2012a\)](#); [Porčić \(2014\)](#); [Premo \(2014a\)](#). Equifinality among transmission models is thus possibly reducible by collecting finer-grained samples during fieldwork, if deposits are well stratified. However, in situations where the depositional environment actively creates temporal aggregation (e.g., in the plowzone, or in deflated aeolian contexts), there may be little that an investigator can do to improve the temporal resolution of data collection. And when we employ published data sets, obviously we cannot easily subdivide the data into assemblages finer than the original investigation supported. When studying living populations, of course, equifinalities may be addressed by converting a purely observational study to a controlled experiment in some cases [Kempe and Mesoudi \(2014\)](#); [Mesoudi \(2014\)](#); [Schillinger et al. \(2014\)](#), but of course this is not an option in archaeological contexts.

Figure 4.1: Simple example of the effect of variable choice in distinguishing models. The variable on the X axis displays quite a bit of overlap between models, while the variable on the Y axis distinguishes the models with fairly high accuracy.

Second, equifinality is partially determined by the predictors or variables we use in trying to separate the behavior of models. Fig. 4.1 shows an artificial example with two distributions, measured on two variables. The marginal distribution of each variable demonstrates how models might be distinguishable given one variable (Y axis) but not another (X axis). In the published literature on transmission modes, single variables are usually examined, but we gain huge power by considering statistical models with multiple variables.

Not all equifinalities may be reducible. The statistical distributions generated by diffusion processes can be highly convergent among related models, and almost all cultural transmission models are, at base, diffusion processes. This type of equifinality is **irreducible**, and is not solved by changing how we perform the analysis or by changing data collection. Irreducibly equifinal models form an **equivalence class** of models that we cannot distinguish given our data. Instead, all we can say is that our data could have been generated by any of the models in the equivalence class. If the equivalence classes of equifinal models are coarse enough (at worst, if they form a single group), then we cannot meet our original inferential goals at all.

In some cases, irreducible equifinalities can become reducible given advances in measurement technologies that open up new sets of predictor variables. After his seminal works of the 1970's on drift and the infinite-alleles neutral model, Warren Ewens stopped working on neutrality tests because tests using allele count data lack statistical power. Ewens moved to studying the population genetics of human diseases instead [Plutinski \(2004\)](#), recognizing that further progress would require sequence data unavailable at the time. This judgment proved accurate: a new suite of neutrality tests did arise starting the late 1980's and 1990's when sequence data became widely available [Fu and Li \(1993\)](#); [Tajima \(1989\)](#).

4.2.2 Equifinality As Classification Error

Since our evolutionary models of cultural transmission are stochastic, and generate a variety of outcomes for the same parameter values, I take a statistical approach to examining equifinality of transmission models in archaeological data. Transmission modes are separable and thus identifiable in archaeological data if the distribution of model outcomes are non-overlapping, when measured in a space created by a set of predictor variables. With stochastic models like the ones currently used by archaeologists, the most efficient method of studying the outcome distribution is to simulate values from the model, and examine our ability to correctly predict which model generated each data point, given a function of the predictor variables.

This general approach can be visualized as in Fig. 4.2. Here, three pairs of probability models are represented by 500 measurements each of two continuous predictors variables (e.g., a diversity index). In the left panel, the pair of models do not overlap in their outcomes. Given a data point, we can assign it to Model 1 or Model 2 with virtually no error, and thus we would consider models 1 and 2 to be distinct and not equifinal at all. The situation in the middle and right panels of Figure 4.1 is different. There is some overlap in the middle panel, and very strong overlap in the right panel. In the right hand panel, in fact, there is enough overlap that on average, our ability to assign a randomly chosen data point to the correct model is no better than chance. Intuitively, we would say that there is some equifinality in the middle panel, and that the two models were strongly equifinal in the right hand panel.

Figure 4.2: Simple example of model outcomes with different degrees of distinguishability: (A) simulated data point from two fully separate models, (B) two models with a limited overlap region, (C) and two models whose outcomes are highly overlapping.

We can formalize the analysis of overlap between models as a problem of “classification” or “pattern recognition” in the sense of statistical or machine learning [Hastie et al. \(2009\)](#). Given a set of models $\mathcal{M}_1 \dots \mathcal{M}_n$, we can measure equifinality as the minimum possible error achievable in cor-

rectly assigning simulated data points to the models which generated them, given measurement of a set of predictor variables. In general, the classification problem asks which model has the highest probability for a given data point, given the conditional density of the data and models. This sounds exactly like Bayes' theorem, and in fact we can write the classification problem as follows, where $Y \in 1, \dots, K$ refers to each of k models, and X_1, \dots, X_p refer to p different predictor variables.

$$\mathbb{P}(Y|X_1, \dots, X_p) = \frac{\mathbb{P}(Y_i)\mathbb{P}(X_1, \dots, X_p|Y)}{\mathbb{P}(X_1, \dots, X_p)} \quad (4.1)$$

$\mathbb{P}(Y)$ plays the role of the prior distribution, and is the prevalence of each model in the population. This is a constant in situations where we are simulating values from each model to test for equifinality. The data points in a classification problem are given, and thus the denominator is a constant. The most probable class for a given data point is just the mode of the likelihood function, which is given by:

$$Y_{\text{pred}} = \arg \max_y \mathbb{P}(X_1, \dots, X_p|Y) \quad (4.2)$$

This is the *Bayes classifier* for a controlled simulation experiment, and its error rate in separating data points by model is called the *Bayes error*. This is the lowest possible error in separating the models given the data [Devijver and Kittler \(1982\)](#); [Fukunaga \(1990\)](#); [Hastie et al. \(2009\)](#). The Bayes error is zero when we can correctly identify each data point as to its model of origin (as in the left panel of [Fig. 4.2](#), and rises as two models overlap in the measurement space. With sufficient overlap, the Bayes error could approach 0.5, which represents a prediction rule which is no better than chance.²

Unfortunately, we can almost never directly calculate the Bayes error rate for a prediction or classification rule, because we rarely have an expression for the likelihood function of our transmission models in the space formed by the predictor variables. Bayes error can be directly calculated, in fact,

²Predictors can achieve even worse error levels, performing more poorly than coin-flipping, but in the current study we will not encounter such rates.

only for a small number of cases, such as Gaussian distributions with a shared covariance matrix.³ Despite the fact that we can rarely calculate the Bayes error rate, it is useful as an operational definition for equifinality, since it measures our uncertainty about model choice given a set of measurable variables. In practice, we approximate the Bayes error by employing algorithms which are known to have near-optimal performance in classification problems. In particular, boosting, bagging, and ensemble approaches that combine many classifier rules are attractive since each achieves some of the best generalization error in prediction tests [Hastie et al. \(2009\)](#), and thus come closest to estimating the Bayes rate [Tumer and Ghosh \(2003\)](#).

4.2.3 Study Design

In order to assess whether transmission bias is identifiable from archaeological samples, this study simulates conformist, anticonformist, and unbiased cultural transmission over a range of innovation rates, recording the outcome of transmission events in the form of counts for individual traits, and for cross-tabulated “classes” of traits which simulate multi-dimensional archaeological types of the kind typically used by archaeologists. These samples of trait and class counts are then subjected to sampling and temporal aggregation, to simulate the kind of assemblage-level often confronted in archaeological samples. For both the raw trait/class counts, and the sampled and time averaged counts, I use a classifier approach with multiple predictor variables to assess the identifiability of transmission bias.

The general process followed throughout the study is:

- Simulate a large number of samples from each cultural transmission model, at a fixed popu-

³There is a large literature, especially in pattern recognition and language classification, on approximating upper bounds for the Bayes error of a classifier, because it is highly useful to know when you cannot improve a recognition system or classifier any further [Antos et al. \(1999\)](#); [Dobbin \(2009\)](#); [McLachlan \(1975\)](#). Most such upper bounds are based upon parametric models, and use estimates of a distance metric between the classes being distinguished (typically, the Mahalanobis or Bhattacharyya distance) [Devijver and Kittler \(1982\)](#). Such bounds are difficult to justify in situations where we have complex social learning models, whose probability density functions in the space of measured variables are typically unknown and are unlikely to be Gaussian. Non parametric bounds are possible, using nearest-neighbor methods [Loizou and Maybank \(1987\)](#), but in most cases the values obtained are not very tight and the performance of boosting and bagged classifiers easily surpasses such methods.

lation size, but with an innovation rate drawn from a uniform distribution of possible values.

Record trait and class counts during sampling intervals and at the end of each simulation run.

- Measure a set of archaeologically relevant variables (e.g., richness, diversity) on each stored sample.
- Perform each variable measurement across different data collection regimes (e.g., duration of accumulation, sample size).
- Train a predictive classifier model for each data collection regime, to predict the model of origin given the measured variables.
- Assess the classifier error rate using additional samples simulated from each transmission model.

4.2.4 Methods

4.2.4.1 Simulated Samples of Cultural Transmission Models

The outcomes of all four transmission models are derived by simulating the dynamics of the model in an agent-based framework that allows each agent to be assigned a different transmission rule. All simulations employ the Moran dynamics, where one individual engages in a copying event at each elemental step Moran (1962, 1958); Aoki et al. (2011). Innovations are modeled using the “infinite alleles” approximation, where every innovation is new to the population Ewens (2004). Simulations were performed using the CTMixtures software package, available as open source software.⁴ The parameters for all simulation runs are given in Table 4.1. Where there is a range given (e.g., innovation rate), the parameter is treated as a prior distribution and each simulation run is assigned a uniform random value from the range. This ensures good coverage of the parameter space given 25,000 replicates for each of the 4 models.⁵

⁴<https://github.com/mmadsen/ctmixtures>

⁵The use of a good prior distribution for parameter ranges also results in simulation data that are usable for later data fitting by approximate Bayesian inference ?Crema et al. (2014); Csilléry et al. (2010); Marin et al. (2012).

Parameter	Value or Interval
Innovation rate (in θ scaled units)	[0.1, 5.0]
Probability of conformism	[0.05, 0.25]
Probability of anti-conformism	[0.05, 0.25]
Sample fractions	0.1 and 0.2
Time averaging intervals (units of 100 individuals)	10, 20, 50, 100
Population size	100
Number of trait dimensions (loci)	4
Initial traits per dimension	10

Table 4.1: Parameters for simulation runs across the four models studied. Intervals are treated as prior distributions, and each simulation run is assigned values derived from a uniform random sample on the interval indicated. Lists of values are all applied to every simulation run (e.g., there is both a 10% and a 20% sample from each simulation run. Single values are applied to every simulation run, and represent a point prior.)

Simulated populations are 100 individuals in size, because most archaeological studies of cultural transmission have focused upon situations where population sizes are assumed to be small. Each simulated individual carries 4 different traits at any time, which are treated as separate loci or dimensions. Trait frequencies are tracked on a per-locus basis, and combinations of loci are tracked in order to simulate archaeological “types” or classes which include multiple dimensions of variation.

Regardless of transmission model, social learning involves no interaction effects between loci in this study. The population is seeded with 10 randomly chosen traits at each locus as a starting configuration. The evolution of each simulated population proceeds for 4 million elemental steps, which is equivalent to about 40,000 copying events on average per individual. This value was chosen by performing simulations at 1 million time step intervals and verifying that the distribution of a key statistic (the number of traits per Loci) had stabilized. This occurred in most cases between 2 and 3 million steps, and in all cases between 3 and 4 million, so the last value was chosen.⁶ At the end of 4 million simulation steps, a suite of variables are measured from each of the 25,000 replicates and stored for analysis.

⁶The analysis underpinning this decision is available in the Github repository at <https://github.com/mmadsen/experiment-ctmixtures/analysis/verification>.

4.2.4.2 Variable Selection

Since most previous work on identifying transmission mode from archaeological data employ single diagnostic variables, and begin to display equifinality under realistic data collection conditions, it is reasonable to examine whether using multiple variables will yield more discriminatory power in the same contexts. By representing the outcomes of transmission models in a higher dimensional space, it should be easier to find a decision boundary (“separating hyperplane”) that correctly predicts the model which generated each data point, if such a boundary exists.

Variable	Model Variable
Cross-Tabulated Class Richness (Class)	num_trait_configurations
Slatkin Exact (Class)	configuration_slatkin
Shannon Entropy (Class)	config_entropy
IQV Diversity (Class)	config_iqv
Neiman T_f (Class)	config_neiman_tf
Slatkin Exact (Max for Locus)	slatkin_locus_max
Slatkin Exact (Min for Locus)	slatkin_locus_min
Slatkin Exact (Mean for Locus)	slatkin_locus_mean
Shannon Entropy of Trait Frequencies (Min)	entropy_locus_max
Shannon Entropy of Trait Frequencies (Max)	entropy_locus_min
Shannon Entropy of Trait Frequencies (Mean)	entropy_locus_mean
IQV Diversity Index (Min)	iqv_locus_max
IQV Diversity Index (Max)	iqv_locus_min
IQV Diversity Index (Mean)	iqv_locus_mean
Trait Richness (Min)	richness_locus_max
Trait Richness (Max)	richness_locus_min
Trait Richness (Mean)	richness_locus_mean
Kandler-Shennan Trait Survival (Min)	kandler_locus_max
Kandler-Shennan Trait Survival (Max)	kandler_locus_min
Kandler-Shennan Trait Survival (Mean)	kandler_locus_mean
Neiman T_f (Min)	neiman_tf_locus_max
Neiman T_f (Max)	neiman_tf_locus_min
Neiman T_f (Mean)	neiman_tf_locus_mean

Table 4.2: Variables measured from each transmission model simulation sample. The parenthetical expression records whether the variable was calculated for cross-tabulations of all 4 loci (Class) or represent the order statistics from individual loci (Min/Mean/Max). The right column records the variable name used within R statistical models, for examining the relative importance of each variable in classifying observations.

The predictor variables chosen in this study focus upon measures of richness and diversity, trait survival over time [Kandler and Shennan \(2013\)](#), and the Slatkin neutrality test [Slatkin \(1996, 1994\)](#). Each has been employed in the archaeological literature on identifying cultural transmission modes, or is a variant on such measures (e.g., IQV is a normalized version of Shannon entropy), and crucially, all are measurable in standard archaeological contexts using type frequency data. This additionally makes most of the variables applicable to the re-analysis of already published data, which is an important usage scenario in archaeological research.

For the locus-centric variables, each statistic was applied to each locus separately, and the mean, minimum, and maximum of the values obtained for each locus were recorded. I collect order statistics in addition to the mean value, since it is possible that minima and maxima might be a better discriminator between models than averages. In addition to the variables calculated upon each of the 4 loci, the traits at each locus were combined into a cross-tabulation of "classes" which simulates the process of archaeological classification. Each class represents a different combination of traits from the 4 loci, and very roughly simulates observing cultural variation through the lens of a standard paradigmatic classification [Dunnell \(1971\)](#). The same variables are then measured as a function of the class counts.⁷ This allows us to understand whether transmission models are better distinguished on a per-locus (dimension) basis or by operating on more complex classes that combine several traits together. The full list of measured variables is given in Table [4.2](#).

As a final note on variable selection, in an exploratory analysis for this project, I tried to include the power law exponent from a log-log transformation of trait frequency, given the important work by Bentley [Bentley et al. \(2004\)](#) and Mesoudi and Lycett [Mesoudi and Lycett \(2009\)](#). It is not clear, however, that previous uses of this variable have been comparable to measurements we can make on archaeological assemblages. As an example, Mesoudi and Lycett [Mesoudi and Lycett \(2009\)](#) use the cumulative number of adoptions of each trait over the entire time span of the simulation as the

⁷The sole exception is the Kandler-Shennan survival time, which is not measured here for the cross-tabulated classes. Understanding the quantitative behavior of this measure for multidimensional classes of traits is an important open research question, however.

“frequency” used to calculate power law exponents.⁸ Given the measurement strategies described in Table 4.3, the number of traits present at any given time is often small, and their prevalence in a small population makes it difficult to fit a power law to the data. Despite its importance in archaeological discussions of neutral versus biased transmission, I have omitted power law exponents from the published analysis, pending investigation of the proper method for calculating them in situations with small N and small numbers of trait categories.

4.2.4.3 Data Collection Treatments

At the end of each simulation run, after the model has reached a quasi-stable equilibrium (measured as stability in per-locus trait richness), a series of samples are taken from the evolving population. These samples are taken in ways that correspond to various real-world data collection strategies. First, a census of the entire population is taken. This functions as a baseline for the “most complete” information we can use to identify transmission modes, and there are also conditions during observational studies or in laboratory experiments where census is possible. In archaeological studies, anything approximating a census is usually impossible, although Jonathan Scholnick’s study of New England gravestones and their makers may approximate this quality of data collection [Scholnick \(2012\)](#). Second, the simulated population is sampled, at the 10% and 20% levels. Sampled data is ubiquitous in archaeological research, and although the issues involved in mapping artifact samples to their meaning for the underlying population of social learners is complex and unresolved, it is useful to determine whether the overall sample fraction has a measurable effect upon model equifinality.

Archaeological data are rarely synchronic or “point in time” samples of the results of human activity, and are typically aggregated over an appreciable duration of time through both data recovery conventions and formation processes [Grayson and Delpech \(1998\)](#); [Lyman \(2003\)](#); [Madsen \(2012a\)](#); [Porčić \(2014\)](#); [Premo \(2014a\)](#). Thus, the sampled data employed in this study is also temporally ag-

⁸I confirmed this by inspection of the source code for their simulation model, which was provided by Alex Mesoudi.

gregated over a number of time steps, and the aggregate trait counts and then used to determine the frequencies of cultural traits over the entire interval. The population census has no temporal aggregation, and thus does represent a synchronic census.

Time averaging is implemented according to the schematic in Fig. 4.3. At the end of the simulation run, sampling begins at a time index calculated to allow time averaged samples to be taken twice, with a gap of 50 “generations” to allow the calculation of the Kandler-Shennan trait survival statistic (although unlike their original study, the values at the start and end times are inherently time averaged in this study, which would be the base in any real archaeological context) [Kandler and Shennan \(2013\)](#).⁹

Figure 4.3: Schematic of how sampling is implemented in this study. Time runs from the start of the simulation run at the top, to the end at the bottom. The interval of time over which we calculate the Kandler-Shennan trait survival is given as a simulation parameter, and represents the gap in the middle of the diagram. Before and after that gap are windows of successive duration, representing aggregation over 10, 25, 50, and 100 “generations” of the simulation.

Sampling Strategy	Time Averaging Duration
Population Census	0
10% Sample	10
10% Sample	25
10% Sample	50
10% Sample	100
20% Sample	10
20% Sample	25
20% Sample	50
20% Sample	100

Table 4.3: Data collection strategies, applied to every simulation run. Time averaging duration is given in units of “generations,” which are units of 100 time steps (given the population size). 100 generations thus represents 10,000 elemental time steps in the Moran simulation dynamics.

The data collection strategies employed in this study are given in Table 4.3. Applied to all 23

⁹The effect of time averaging on the start and end values used to calculate the Kandler-Shennan trait survival is not directly studied in this paper, but is a necessary component of using their method to study archaeological assemblages, I believe.

variables, the study yielded approximately 900,000 samples from the four transmission models.¹⁰ This raw data was then formed into the three pairwise comparisons shown in Table ?? for equifinality analysis with a classifier model.

4.2.4.4 Classifier Selection and Training

Classifier algorithms are supervising learning models from statistics and machine learning that predict a categorical response from a mixture of discrete or continuous variables [Hastie et al. \(2009\)](#). The most familiar classifiers in archaeological practice are logistic regression and discriminant function analysis, but neither is competitive with contemporary “ensemble” methods which combine many classifier rules into a single prediction. In such models, combining predictors can both reduce the variance of prediction (e.g., bagging added to traditional classifiers and random forests), and reduce bias. Some classifiers, like boosted trees, can do both.

Since the Bayes error rate of comparing two complex transmission models is not something we can calculate or even estimate, we must approximate it using the best performing classifier model available. A very general result in statistical decision theory (called, appropriately, the “No Free Lunch” theorems) guarantee that there is no single prediction model that can achieve the best result with every data set and problem [Wolpert \(2002\)](#); [Wolpert and Macready \(1997\)](#). Thus, I took a compromise approach, selecting several algorithms that are known to have excellent performance across a range of data sets, and then performing a pilot study using the four transmission models previously described. A recent study compared 179 classifier algorithms on 121 different data sets (representing the entire UC Irvine Machine Learning Database), and found that random forests [Breiman \(2001\)](#), support vector machines, and gradient boosted classifiers performed the best [Hastie et al. \(2009\)](#). Additionally, some ensemble methods (random forests and gradient boosted classifiers) provide information on variable importance as an integral part of the algorithm. Since understanding which of

¹⁰All data and analyses for this study are available as part of a Github repository, although large data files are kept on Amazon S3 for long-term storage. See <https://github.com/mmadsen/experiment-ctmixtures> for details. The published analysis described here is the “equifinality-4” data set.

our 23 variables are useful for separating transmission models is an important aspect of this study, I evaluated random forests against gradient boosted classification trees using small simulated samples from each transmission model.¹¹ Gradient boosted models outperformed random forests on these simulated data, are comparable in computational costs, and are used for all further results in this paper.

Gradient boosted classification operates by repeatedly fitting a set of decision trees to the data [Alexey Natekin \(2013\)](#); [Hastie et al. \(2009\)](#). In each round, decision trees are fit to the training data, and individual data points scored as errors or successful predictions. Subsequent trees are fitted by modifying the trees in the direction that minimizes the residual error. This is equivalent to finding the gradient of the loss function in the space of possible classifier functions, hence the name of the method. The impact of each gradient step is smoothed by including a “shrinkage” factor. Finally, the gradient steps are “boosted” to weight data points by the success in prediction, such that data points that are frequently misclassified become targeted by the algorithm until they can be correctly predicted [Freund \(1995\)](#); [Freund et al. \(1999\)](#); [Schapire and Freund \(2012\)](#). After a specified number of iterations, the class or label membership of each data point is obtained by having each gradient step classifier tree “vote” for class membership, and the final answer is the majority vote. This class of models can also be visualized as repeated refitting of residuals until error is minimized [Friedman \(2001\)](#). This combination of boosting and iterative function search is very powerful, and gradient boosted models regularly achieve top accuracy in benchmark studies.

In this study, I employ the R package (**gbm**) for gradient boosted classification [Ridgeway \(1999\)](#), with the binomial deviance $\log(1 + \exp(-2y\hat{y}))$ as our loss function, where y is the true model for a data point, and \hat{y} is the classifier model’s prediction. Binomial deviance approximates the “zero-one” loss function with one which is differentiable, which is needed for a gradient descent method. The tuning parameters for this study (number of boosting iterations, depth of classification trees) were selected using 5 rounds of repeated 10-fold cross-validation on the training data [Kim \(2009\)](#); [Kuhn](#)

¹¹The data for this initial comparison are available in the <https://github.com/mmadsen/experiment-ctmixtures> repository under the experiment name “equifinality-2”.

and Johnson (2013).

The full data set is split into two chunks. 80% of the data are used to train the classifier model, and 20% are held back to provide an unbiased evaluation of classifier performance. For each comparison of models reported here, the training data are thus fitted 50 times across different values of the tuning parameters (number of boosting iterations, and depth of decision trees), and the best performing parameters chosen from the repeated cross-validation sets. The final model is then constructed using the entire training set and the optimal parameter values. All classifier tuning, final model fitting, and test error evaluation was performed using Max Kuhn’s superb `caret` package for R Kuhn (2008); Kuhn and Johnson (2013).

Predicted	Actual Model:	
	Model 1	Model 2
Model 1	9000	2500
Model 2	1000	7500

Table 4.4: Example confusion matrix. Columns correspond to the actual model for data points, rows correspond to predictions from a classification model. Bold numbers on the diagonal correspond to correct predictions, the off diagonal elements correspond to classification errors.

4.2.4.5 Classification Error and Equifinality Assessment

The basic data for assessing the quality of a classifier model is the *confusion matrix*, which compares classification successes and errors for a data set. A hypothetical example is given in Table 4.4. The most basic measure of classification quality is the *accuracy*, or the ratio of correct predictions to the total number of data points. In the confusion matrix, this is the ratio of the sum of diagonal elements to the sum of off-diagonal elements. In the example given in Table 4.4, the classifier is 82.5% accurate. We often also use the misclassification rate, which is simply $1 - \text{accuracy}$.

When the classes being predicted are not balanced, and especially if there are a small number of one class compared to another, a better statistic is Cohen’s “kappa” Kuhn and Johnson (2013), which compares observed accuracy to what one would expect purely from chance, given the marginal totals:

$$\kappa = \frac{O - E}{1 - E} \quad (4.3)$$

where O is the observed accuracy, and E is the expected accuracy due to chance given the ratio of classes in the marginal totals of the confusion matrix. Kappa ranges from -1 to $+1$, with 0 indicating no agreement between predictions and the real class memberships. High values indicate good agreement, while values below 0.5 and especially less than 0.2 indicate very poor predictive ability [Altman \(1991\)](#). In the present context, a classifier comparison (for example, biased versus neutral models with no sampling or time averaging) that yield a high kappa value are strong evidence that no equifinality exists between the two situations, since the classifier is highly accurate. Low kappa values are evidence that despite strong statistical methods and many variables to choose from, we cannot distinguish between models, and thus the models may be equifinal.

In studies where one outcome or class represents the presence of something (e.g., a positive test for a disease marker) and the other the absence, we may look at the individual cells of the confusion matrix rather than the bulk accuracy. The “false positive rate” (FPR), for example, is the number of cases which are not members of the “positive” class, but which the classifier falsely identifies as such (in the example shown here, if Model 1 is the positive class, the cell in the upper right corner of the matrix is the FPR. A number of other statistics build from FPR and the false negative rate to handle asymmetric experiments. In the present study, we are interested simply in the misclassification rate, or bulk accuracy, of predicting the correct model. Throughout these results, I use the misclassification rate and Cohen’s kappa values exclusively.

4.3 Results

In the next three sections, I review the results of applying the gradient boosted classifier to the three pairwise comparisons described in Table ??.

4.3.1 Unbiased Versus Biased Cultural Transmission

In the first comparison, all data points generated by unbiased (neutral) cultural transmission form one class, and the data points generated by each of the 3 biased models. As a reminder, the latter are:

1. Mixture of equal numbers of conformists and anti-conformists.
2. A mixture dominated by conformists, but with 30% anti-conformists.
3. A mixture dominated by anti-conformists, but with 30% anti-conformists.

This comparison examines the question of whether multiple predictor variables give us the power to discriminate between unbiased and any mixture of biased transmission, across different data collection regimes. For this comparison, classifier models were also developed for all of the predictor variables, and just for the per-locus variables, to determine the effect of using multidimensional classes that mimic archaeological classification, as opposed to simply examining single dimensions of variation (which has been the most common practice in archaeological studies to date).

The results are summarized in Fig. 4.4 as Cohen's kappa values across the different predictor variable sets and data collection regimes. It is immediately apparent that multiple variables in our classifier model gives us great power in distinguishing biased from unbiased transmission, in the case where we have population census data which is not subject to temporal aggregation. The use of multidimensional classes *in addition* to per-locus variables offers a tiny increase in accuracy, but these two comparisons are otherwise equivalent and display no equifinality given 97% accuracy in predicting biased versus unbiased transmission in the hold-out test set.

Figure 4.4: Cohen's kappa for correctly predicting whether simulated data points originate from unbiased copying or any of 3 other biased transmission models. High values of kappa correspond to high accuracy in correctly distinguishing between transmission models, while values well below 0.5 indicate great difficulty and low classifier accuracy. Each line in the dotchart represents a different data collection treatment, and overall the results indicate that significant equifinality exists except when time averaging is absent and a population census (or near equivalent) is available.

Accuracy rapidly declines, however, when data points are derived from samples of the evolving population and where time averaging is present. As one might expect, larger samples offer more accurate predictions than smaller samples. Within the larger, 20% sample, when cross-tabulated class and per-locus predictors are included, accuracy is highest with the smallest amount of time averaging (10 generations), and decreases as time averaging increases. When we remove cross-tabulated class predictors, and simply look at per-locus variables, this clean pattern is not apparent, and accuracy is not a function of time averaging duration. Furthermore, for the smaller 10% sample with all variables included, accuracy is not a function of time averaging duration. In these cases, Cohen's kappa values are close to 0.25, indicative of a very poor classification model whose output bears little relation to the underlying transmission models. Finally, pooling all sample sizes and time averaging durations simply yields the average performance of the sampled and aggregated models, as one might expect.

Importance	Predictor Variable
100.00	Cross-Tabulated Class Richness
50.71	Slatkin Exact for Classes
29.50	Shannon Entropy (Mean for Locus)
23.13	Shannon Entropy for Classes
19.66	IQV Diversity (Mean for Locus)
11.58	Kandler-Shennan Trait Survival (Mean for Locus)

Table 4.5: Relative importance of predictor variables for population census data, in the comparison between unbiased transmission and all biased models. The most important variable is (by convention) scaled to 100, and the values indicate the ratio of variable importance to the variable which is most effective at classifying data points. Only values greater than 10 are shown. The remainder of the predictor variables are 1/100th as effective as class richness or less.

Gradient boosting algorithms allow measurement of how much each predictor variable contributes the classification model. The importance of a variable is assessed over the iterations of tree construction by estimating the relative improvement in training set misclassification error from adding the variable to the model. The importance values are usually scaled such that the most important variable has a score of 100, and variables with smaller importance values are less important to classification power. Table 4.5 gives the relative importance of predictor variables for the compar-

ison between biased and unbiased models using population census data, and we can see that most of the classification power comes from the richness of cross-tabulated classes, about half as much from the Slatkin Exact test for cross-tabulated classes, and then an entropy measure of diversity among traits and classes. This is followed by a normalized version of the Shannon entropy, and finally by the Kandler-Shennan survival time, averaged across the 4 loci.

4.3.2 Unbiased Versus Balanced Conformist/Anti conformist Bias

The second comparison pairs unbiased transmission with a model the simulated population is composed of an equal number of conformists and anti-conformists. The probabilities of biased copying events are simulation parameters and are chosen uniformly from the prior distribution given in Table 4.1. This comparison examines the question of whether mixtures of biases can cancel each other out and appear to be unbiased, previously raised by Mesoudi and Lycett [Mesoudi and Lycett \(2009\)](#) and others. I believe this to be a likely scenario, and the likelihood that such mixtures would be indistinguishable from unbiased or neutral transmission when sampled, time averaged, or observed at larger regional scales was the original impetus for this study. The comparison was performed in the same manner as the first, except that the minor differences between using all predictors and only per-locus variables in the first comparison led to dropping separate comparisons given the computational cost of doing so. In this and the third comparison, all results refer to the full suite of 23 variables, across the same set of data collection regimes.

Figure 4.5: Cohen's kappa for correctly predicting whether simulated data points originate from unbiased copying or a balanced mixture of pro- and anti-conformist individuals. Each line in the dotchart represents a different data collection treatment, and overall the results indicate that significant equifinality exists except when time averaging is absent and a population census (or near equivalent) is available.

Fig. 4.5 displays the results of comparing “balanced biases” against unbiased transmission. We can see again that excellent separation is achieved with population census data, but with all of the

sampled and time averaged data collection strategies, there is considerable difficulty in correctly predicting the model from which a data point originated. With larger sample sizes, of course, there is less equifinality than with the smaller 10% but in both cases Cohen's kappa is 0.5 or less, indicating substantial equifinality though not complete overlap in the model outcomes.

Importance	full_variable
100.00	Cross-Tabulated Class Richness
85.49	Slatkin Exact for Classes
47.12	Shannon Entropy (Mean for Locus)
24.12	Kandler-Shennan Trait Survival (Mean for Locus)
18.88	IQV Diversity (Mean for Locus)
10.85	Shannon Entropy for Classes

Table 4.6: Relative importance of predictor variables for population census data, in the comparison between unbiased transmission and a balanced mixture of pro- and anti-conformists. The most important variable is (by convention) scaled to 100, and the values indicate the ratio of variable importance to the variable which is most effective at classifying data points. Only values greater than 10 are shown. The remainder of the predictor variables are 1/100th as effective as class richness or less.

The same predictor variables are responsible for almost all of the classification power, but there are subtle differences. Slatkin's "exact" test has more relative importance for this comparison than in differentiating between unbiased and all biases, and the entropy measures of diversity also have higher importance. This suggests that subtle differences in the evenness of classes and individual loci are very important in determining whether a population is truly engaged in unbiased transmission, or whether transmission biases are simply "canceling out" at the macroscopic scale. Unfortunately, it appears that working with small samples of the population in the presence of time averaging strongly compromises our ability to differentiate those scenarios.

4.3.3 Conformist Dominated Versus Anti conformist Dominated Populations

The final comparison pairs two simulated populations, one of which is dominated by 70% conformists, with 30% anti-conformists, and the opposite with 70% anti-conformists and 30% conformists. In previous efforts to model the statistic signatures of conformism and anti-conformism, several au-

thors have argued that there are clear patterns which separate these two modes of transmission (especially see Mesoudi and Lycett [Mesoudi and Lycett \(2009\)](#)). My own view is that these modes of transmission are much harder to detect in heterogeneous populations. This comparison is meant to test a simplified version of this conjecture. In this analysis, the number of conformists and anti-conformists is fixed by each of the models to the ratios given above, but the probability of a biased copying event is set for each simulation run to randomly chosen values drawn from the prior distribution given in [Table 4.1](#).

Figure 4.6: Cohen's kappa for correctly predicting whether simulated data points originate from a conformist-dominated mixed population versus a mixed population dominated by anti-conformists. Each line in the dotchart represents a different data collection treatment, and overall the results indicate that strong equifinality exists regardless of the data collection treatment.

Fig. [4.6](#) displays the result of this comparison across data collection treatments. None of the results indicate an ability to cleanly separate these two models. Population census data and the absence of time averaging certainly help, but the accuracy of classification is dismal in all cases. Strong equifinality exists between these models, as one might expect given their similarity. It is possible that with even stronger propensities to engage in conformity or its opposite, that we may be able to detect it in a heterogeneous population, but at the levels probed here, the models are indistinguishable, even in the high-dimensional space created by all 23 predictor variables.

4.4 Discussion

The classifier models used in this study provide a sensitive probe into the issue of equifinality between models of cultural transmission modes. Using both accuracy measures and measures of variable importance, this work highlights the variables we need to use in order to reliably distinguish between modes of transmission, given particular data collection conditions, in population models that are more realistic than those previously used.

This study seems to substantiate previous claims that time averaged data make the task of identifying the mode of transmission difficult. I propose to extend those claims by noting that small sample sizes dramatically worsen our ability to separate models, and to note that distinguishing *among* detailed models of transmission bias given frequency data alone (on individual dimensions/loci and multidimensional classes) appears to be impossible without new predictor variables. A better understanding how we can best calculate and use the power law exponent for trait or class diversity may help. To date I believe there are inconsistent ways in which the statistic has been applied to simulated data, some of which seem incompatible with the measurements we can make on archaeological assemblages.

But simple equifinality is not the whole story. It is not simply the case that sampling and time averaging render our predictions of transmission mode random with respect to the set of models tested. There is substantial bias (in the statistical sense) in the classifier models for sampled and time averaged data collection regimes. We can see this by looking at individual confusion matrices from predictions made on the hold-out test data.

Table 4.7: Two confusion matrices arising from the first model comparison, between unbiased and all biased models.

(a) Population Census Data			(b) Sample Size: 20 Duration: 50		
	biased	neutral		biased	neutral
biased	14898	132	biased	13926	2724
neutral	102	4868	neutral	1074	2276

The left hand side of Table 4.7 shows the confusion matrix for the population census data collection treatment, while the right hand panel represents predicts for a sample size of 20%, time averaged over 50 generations. The top row of the table shows data points for which the model predicted an origin in a biased model, with the columns representing the “real” origin of the data points. In the left panel, the population census data only identified 132 data points as biased, when they really arose from an unbiased model. However, in the right panel, we see a very different pattern. Of the 5000 data points arising from an unbiased model, *more* of the points were identified as coming from biased

transmission models than as unbiased.

Data Collection Treatment	% of Unbiased Data Misclassified
Population Census	2.6
Per-Locus Population Census	3.4
Sample Size: 20 Duration: 10	49.1
Sample Size: 20 Duration: 25	49.5
Per-Locus Sample Size: 20 Duration: 25	49.7
Per-Locus Sample Size: 20 Duration: 10	50.1
Per-Locus Sample Size: 20 Duration: 50	54.4
Sample Size: 20 Duration: 50	54.5
Sample Size: 20 Duration: 100	57.6
Per-Locus Sample Size: 20 Duration: 100	58.1
All Sample Sizes and TA Durations	68.0
Per-Locus Sample Size: 10 Duration: 25	73.5
Sample Size: 10 Duration: 25	73.6
Sample Size: 10 Duration: 50	73.7
Per-Locus Sample Size: 10 Duration: 10	73.8
Per-Locus Sample Size: 10 Duration: 100	74.0
Per-Locus Sample Size: 10 Duration: 50	74.1
Sample Size: 10 Duration: 100	74.4
Sample Size: 10 Duration: 10	74.7

Table 4.8: REDO!!! omPercentage of data points from the unbiased transmission model that are falsely identified as arising from a biased model.

By looking at the ratio of the right column in each confusion matrix, across all data collection treatments, we can see the magnitude of this “preference” for predicting data points as coming from biased transmission models (Table 4.8). Immediately apparent is that sampling and time averaging have a dramatic effect on predictions of transmission bias, making it extremely likely that we will find sampled and time averaged data samples to fit our models of conformist and anti-conformist bias.

I believe that this asymmetry in discriminatory ability means that archaeologists must be extremely careful in identifying transmission bias from archaeological samples. Only under very rare preservation and sedimentary conditions, or in historical contexts, will we find data collection regimes that approximate the population census treatment studied here. Whenever we deal with small samples and data that come from aggregated deposits, we would do well to exhibit healthy skepticism

about our ability to detect transmission bias, or indeed to say much about social learning modes. In the terms developed in this study, we face some irreducible equifinalities (as between conformism and anti-conformism), and many equifinalities that are reducible given more precise and complete data collection. Unfortunately, some of these potentially reducible equifinalities may be irreducible in practical terms.

This conclusion, however, is relative to the exact details of transmission models, predictor variables, and data collection regimes. As we develop better models and additional predictor variables that are measurable from archaeological data, we may be able to achieve better resolution of social learning processes. The classifier approach demonstrated here is capable of identifying whether we have successfully reduced equifinalities, or whether social learning modes remain out of reach for most archaeological contexts, and whether our efforts at applying cultural transmission modeling to the archaeological record would be better served by focusing upon different questions tailored to the data we possess.

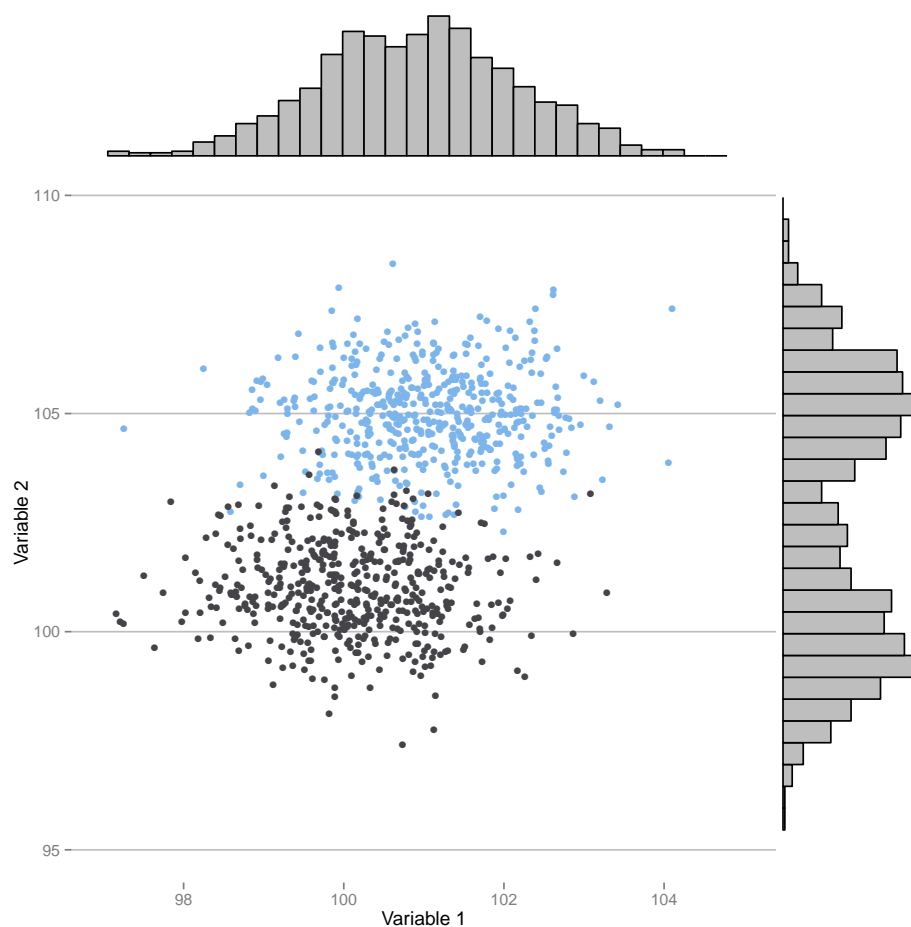
FIGURES IN DRAFT - REMOVE THIS SECTION FOR SUBMISSION

Figure 4.1: Simple example of the effect of variable choice in distinguishing models. The variable on the X axis displays quite a bit of overlap between models, while the variable on the Y axis distinguishes the models with fairly high accuracy.

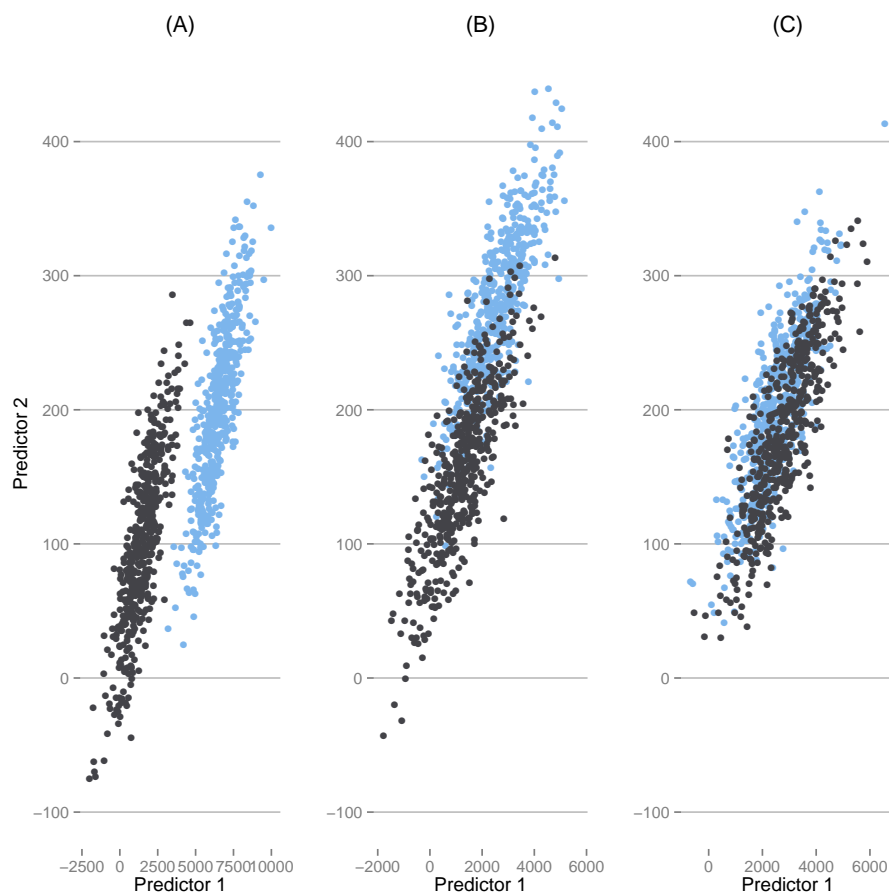


Figure 4.2: Simple example of model outcomes with different degrees of distinguishability: (A) simulated data point from two fully separate models, (B) two models with a limited overlap region, (C) and two models whose outcomes are highly overlapping.

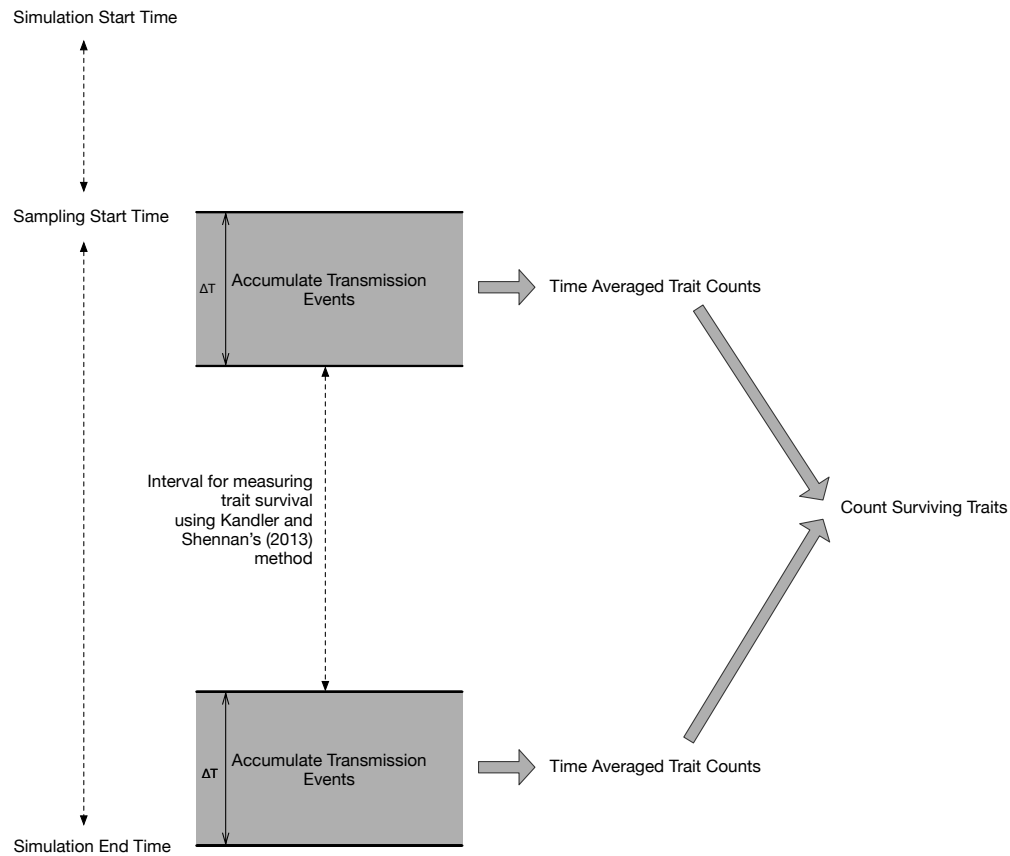


Figure 4.3: Schematic of how trait survival as described by Kandler and Shennan [Kandler and Shennan \(2013\)](#) is extended to time averaged samples of transmission events. Time runs from the start of the simulation run at the top, to the end at the bottom. The interval of time over which we calculate the Kandler-Shennan trait survival is given as a simulation parameter, and represents the gap in the middle of the diagram. Before and after that gap are sampling windows during which transmission events are accumulated over some number of simulated “generations” (values of 10, 25, 50, and 100 are used in this paper). Trait survival is then calculated as the number of traits present in the starting time averaged sample of transmission events, which are still present in the ending time averaged sample of events.

Combinatorial Structure of the Deterministic Seriation Method with Multiple Subset Solutions

ABSTRACT Seriation methods order a set of descriptions given some criterion (e.g., unimodality or minimum distance between similarity scores). Seriation is thus inherently a problem of finding the optimal solution among a set of permutations of objects. In this short technical note, we review the combinatorial structure of the classical seriation problem, which seeks a single solution out of a set of objects. We then extend those results to the iterative frequency seriation approach introduced by Lipo et al. (1997a), which finds optimal subsets of objects which each satisfy the unimodality criterion within each subset. The number of possible solutions across multiple solution subsets is larger than $n!$, which underscores the need to find new algorithms and heuristics to assist in the deterministic frequency seriation problem.

SOURCE Posted to Arxiv.org (<https://arxiv.org/abs/1412.6060>), in December 2014. Co-authored with Carl P. Lipo.

5.1 Single Seriation Combinatorics

Seriation, whether employing class frequencies or simple occurrence to order assemblages, yields solutions which are permutations of the set of assemblages. Because we cannot determine the “polarity” of a seriation solution—which ends represent early and late—from the class data alone, a unique seriation solution is thus formally a pair of mirror-image permutations:

$$\{a, d, b, c, e\} \equiv \{e, c, b, d, a\} \quad (5.1)$$

This means that a set of n assemblages can yield $n!/2$ distinct solutions, regardless of whether solutions are composed of ordered similarity matrices or “Fordian” frequency curves. With small numbers of assemblages, enumeration and testing of all possible solutions is easy, even without parallel testing across many processors. The ability to test solutions by enumeration quickly breaks down with only a modest number of assemblages. Table 5.1 gives the number of unique solutions for selected problem sizes between 4 and 100 assemblages, and estimates of processing time to enumerate and test all solutions, assuming a cluster of 64 cores, and 5×10^{-4} seconds per solution test.¹ With 10 assemblages, we can test all solutions quickly enough that even a serial algorithm on a single core will be adequate to find the global best solution in a matter of hours, with parallelism improving this to real time responses.

A typical characteristic of many combinatorial algorithms is that small changes in problem size can have massive changes in processing time. 13 assemblages will turn out to be the practical limit for direct enumeration, even given parallel processing with circa-2012 technology, with total processing time of nearly 3 days running 64 cores at full capacity.² Problems involving 14 and 15 assemblages reach the point where large clusters require more than a month and 19 months respectively, to solve.

¹These assumptions concerning per-trial processing time and parallelism are arbitrary but within reach of social scientists given Amazon’s EC2 cloud computing infrastructure, without requiring formal “supercomputer” access. Modification by a factor of 10 has little effect on the results, perhaps shifting feasibility upward slightly before combinatorial explosion occurs.

²Realistically, almost nobody would contemplate doing this, given the expense of the computing time relative to the value of guaranteeing the optimal solution, but the hypothetical example demonstrates that such solutions are *feasible*.

N	Seriation Solutions	Seconds	Years
4	12	9.4e-05	3e-12
6	3.6e+02	0.0028	8.9e-11
8	2e+04	0.16	5e-09
10	1.8e+06	14	4.5e-07
12	2.4e+08	1.9e+03	5.9e-05
13	3.1e+09	2.4e+04	0.00077
14	4.4e+10	3.4e+05	0.011
15	6.5e+11	5.1e+06	0.16
16	1e+13	8.2e+07	2.6
20	1.2e+18	9.5e+12	3e+05
40	4.1e+47	3.2e+42	1e+35
60	4.2e+81	3.3e+76	1e+69
80	3.6e+118	2.8e+113	8.9e+105
100	4.7e+157	3.6e+152	1.2e+145

Table 5.1: Number of unique seriation solutions and parallel processing time for sets of assemblages $4 < n < 100$, testing solutions across 64 cores, assuming 5ms per trial

Beyond 15 assemblages, a “combinatorial explosion” sets in, with 20 assemblages requiring more than 3 million years, before solution times quickly exceed the lifetime of the universe.

In short, top-down enumerative methods are feasible for small sets of assemblages, and given widespread availability of multiple core computers, seriation packages should employ enumeration for small problems, or to build and test smaller parts of larger seriation solutions.

5.2 Deterministic Seriation with Multiple Solution Groups

In an earlier paper (Lipo et al., 1997a), we introduced an iterative method for finding deterministic solutions to the frequency seriation problem by partitioning assemblages into subsets, each of which meets the unimodal ordering principle, within tolerance limits governed by sample size. Lipo (2001b) extended and refined the method in his dissertation research. Our initial work on the method employed a combination of automated calculations (e.g., bootstrap significance tests for pairwise orderings), and manual sorting of assemblages into groups and specific positions (using an Excel macro package available at <http://lipolab.org/seriation.html>). Figure 5.1 is an example of seriation

5. COMBINATORIAL STRUCTURE OF THE DETERMINISTIC SERIATION METHOD WITH MULTIPLE SUBSET SOLUTIONS

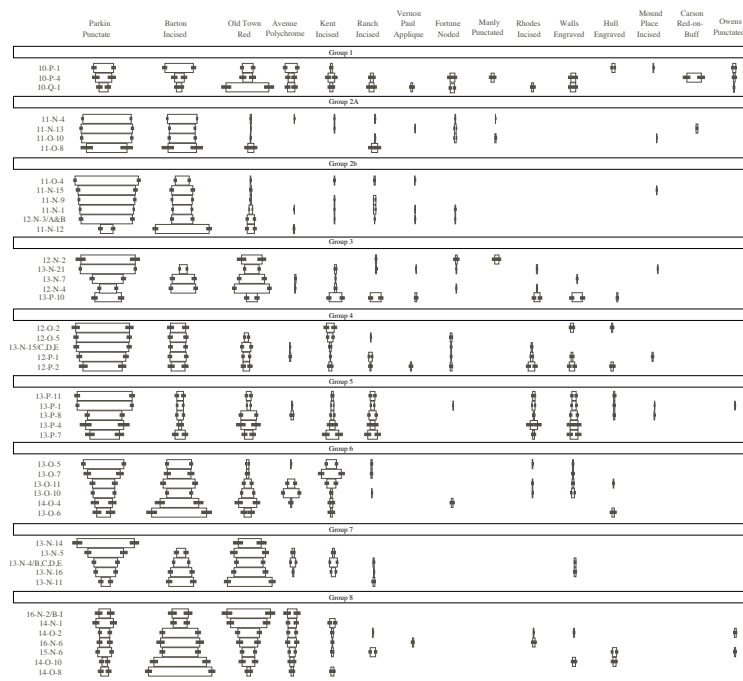


Figure 5.1: Example of a deterministic frequency seriation with assemblages partitioned into multiple subsets or solution groups. From [Lipo \(2001b\)](#), Figure 4.4.

with multiple solution groups, from Lipo's dissertation research in the Lower Mississippi Valley.

Our initial work suggests assemblages seriate together into groups reflecting variation in the intensity of cultural transmission among assemblages, over their duration of accumulation. In most cases, solution groups tend to be spatiotemporally compact, and form clusters when mapped on the landscape, although long-distance connections between past communities can also yield patterns which are more complex and less cohesive when mapped. Madsen's dissertation research is aimed at tying the properties seriation solution groups to their causes in regional patterns of interaction and the dynamics of specific cultural transmission models.

In this section, the goal is to understand the complexity of the multiple seriation groups problem, constructing reasonable upper bounds for a given problem size, even if some problems encountered in real analyses do not approach the worst case. From a combinatorial standpoint, seriation with multiple solution groups has the following structure. We begin with n assemblages in total, and seek a solution or solutions whereby we end up with m solution groups, where $m < n$. Each solution

# of Solution Groups (m)	20	40	60
3	5.8e+08	2e+18	7.1e+27
4	4.5e+10	5e+22	5.5e+34
6	4.3e+12	1.8e+28	6.8e+43
8	1.5e+13	3.2e+31	3.8e+49
10	5.9e+12	2.4e+33	2.7e+53
15		2.9e+34	2.2e+58
20		1.6e+32	1.7e+59
25			3.7e+57
30			9.6e+53

Table 5.2: Number of ways to form m subsets (seriation solutions) from 20, 40, and 60 assemblages

must have at least one assemblage, and in practice will often have 3 or more (singletons may indicate assemblages which simply do not “fit” with anything else in the data set). The number of ways that n objects can be partitioned into m non-empty subsets (or solution groups) is given by the Stirling numbers of the second kind, which are given by the recursion equation:

$$\left\{ \begin{matrix} n \\ m \end{matrix} \right\} = m \left\{ \begin{matrix} n-1 \\ m \end{matrix} \right\} + \left\{ \begin{matrix} n-1 \\ m-1 \end{matrix} \right\} \quad (5.2)$$

Table 5.2 gives the number of ways to form a specific number of subsets (or seriation solution groups) from sets of assemblages ranging from 20 to 60. Each column runs from 3 solution groups to half of the number of assemblages, since the number of possible subsets is maximized just before $n/2$ and declines thereafter (Figure 5.2).

We can immediately see that there are an enormous number of possible subsets for any assemblage size. There are fewer subsets, of course, than complete permutations of the set of assemblages since subsets are unordered (i.e., $\left\{ \begin{matrix} n \\ m \end{matrix} \right\} < n!$ for all m). However, in the multiple seriation group problem, the problem size is larger than the corresponding Stirling number because we do not know in advance how many groups (subsets) a set of assemblages will seriate into. Thus, the total number of unique subsets which might contain the optimal solution is the total of the number of subsets, across all subset sizes:

$$\sum_{i=1}^n \left\{ \begin{matrix} n \\ i \end{matrix} \right\} \quad (5.3)$$

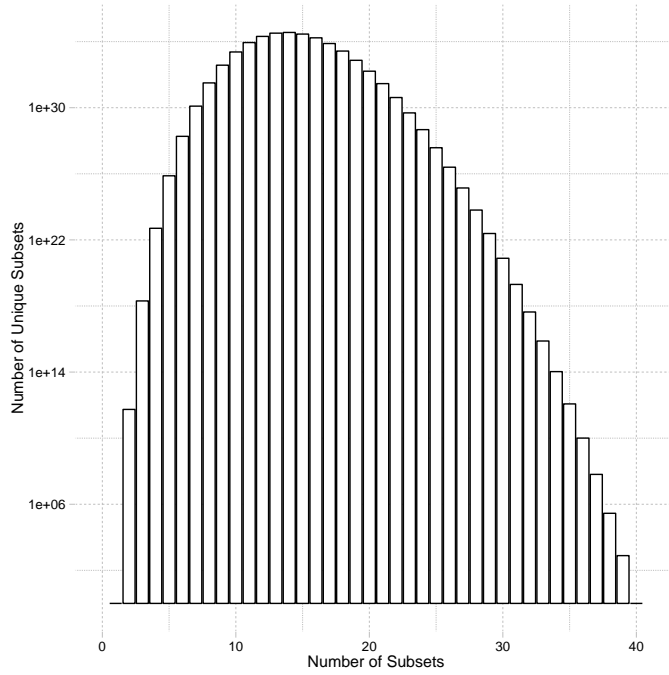


Figure 5.2: Number of Unique Solution Sets for 40 Assemblages When Partitioned Into m Solution Groups

This result is still smaller than the total permutations for a set of n assemblages. For example, given 40 assemblages, $n! = 8.159 \times 10^{47}$, whereas the total from Equation 5.3 for 40 assemblages is 1.575×10^{35} .

Another factor to consider is that each of these unique subsets resulting from a partition of n assemblages into seriation groups is still unordered. For example, if we partition 10 assemblages into 3 solution groups, there are 9330 unique ways of assigning the 10 assemblages to the 3 solution groups. Each group within a partition will have n_i members, where $\sum n_i = n$. The number of unique seriations for each of the 3 solution groups is $n_i!/2$, but we cannot assume that solution groups will have a balanced or equal number of assemblages (as Figure 5.1 does). Partitions such as:

$$\{1, 2, 3, 4, 5, 6\}\{7, 8\}\{9, 10\}$$

are common in seriating real assemblages (Lipo, 2001b).

Since the factorial function grows so quickly, the computational cost of determining the correct

permutation within a given seriation solution group is controlled by the size of the largest subset, especially if the other subsets are relatively small, as in the previous example. At worst, for a solution set with m solution groups, $m - 1$ solution groups will contain 1 assemblage each, and the last solution group will consist of the remaining $n - m - 1$ assemblages. This means, of course, that the worst case would involve consideration of on the order of $(n - m - 1)!$ permutations within each solution group, for each of the subsets given by Equation 5.3. This yields:

$$\sum_{m=1}^n \left\{ \begin{matrix} n \\ m \end{matrix} \right\} (n - m - 1)! \quad (5.4)$$

Table 5.3 gives the total number of possible solutions for assemblages ranging from 4 to 100, where solutions may fall into multiple seriation groups of any size.

N	Total Solutions	Seconds	Years
4	15	0.00012	3.7e-12
6	4.7e+02	0.0037	1.2e-10
8	5.2e+04	0.4	1.3e-08
10	1.5e+07	1.1e+02	3.6e-06
12	8.5e+09	6.6e+04	0.0021
13	2.6e+11	2e+06	0.064
14	8.9e+12	7e+07	2.2
15	3.5e+14	2.8e+09	87
16	1.6e+16	1.2e+11	3.9e+03
20	1.7e+23	1.3e+18	4.2e+10
40	9e+65	7e+60	2.2e+53
60	5.1e+116	4e+111	1.3e+104
80	5.1e+172	4e+167	1.3e+160
100	4.4e+232	3.4e+227	1.1e+220

Table 5.3: Number of total solutions with multiple seriation groups and processing time for sets of assemblages $4 < n < 100$, testing solutions across 64 cores

5.3 Discussion

Clearly, in the worst case, the combinatorial complexity of the multiple seriation groups problem is much worse than even the straight factorial case involved in single solution permutations. The

feasibility of parallelized enumerative methods still explodes after 13 assemblages, but much more steeply. The goal of a new algorithm for deterministic multiple group seriations is, therefore, to employ heuristics to drastically reduce the size of the solution space. Vast amounts of the solution space involve partial orders which violate unimodality, but of course we cannot easily identify those regions of solution space *a priori* without testing possibilities. But given small partial solutions which do meet the seriation model, we can easily test solutions which are “adjacent” to the partial solutions, suggesting that agglomerative heuristics may be the best approach to finding a computationally feasible method.

Measuring Cultural Relatedness Using Multiple Seriation Ordering Algorithms

ABSTRACT Seriation is a long-standing archaeological method for relative dating that has proven effective in probing regional-scale patterns of inheritance, social networks, and cultural contact in their full spatiotemporal context. The orderings produced by seriation are produced by the continuity of class distributions and unimodality of class frequencies, properties that are related to social learning and transmission models studied by evolutionary archaeologists. Linking seriation to social learning and transmission enables one to consider ordering principles beyond the classic unimodal curve. Unimodality is a highly visible property that can be used to probe and measure the relationships between assemblages, and it was especially useful when seriation was accomplished with simple algorithms and manual effort. With modern algorithms and computing power, multiple ordering principles can be employed to better understand the spatiotemporal relations between assemblages. Ultimately, the expansion of seriation to additional ordering algorithms allows us an ability to more thoroughly explore underlying models of cultural contact, social networks, and modes of social learning. In this paper, we review our progress to date in extending seriation to multiple ordering algorithms, with examples from Eastern North America and Oceania.

SOURCE Submission to Electronic Symposium, “Evolutionary Archaeologies: New Approaches, Methods, And Empirical Sufficiency” at the Society for American Archaeology conference, April 2016
Co-authored with Carl P. Lipo. Posted as Arxiv.org <http://arxiv.org/abs/TBD>.

6.1 Introduction

Seriation is a set of methods that uses patterns in the occurrence or abundance of historical classes to construct an ordering among otherwise unordered assemblages or objects (Dunnell, 1970). Its early 20th century developers built seriation as a relative dating method and orders constructed by seriation were intended to be chronological (O'Brien and Lyman, 2000, 1998; Lyman and O'Brien, 2006; O'Brien and Lyman, 1999; Lyman et al., 1997). While practitioners such as James Ford (Ford, 1938; Phillips et al., 1951; Ford, 1935) noted that seriation techniques also create orderings which incorporate the effects of spatial variation in addition to temporal change, the dominant use of seriation in archeology has been chronological.

As a chronological tool, seriation has been success in developing an understanding the large-scale temporal structure of the archaeological record in the New World (Beals et al., 1945; Bluhm, 1951; Evans, 1955; Ford, 1949; Kidder, 1917; Mayer-Oakes, 1955; Meggers and Evans, 1957; Phillips et al., 1951; Rouse, 1939; Smith, 1950). Despite this success, the method has largely been ignored since the advent of radiocarbon dating given its primary association as a relative dating method. But seriation is only a dating method in the sense that chronology is one possible inference that can be obtained by mapping the spatiotemporal pattern of change in cultural variants. Other inferences are possible, and in particular, there is a growing understanding that seriation is one of several methods for inferring historical and heritable continuity and thus documenting the evolutionary history of past populations (e.g., Lipo et al., 1997b; Lipo and Madsen, 2000; Lipo, 2001c; Lipo, 2001a; Lipo, 2005; Lipo and Madsen, 1997; Lipo et al., 2015; Neiman, 1995; O'Brien and Lyman, 1999, Ch. 3; Teltser, 1995).

Seriation is based on the notion that the frequencies of classes of artifacts reflect heritable continuity when it arises from information being passed between populations over time; that is, from cultural transmission processes. Although the fact that seriation, in some sense, measures cultural transmission has been implicit since the earliest discussions of the method (e.g., [Kroeber, 1923](#)), the connection remained a common sense generalization until the mid 1990's. Fraser Neiman, in his dissertation ([Neiman, 1990](#)) and later his seminal 1995 article ([Neiman, 1995](#)), noted that the unimodal patterns that form the core of the traditional frequency seriation technique are regularly seen in the trajectories seen when simulating unbiased transmission. In order to make this connection both rigorous and useful in empirical work, we began a research program aimed at exploring the connection between cultural transmission models and seriation methods ([Lipo et al., 1997b](#)). Our investigation into seriation has resulted in numerous publications, new seriation software algorithms, and many conference papers ([Lipo and Eerkens, 2008](#); [Lipo and Madsen, 2001](#); [Lipo, 2001a, 2005](#); [Lipo and Madsen, 1997](#); [Lipo et al., 2015](#); [Madsen and Lipo, 2014, 2015](#); [Madsen et al., 2008](#); [O'Brien et al., 2015](#)).

The core of the all seriation techniques are a set of “ordering principles” which describe how the data points making up each assemblage or object are rearranged in order to achieve a valid seriation solution. Traditionally, there are two principles: occurrence and frequency ([Dunnell, 1970](#); [Rouse, 1967](#); [Whitlam, 1981](#)). The “occurrence principle” states that a valid ordering leaves no temporal gaps in the distribution of the historical classes used, and thus that temporal orders are continuous ([Dempsey and Baumhoff, 1963](#); [Rowe, 1959](#)). The “frequency” or “popularity” principle states that in a valid ordering, the frequencies making up the continuous distribution of each historical type will be unimodal, possessing a single peak of “popularity” ([Nelson, 1916](#)).

Both the frequency and occurrence principle work to sort descriptions of assemblages through time. The robustness of methods built on these principles is easily demonstrated by the continued utility of the basic chronological frameworks erected by culture historians in the first half of the 20th century using seriation along with stratigraphy and marker types ([Lyman et al., 1997](#)). It is intrigu-

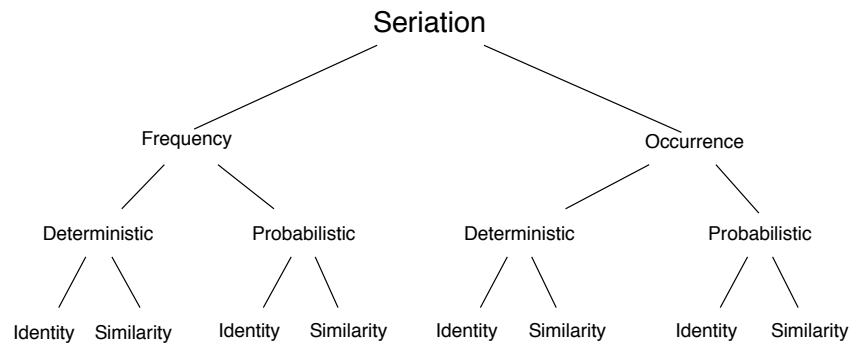


Figure 6.1: [Dunnell \(1981\)](#) defines seriation to be a set of methods which use historical classes to chronologically order otherwise unordered archaeological assemblages and/or objects. Historical classes are those which display more variability through time than through space. Occurrence seriation uses presence/absence data for each historical class from each assemblage ([Kroeber, 1916](#); [Petrie, 1899](#)). Frequency seriation uses ratio level abundance information for historical classes ([Spier, 1917](#); [Ford, 1935, 1962](#)). Frequency and occurrence seriation techniques can take the form of deterministic algorithms that require an exact match with the unimodal model or probabilistic algorithms that accept departures from an exact fit. Identity approaches employ raw data (whether frequency or occurrence) to perform the ordering. Similarity approaches transform the raw data into a non-unique coefficient (e.g., Brainerd Robinson, squared Euclidean distance); the coefficients then form the basis for ordering.

ing to note, however, that the frequency principle remains an empirical generalization that is only suggested by the generalized behavior of cultural transmission models, rather than being a necessary consequence. From Neiman’s simulations (i.e., [Neiman, 1995](#)), one can see that the results of cultural transmission are not strictly or necessarily unimodal. This possibility suggests to us that seriation as a method requires further methodological development, especially if it is to be one of our major tools in tracing historical and heritable continuity in the archaeological record.¹

In this paper, we explore an alternative to unimodality and the “popularity principle” that drives classical frequency seriation: exact minimization of inter-assemblage distance metrics, or “continuity” seriation. Although not a new principle, it was underappreciated especially prior to the contemporary explosion of computing power. We demonstrate that an exact form of distance minimization,

¹Cladistics and phylogenetic methods, especially those which take into account temporal differences in the samples being studied (stratocladistics) and which are capable of yielding phylogenetic networks in addition to trees, are the other major tools by which we can measure heritable and historical continuity.

in contrast to the statistical or approximate minimization associated with multidimensional scaling, generates solutions that are usually identical to the application of unimodality to the same data. Furthermore, using simulated data, we examine situations where frequency and continuity seriations may differ in minor ways, without affecting the overall ordering of the data set. Although there is still great value in the classical approach, the advantage of developing new seriation approaches is that we can often apply distance minimization to classes and types which do not necessarily display the classical unimodal form, which opens seriation to wider classes of data. In addition, distance minimization can be formulated within large scale, parallel machine learning frameworks, and thus made applicable to contemporary data sets which are often orders of magnitude larger than those we face in archaeological contexts, as well as archaeological data sets for which frequency seriation analysis performs poorly.

6.2 Seriation and the Frequency Principle

Seriation, in the Americanist sense, was initially developed by Alfred Kroeber ([Kroeber, 1916](#)) in the Southwest, based on his observations of changes in the relative abundance of forms of ceramic decorations found on sherds located in assemblages near Zuni Pueblo. The primitive seriation proposed by Kroeber was quickly amended by Leslie Spier, Alfred V. Kidder and Nels C. Nelson all of whom were conducting stratigraphic excavations in the American Southwest ([Kidder, 1917](#); [Nelson, 1916](#); [Spier, 1917](#)). This group of researchers all noticed that when ceramics were described in a particular way – called “stylistic” by Kidder ([1917](#)) – the temporal distribution of the types took the form of “normal curves.” Using such types, it was apparent that a series of assemblages collected from the surface or otherwise undated could be arranged in chronological order by rearranging them so that all type distributions approximated “normal curves” simultaneously. The orders constructed in this way could also be tested by finding stratified deposits and were found to be correct. The resulting method then went on to dominate archaeological practice for much of the next 50 years ([Lyman et al.,](#)

1997).

As powerful as seriation proved to be, these early formulations were entirely intuitive and based on the generalization that greater temporal differences between assemblages caused larger differences between frequencies of decorated types, and that properly constructed historical types displayed a clear pattern of change (Phillips et al., 1951, p. 220):

If our pottery types are successful measuring units for a continuous stream of changing cultural ideas, it follows that when the relative popularity of these types is graphed through time, a more or less long, single-peak curve will usually result. Put in another way, a type will first appear in very small percentages, will gradually increase to its maximum popularity, and then, as it is replaced by its succeeding type, will gradually decrease and disappear.

This compactly describes the “popularity principle,” originally articulated by Nelson (1916) and Wissler (1916). A key word in the above is “usually,” since not all types display the unimodal distribution described, even when the attributes chosen are explicitly stylistic and decorative. Types suitable for frequency seriation were a subset of stylistic variation, comprising those which displayed spatial and temporal contiguity, a long enough duration that the types overlapped in their representation among sites and assemblages, and those whose distribution through time displayed the characteristic unimodal form which allowed the analyst to arrange them by eye. Culture historians also minimized the effect of chance and potential recurrence by insisting that the classes used for measurement were constructed from multiple dimensions (Phillips et al., 1951; Lipo, 2001c). The overall process of constructing and testing such types became known, after Krieger (1944), as applying the “test of historical significance.”

6.2.1 Unimodality and Cultural Transmission Processes

In most cases (such as the above quote from Phillips, Ford, and Griffin), the popularity principle is simply assumed to hold in culture-historical applications. It is clear that culture historians assumed that what generates heritable continuity, and thus allows the tracing of chronological relations, is cultural transmission. As Lyman (2008) documents in careful detail, early 20th century anthropology and archaeology understood and discussed a variety of transmission processes informally, as generating the patterns they studied, even if they used different terms and did not form quantitative models for it. Rouse (1939), for example, explicitly discussed the diffusion of cultural traits, in terms that we now recognize as a spatiotemporal model of transmission. Kroeber, the father of frequency seriation, clearly understood the connection between his previous work and trait diffusion (Kroeber, 1937). Deetz and Dethlefsen (1965; 1971) noted the spatial dimension to trait diffusion. There are many more examples (Lyman, 2008).

Interest in studying cultural transmission in an explicit way has a long history in archaeology. Since the 1970s, archaeologists have worked with models of diffusion, with those models becoming increasingly quantitative, statistical, and even explicitly mathematical (e.g., Ammerman and Cavalli-Sforza, 1971). These models of diffusion, however, tended to be deterministic, especially those stemming from the interdisciplinary literature on the diffusion of innovations (e.g., Rogers, 2003). Deterministic models, however, ignore the essential historically contingent pathways of culture transmission that produce the patterns noted by culture historians as historically significant. More recently archaeologists have become interested in developing models for individual social learning events (e.g., ?). Individual social models, however, do not necessarily “add up” to produce a population level effect, and the latter is what we need to understand in order to solidly ground a seriation ordering algorithm in cultural transmission.

It was not until archaeologists began working with stochastic models of cultural transmission, however, that we could easily visualize the sheer variety of patterns that cultural transmission processes can, and do, generate. Stochastic models of transmission allow us to easily explore the pre-

cise conditions under which unimodal distributions occur in type frequencies, what classification methods tend to produce it, and what dimensions of variation combine to produce mostly unimodal behavior.

Dunnell's (1978b) exposition of style as neutral variation was one key step in the adoption of stochastic models of drift from population genetics as the main tool for exploring cultural transmission dynamics. Neiman (1995) took this step substantially further when he simulated drift in cultural variants as an unbiased transmission process, as shown in Figure 6.2. Immediately apparent is the fact that some variants do display unimodal patterns, but most variants are multimodal or display violations of unimodality at small scales even if the macroscopic shape seems to conform to the popularity principle.

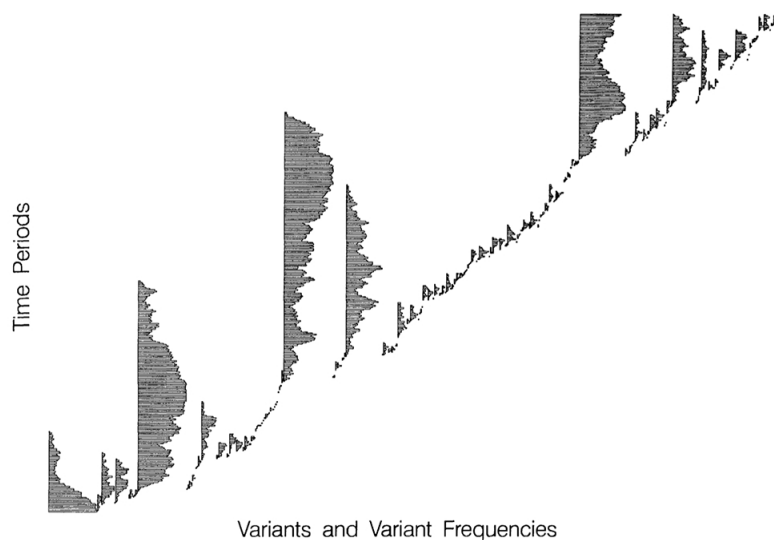


Figure 6.2: Neiman's simulation of drift in cultural variant frequencies under unbiased cultural transmission (reproduction of Figure 2a from Neiman 1995.)

The lesson of Figure 6.2 is that there is nothing necessary about unimodality given cultural transmission, but that it can occur. But culture historical types used in seriation were **constructed** to yield unimodal distributions, and a key element in such construction is ensuring that types are composed of multiple dimensions of variation which co-occur on artifacts identified to that type. We

can imagine selecting the traits shown in Figure 6.2 and intersecting combinations of them to form multidimensional classes. In doing so, it is likely that unique combinations of those variants would not recur and the role of chance in the occurrence of combinations of traits would be minimized. Thus, such practices likely contribute to the presence of unimodal distributions. It is also likely that time averaging (ubiquitous in the archaeological record) smooths out some of the minor variation in variant frequencies, as will the vagaries of sampling archaeological deposits.

Taken together, these factors seem to explain why the intuitive construction of historical types, from the continuous flow of the products of cultural transmission processes, worked to produce chronology through application of the common-sense popularity principle, and why not all artifact classes constructed from otherwise “stylistic” dimensions of variation, are suitable for frequency seriation using unimodality as the ordering criterion. From the perspective of culture historians, unimodality was a sufficient criteria for recognizing patterns that were likely chronological from those that were likely not. While focusing on only those classes that produced unimodal distributions in class frequencies might have ignored other potentially historical significant classes, without any other means of identifying chronological patterns, culture historians were satisfied with the subset that worked.

6.2.2 Continuity: An Alternative to Unimodality

There are several reasons why we should explore alternatives to unimodality as an ordering algorithm for frequency seriation. First, from a performance perspective, searching for unimodal orders is computationally expensive, even for relatively small data sets (Madsen and Lipo, 2014). Even with the iterative, agglomerative method that we introduced recently (Lipo et al., 2015), the computation time can grossly exceed computing capacity for data sets as small as 30. While 30 is a large number of assemblages by most archaeological standards especially when adequate sample size requirements are met, it is a serious limitation. Without good techniques and ordering principles seriation may not scale to much larger problems, and even be applicable to the flood of data seen in modern day life.

Second, and more importantly from a theoretical perspective, it is important to be able to trace heritable continuity even if does not display a particular type of temporal frequency distribution. Using traditional type construction methods and the test of historical significance, culture historians were able to find **enough** conforming types and classes to construct regional chronologies. The goal of culture historians was to build chronologies using the most efficient means possible to do so, not study combinations of trait transmission through time and space. The use of seriation as a method for tracing evolutionary relationships is a more demanding task than establishing rough chronology in a region. Thus, it is worth searching for additional ordering principles that may be useful for seriating more classes of cultural variants. Specifically, there is strong relationship between the number of classes in a seriation, and our ability to map differences across space and time. We need methods that can evaluate arbitrary sets of classes to arrive at the most detailed understanding of cultural transmission landscapes.

For example, Madsen (2015) is presently working on classifying regional interaction models by the structural properties they leave behind when cultural transmission is simulated on such regional models and then seriated. Doing this kind of detailed analysis requires many types and frequently, many assemblages to be successful. Even if unimodality suffices for rough chronology, additional ordering principles will be highly useful for studying regional interaction and the evolutionary history of technology.

A theoretically sound ordering principle for seriation should be derivable from characteristics of the underlying cultural transmission processes that we believe drive the spatiotemporal variation seriation measures. Formal models of cultural transmission, such as those formulated by Boyd and Richerson, Cavalli-Sforza and Feldman, and borrowed from population genetics (Boyd and Richerson, 1985b; Cavalli-Sforza and Feldman, 1981b; Neiman, 1995) provide a good starting place. Their models incorporate stochastic autoregressive processes in which the probability distribution of outcomes at a given time are dependent upon the outcomes from the immediate past. Mathematically, then we can treat cultural transmission models as Markov processes, usually of first order (i.e., with-

out dependencies on states previous to the immediate past state). Such models are certainly capable of making large changes in state over short time intervals, but large jumps are rare compared to small changes in state, especially in large populations. This is the reason why we (and culture historians) often have an expectation that cultural transmission has a “gradual” character to it.

The probabilistic gradualism of change over small time periods in our cultural transmission processes explains the “continuity” principle that is embedded in traditional forms of seriation. Continuity is strongly related to notions of continuous functions in mathematics: samples which originate close together in time, space, or both will be close in type frequency and the presence/absence of types, especially compared to samples which are further apart. This continuity principle immediately leads to considering ordering algorithms based upon minimizing a suitable distance metric, with assemblages represented by points in a multidimensional space of type frequencies or counts.

6.2.3 Statistical Seriation Methods

The earliest statistical techniques for seriation were also built upon using interassemblage distance metrics. Brainerd and Robinson ([Brainerd, 1951](#); [Robinson, 1951](#)) pioneered a method for seriation based upon the similarity between assemblages, measured as a scaled version of the Manhattan (or city-block) distance between assemblage frequencies. When these scaled distances (which became known as Brainerd-Robinson coefficients) are arranged in a matrix with the largest values nearest the diagonal and the lowest values in the corners and away from the diagonal, the order of assemblages by row or column provides the seriation solution. In practice, most real data matrices cannot be put in perfect Robinson form without violations from the assumptions of the seriation model.

Brainerd and Robinson’s pioneering work became the basis of a minor industry that developed methods for matrix ordering in the face of the practical difficulties in coercing most data sets into a perfect linear ordering (e.g., [Dempsey and Baumhoff, 1963](#); [Kendall, 1963](#); [Matthews, 1963](#); [Bordaz and Bordaz, 1970](#); [Gardin, 1970](#); [Kendall, 1970, 1971](#)). As access to computers by researchers in the social sciences increased, computerized algorithms for examining permutations quickly proliferated

(Ascher and Ascher, 1963; Craytor and Johnson, 1968; Kuzara et al., 1966). Kendall (1969) and others attacked the ordering problem through the use of multidimensional scaling. For a detailed review of the many variants on this type of probabilistic seriation solution through the late 1970s, see (Marquardt, 1978). Most recently correspondence analysis has been used with success in determining probabilistic seriation orders, and just as importantly, quantifying the degree of departure from the ideal seriation model (Smith and Neiman, 2005).

Not all of the similarity measures used in this literature are true distance metrics, but many are, and there have been calls to simplify the problem by directly minimizing inter-assemblage distance, and thus the total “path length” of a candidate seriation solution. Kadane (1971) describes this approach, and it was adopted later by Shepardson (2006) in his construction of the “Optipath” seriation algorithm, which has distance minimization at its core.

Where existing distance/similarity methods encounter a problem is the assumption that a seriation solution must be a single linear order. In an earlier paper, we describe a seriation algorithm (iterative deterministic seriation solutions, or IDSS) that finds all of the possible orders in a set of data that conform to an ordering principle, and where those orders have overlap in assemblages (Lipo et al., 2015). Using this ordering principle, IDSS constructs a graph with branches that recognizes that the best solutions may not be linear. In probabilistic approaches to seriation such as MDS or correspondence analysis, departures from linear solutions have always been treated as “stress” or “error.” Practitioners usually recognize that such departures arise from coercing data which naturally sit in a larger number of dimensions – because of spatial variation and other factors – into a one-dimensional order. In essence, methods which attempt to coerce a complex spatiotemporal pattern into a linear ordering tend to treat departures from linearity as noise, which is then ignored.

But the departure from linearity is not “noise,” in the statistical sense. Especially if one accounts for sampling error in constructing seriation orders (as we do in IDSS by using the bootstrap to construct confidence intervals around the empirical frequencies), then departures from a linear ordering are **signal**, not noise. Such solutions reflect the fact that an assemblage at time T_1 , for example, may be

the closest match to two different assemblages at later times T_2 and T_3 for example, given slightly different areas of overlap in their type frequencies. This pattern can occur because the seriation method is inherently spatiotemporal, instead of simply measuring time (as culture historians have always known), and it can also reflect the splitting of populations into separate lineages (or their merger).

6.2.4 Exact Distance Minimization Ordering: “Continuity” Seriation

Instead of the “approximate” distance minimization algorithms employed in multidimensional scaling, we explore exact solutions using our IDSS algorithm. For simplicity in the configuration of the software, we summarize our approach by calling it “continuity” seriation, to distinguish it from unimodal-based frequency seriation and to emphasize that we want solutions that have the smoothest, most continuous transition of type frequencies when we consider pairs of assemblages. We achieve this by locally minimizing the inter-assemblage distance within the solution graph, which automatically yields the minimum total “path length” for a seriation solution.

Our algorithm makes no use of the unimodality criterion, and produces equivalent results in almost all cases, as we show in the next section. The algorithm currently employs the Euclidean distance between assemblage counts or frequencies, although it can use any distance metric. The Euclidean distance has the advantage of treating each class as equivalent measures, a property consistent with the use of paradigmatic classification (sensu [Dunnell, 1971](#)) for generating measurement classes. Given a table of inter-assemblage distance metrics, we first construct pairs of two-vertex graphs which represent the “closest” assemblage for each assemblage in the data set (mirrored pairs are filtered out since they are isomorphic). The edge weight given to each edge is the Euclidean distance between the assemblages represented by vertices. For each of the minimal graphs in this initial set, we then find the assemblage with the shortest distance to each of the two ends, and continue iterating. Crucially, if there are equal-distance options, both possible solutions are retained. The result of this iteration is a collection of graphs which represent partial minimum-distance paths through the set of assemblages. This collection of partial graphs are then overlaid to form a single solution using a “minmax”

approach as described in our paper on the IDSS algorithm in general ([Lipo et al., 2015](#)).

The general approach is the same one we take to frequency seriation; what differs here with “continuity” seriation is how we form the set of candidate partial solutions. Instead of enforcing unimodality within each partial solution, we minimize Euclidean inter-assemblage distance. The resulting minmax graph is linear only if all of the candidate partial solutions perfectly overlay themselves into a linear solution, and otherwise will have a tree structure with branches. The possibility of branching is what allows a seriation solution to express both spatial and temporal structure simultaneously. The ability to inform on both allows investigation of social network structure, and interaction and social learning patterns in past populations, at scales more detailed than entire cultural manifestations or phases. We believe that seriation, augmented in this way, sits between the microevolutionary level where we investigate evolution in single populations, and the macroevolutionary level, best explored using the tools of phylogenetic analysis and cladistic techniques.

6.3 Comparing Frequency and Continuity Seriation

In this section we compare the results of our IDSS frequency seriation algorithm, described in a recent paper ([Lipo et al., 2015](#)), and our exact distance-minimization or “continuity” algorithm. It is difficult to compare the algorithms on a very large set of empirical data sets, so we begin by examining a large sample of data sets generated by sampling simulated cultural transmission, within a regional metapopulation model of multiple communities. We described the overall model, called “SeriationCT,” in a conference paper last year, but we review the essentials here.²

Seriation of artifact assemblages is inherently a regional-scale problem, whether for chronology or tracking interaction and social learning processes. Thus, the fundamental abstraction for modeling is a graph or network which (a) represents the intensity of contact, migration, and interaction between communities of people at any given point in time, (b) allows the set of communities to evolve, with

²The SeriationCT software is open source, and is located at [Github](#). Experiments using it to generate the data analyzed here, and more network models, are described and linked on [Madsen’s website and lab notebook](#).

some communities going away and others originating over time, and (c) representing how both the pattern and intensity of inter-community contacts evolves over time. Social network or graph models, especially weighted graphs, form an essential ingredient for this type of modeling, but need to be extended to the temporal dimension.

Extending networks for modeling time-transgressive change employs so-called “temporal network models,” which record the changing structure a network or graph over a series of time points (Holme and Saramäki, 2012). For our purposes, “interval” temporal networks are the right abstraction. Such graphs represent interactions that occur and persist over a measurable duration as edges that carry time indices. Interval graphs can be modeled mathematically in a number of ways, but in an algorithmic setting the most convenient is to define a sequence of separate graphs, where each graph G_t in the sequence represents one or more change events within the network between times t and $t + \delta t$ (where $\delta t = t + 1 - t$). In a fully continuous temporal representation, each graph in the sequence specifies a single change event, and thus is equivalent to the way that a continuous-time stochastic process represents events. In situations where our observations are coarse grained due to time averaging or recovery methods (or both), each graph in the sequence may represent a number of change events which occur over the duration assigned to that graph in the sequence.

Change events encompass anything that modifies the graph. Vertices may be added or removed, and edges may be added or removed. In addition to addition and removal, if the graphs in the sequence are weighted, slices may record events where the strength of an edge changes, without other topological changes to the graph. If other attributes are present on vertices or edges (e.g., labeling edges for a type of interaction), changes to those labelled attributes would also constitute a change event and would be recorded by a graph in the sequence with changed attribute values. An interval temporal network is thus defined as an ordered set of graph “slices,” each slice associated with a time index. The changes themselves can be found by “subtracting” two graph slices and obtaining lists of vertex and edge changes.

Constructing a time-transgressive regional metapopulation from an interval temporal network

occurs by giving interpretations to vertices, edges, and other attributes of the graph. In our research, vertices represent communities of individuals, with population sizes which may change or not over time. Edges represent the presence of interaction between two communities, which could represent learning between individuals, or migration of individuals bringing portions of a cultural repertoire between communities. The weight given to an edge is typically a relative measure of interaction between communities, normalized by the rest of the communities, since there is no good way in a simple structure like this to model the absolute intensity of such interaction. When communities come into existence, by members of an existing community founding a new settlement, a vertex is added to the network and it acquires connections to other communities (according to the class of model we are constructing). Similarly, communities may go away over time, and the vertex is then removed. Interaction patterns may change as well, resulting in the addition or removal of edges over time, or change in the edge weights.

For example, we can create a model whereby two clusters of communities are tightly interconnected internally, and have some sparser relationship between the clusters, and slowly lose that interconnection to become separate, non communicating lineages, using a model similar to that shown in Figure 6.3.

The third and fourth columns in the figure describe the change events. The third describes changes to the network structure in each time slice, and the fourth describes the interpretation of those structural changes in terms of a regional metapopulation model.

Interval temporal networks, interpreted as regional metapopulation models, thus form a basic tool for modeling many classes of regional histories and interaction patterns. For purposes of comparing frequency and our continuity seriation algorithms, we focus on a regional model of the type depicted in Figure 6.3, but with a larger number of communities than shown. In that model, four clusters of communities start out at the beginning of the time period under consideration being tightly interconnected within each cluster, and more loosely connected among the four clusters. At any given time, each cluster has 8 communities spread over a geographic area, so with four clusters, there are

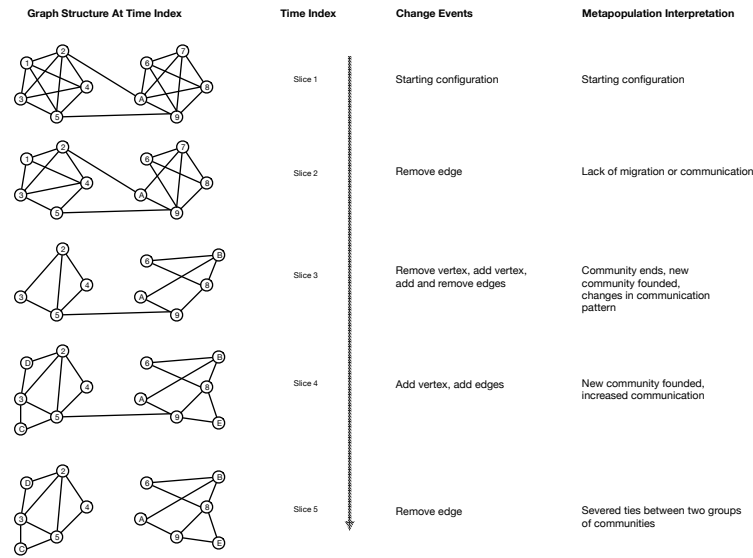


Figure 6.3: Example of an interval temporal network interpreted as a regional metapopulation model, with vertices representing communities, weighted edges representing intensity of interaction and migration, and changes in each representing their respective evolution over time.

32 communities in the region under consideration. At a late point in the time interval under consideration, the connections between pairs of clusters is removed, creating two non-interacting sets of community clusters, to model the origin of separate “lineages” of cultural transmission in a region.³

Given this model of interaction between communities, we then simulate the standard unbiased cultural transmission model across this network. The changes specified by the temporal network guide the addition of new subpopulations or their demise in the model, and the edge weight pattern defines migration of individuals between communities, and thus the possibility of cultural variants flowing between communities. Simulation of transmission occurs for 12,000 time steps, with the change events occurring regularly over that interval, creating change in interaction over time as social learning proceeds.

During the evolution of the model, we record the frequencies of individual variants, and their

³This model is available for inspection as a set of GML network files in experiment “sc-2” in the [experiment-seriation-classification](#) repository maintained by Madsen. That experiment focused on differentiating different classes of lineage-splitting or coalescence models through their seriation solutions, and here I focus only on the data resulting the “early lineage splitting” model.

co-occurrence to mimic archaeological classes or types which are defined by multiple dimensions of variation. Recording of frequencies occurs within each of the 32 communities present at any given point in time, so we can measure spatial and temporal variation in cultural variants. For purposes of the experiments reported here, we sample innovation rates from a prior distribution which allows any given simulation run to have a very low innovation rate, through relatively high innovation rates.⁴

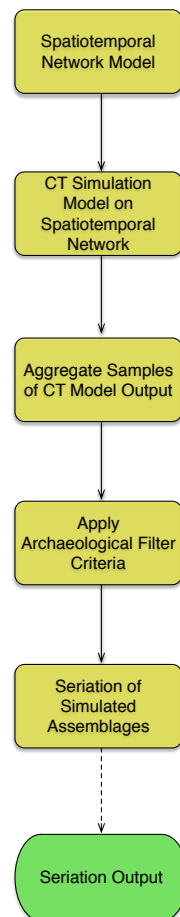


Figure 6.4: Processing steps in simulating cultural transmission on a regional metapopulation model of lineage splitting, to compare seriation ordering algorithms.

Following simulation and data recording, the raw data are processed in ways that mimic the time

⁴The details of the prior parameter distributions are relatively unimportant for purposes of comparing seriation algorithms, but are found in the [experiment-seriation-classification](#) repository under experiment SC-2 in the file “seriationct-priors.json”.

averaging that occurs in archaeological deposits, and the sampling that archaeologists do when taking surface collections from such aggregated deposits. This chain of processing is depicted in Figure 6.4. First, recorded cultural variants are aggregated for each community across the simulated time that community existed, so that all variant frequencies are time averaged in the manner described and modeled by Premo (2014b) and Madsen (2012b). Then, from the time averaged data for each community, an assemblage of 500 simulated artifacts is drawn from the raw data. This has a tendency to represent common variants well, and capture some but not all rare variants. From this sampled data, we then take a sample of the available communities, since seriations are always performed on a sample of archaeological deposits selected by the archaeologist (whether in rigorous or ad hoc ways). Finally, we filter the types present in each group of assemblages, to remove those types which are present only in one assemblage (as one would do in a manually constructed seriation), since those types do not contribute to ordering.

The resulting set of assemblage-level type frequencies were then fed into our IDSS seriation program, asking it to produce both a frequency seriation using unimodality as the ordering criterion, and a continuity seriation, using exact distance minimization as the ordering criterion. We did this for 50 simulation runs with different parameters across the “lineage splitting” regional model described above, and compared the resulting seriation solutions. We measure whether frequency and continuity solutions are identical by testing whether the solution graphs are isomorphic, which means that the same vertices are connected to the same neighbors by the same edges. Of the 50 simulation runs examined here, in 80% of cases the continuity and frequency seriations give an exactly identical solution. Of the remaining non-identical solutions, we find that the differences nearly always involve the repositioning of a single assemblage. In the next section, we examine such a case in detail to understand what drives such differences when they occur.

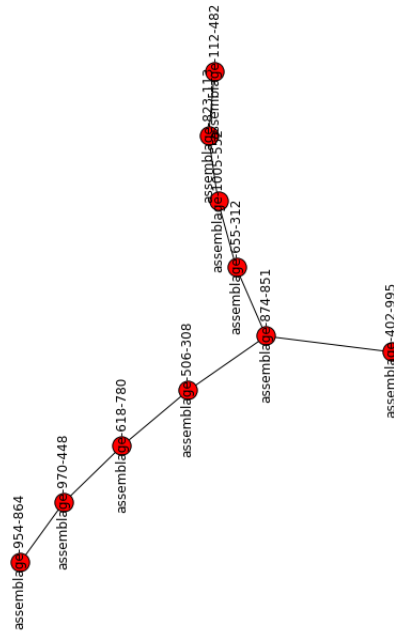


Figure 6.5: Frequency seriation solution for simulation run f8a6f378 on the “lineage splitting” regional interaction model.

6.3.1 Examining a Solution Which Differs

Of the differing solutions, we selected one (f8a6f378) at random to show the details of how frequency and continuity solutions differ. Figures 6.5 and 6.6 depict the frequency and continuity seriations, respectively, in the form of graphs which connect assemblages which are “adjacent” in the seriation solution. This makes it easier to see where an assemblage is really part of several solutions, which can indicate lineage splitting or differentiation occurring over space. We introduced this format for seriation solutions in our recent article on IDSS seriation (Lipo et al., 2015).

Although the graphs are laid out slightly differently (as a function of an automated graph layout algorithm), it is apparent that most of the seriation ordering is the same. Simulated assemblage 954-864 anchors one end of the ordering, while assemblage 112-482 anchors the other.⁵ Both solutions also show a branch for assemblage 402-995, which belongs to one of the two lineages after the connections between two sets of communities is lost. It is a single assemblage branch because of the

⁵Simulated assemblage names here reflect geographic coordinates, since regional interaction models often bias interaction and migration by location or neighborhood.

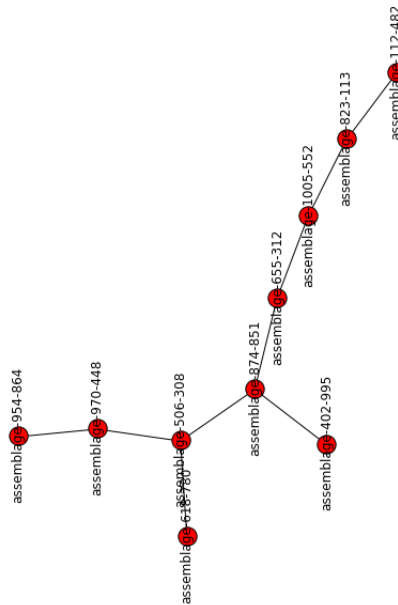


Figure 6.6: Continuity seriation solution for simulation run f8a6f378 on the "lineage splitting" regional interaction model.

vagaries of sampling assemblages out of the total set of communities in this example. The main difference between the solutions comes in assemblage 618-780 and where it connects. In the frequency solution it occurs "inline" while in the continuity solution, interassemblage distance is minimized by removing it to a small branch of its own.

Viewed in traditional tabular view of the type counts in Tables 6.1 and 6.2 or as traditional centered bar charts in Figures 6.7 and 6.8, several features are apparent. First, there are apparent violations of unimodality in the frequency seriation. But given our IDSS algorithm, we calculate a 95% confidence interval around each type count given the total sample size, and thus there are small differences (compared to the larger values) which are not statistically significant. Second, we can see that continuity solutions allow violations of unimodality (e.g., assemblage 823-113) but come up with the same overall structure. To us, this shows that unimodality is sufficient but not necessary for using a seriation method to track the spatiotemporal structure of cultural transmission.

Assemblage Name	6022-0-1767	36526	36557	7005-0-1767	7628-0-1767	0-9222-3	1-0-1767	3771
assemblage-954-864	10	160	0	49	92	0	0	0
assemblage-970-448	0	155	0	74	128	0	0	0
assemblage-618-780	123	50	0	164	121	0	13	0
assemblage-506-308	107	58	0	199	114	0	9	0
assemblage-874-851	81	66	0	165	0	0	162	6
assemblage-874-851	81	66	0	165	0	0	162	6
assemblage-655-312	0	52	16	111	0	20	269	6
assemblage-1005-552	0	53	32	72	0	61	182	41
assemblage-823-113	0	145	81	0	0	64	132	10
assemblage-112-482	0	24	151	0	0	157	81	49
assemblage-874-851	81	66	0	165	0	0	162	6
assemblage-402-995	106	65	0	29	0	0	192	0

Table 6.1: Raw data for frequency seriation for simulation run f8a6f378, grouped into blocks corresponding to the branches of the solution graph

6.3.2 Multiple Seriations for Phillips, Ford and Griffin (1951) data

Simulations of cultural transmission may give us the ability to probe the consequences of altering a model, and simulations are very useful for developing large samples of seriation solutions and understanding their properties. But simulations do not replace seriations of real data. To that end, we extend the Lower Mississippi River Valley example from our recent work (Lipo et al., 2015) by comparing frequency and continuity seriation algorithms on the same set of assemblages.⁶ The result is depicted in Figure 6.9. The result is identical – the two solutions are isomorphic.

6.4 Discussion

The fact that distance minimization can function as a seriation ordering algorithm is not a new idea. Not only has there been development of the idea within archaeological circles in the work of Kadane,

⁶We are archiving seriation datasets, with supporting information, licenses if available, and often with accompanying geographic information, and scripts to perform seriations on the data using our IDSS program, in the [seriation-datasets repository](#) in Github. If you would like to contribute a dataset, please contact Mark Madsen or send a pull request.

Assemblage Name	6022-0-1767	36526	36557	7005-0-1767	7628-0-1767	0-9222-3	1-0-1767	3771
assemblage-954-864	10	160	0	49	92	0	0	0
assemblage-970-448	0	155	0	74	128	0	0	0
assemblage-506-308	107	58	0	199	114	0	9	0
assemblage-874-851	81	66	0	165	0	0	162	6
assemblage-655-312	0	52	16	111	0	20	269	6
assemblage-1005-552	0	53	32	72	0	61	182	41
assemblage-823-113	0	145	81	0	0	64	132	10
assemblage-112-482	0	24	151	0	0	157	81	49
assemblage-874-851	81	66	0	165	0	0	162	6
assemblage-402-995	106	65	0	29	0	0	192	0
assemblage-506-308	107	58	0	199	114	0	9	0
assemblage-618-780	123	50	0	164	121	0	13	0

Table 6.2: Raw data for continuity seriation for simulation run f8a6f378, grouped into blocks corresponding to the branches of the solution graph

Shepherdson, and others, but distance minimization of one type or another underpins most classical multivariate statistics and nearly all of contemporary machine learning. Our principal contributions here have been to explicate the relationship between different seriation ordering algorithms, and to reintroduce distance minimization in an “exact” rather than statistical form.

Exact distance minimization as a means of tracing patterns of cultural transmission is only possible if we do not coerce the data into a single linear ordering, as has been the practice in all previous work. In these previous applications, the departures from linearity have been considered statistical noise or “stress,” and disregarded. From a culture transmission model, however, noise only enters the seriation problem as sampling error of counts or frequencies given the size of sample taken by the analyst. We can control this type of noise by using bootstrap confidence intervals around the empirical frequencies when we make ordering decisions. Our IDSS software system does so by default. Thus, once the effects of sampling are controlled departures from linearity cannot be noise, but are telling us something else about our data. In our judgment, those departures from perfect linearity are telling us about the simultaneous effects of spatial variation, temporal order, and the structure of the

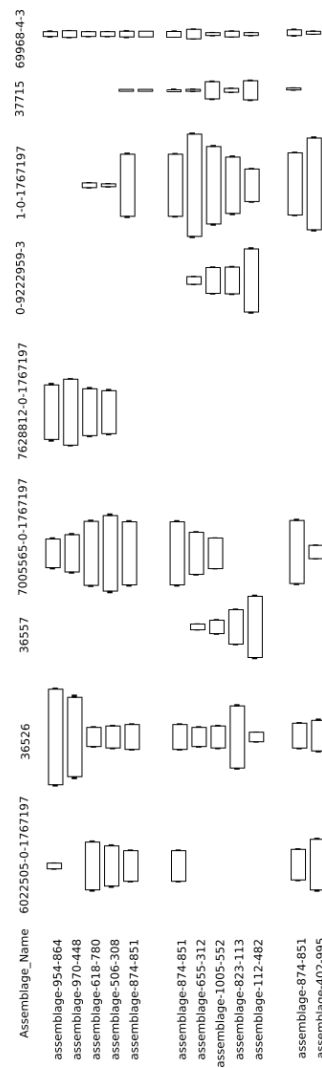


Figure 6.7: Centered bar chart representation of the relative frequencies of type for simulation run f8a6f378 built with the IDSS frequency seriation algorithm. The groups correspond to the branches of the solution graph.

social networks of interaction within which past cultural transmission occurred.

Thus, our approach to both frequency and continuity seriation allows partial solutions (each of which is a valid linear ordering) to agglomerate to form graphs or networks of solutions, given vertices (assemblages) which overlap between the sub-solutions. The resulting seriation graphs give us a more complete picture of the multiple causes that drive seriations than do traditional linear orders, whether perfect or coerced by a statistical method.

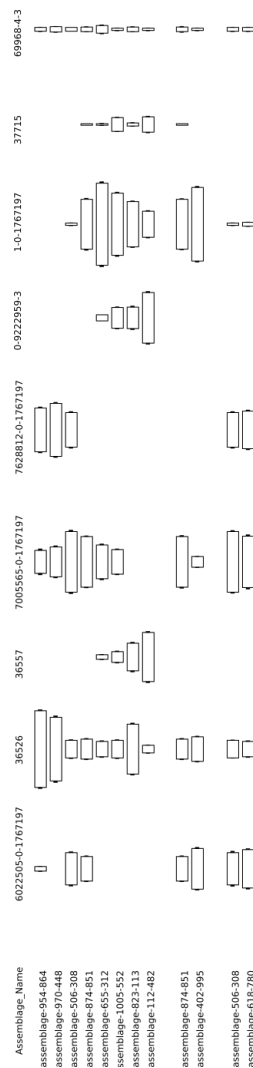


Figure 6.8: Centered bar chart representation of the relative frequencies of type for simulation run f8a6f378 built with the IDSS continuity seriation algorithm. The groups correspond to the branches of the solution graph.

The search for additional ordering methods led us to reconsider distance minimization methods, and although it is not unexpected that such methods work, it is a happy result. Continuity techniques have a much lower computational burden than searching for unimodality, especially as the number of assemblages gets large. For the Phillips, Ford and Griffin assemblages discussed here, the frequency solution took 25.2 seconds on an 8 core system, while continuity analysis took 0.955 seconds, for a speedup of 26x. This performance difference should be taken as a minimum on the difference be-

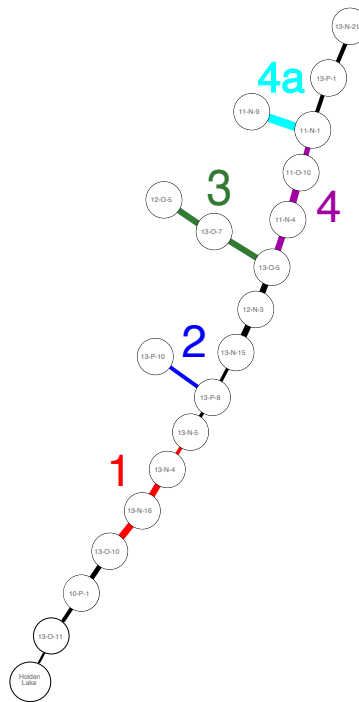


Figure 6.9: Seriation solution with frequency and continuity seriation for PFG (1951) ceramic assemblages in the Lower Mississippi River Valley, as analyzed by Lipo (2001a) and re-analyzed by Lipo et al. (2015). There are no differences between frequency and continuity ordering algorithms in analyzing this set of assemblages, and thus only one graph is shown.

tween algorithms, because our current algorithm for unimodality analysis is parallelized for a critical section across all of those cores, while continuity is still a serial algorithm and only uses a single core. Realistically, we should see a much larger speedup with further development, especially given the wealth of parallel algorithms for distance metric computations in contemporary machine learning. The latter will allow continuity methods to be fruitfully used even for “big” datasets of the type easily gathered in online settings. This method effectively has no limit as to the number of assemblages that can be analyzed.

Seriation is among the oldest of the purely archaeological methods for determining both chronology and cultural relatedness, but we find that it continues to repay detailed exploration by archaeologists and students of cultural evolution. It is fully complementary to phylogenetic methods and cladistics in many ways, especially in its ability to use detailed information about trait abundances and

the spatial pattern of those abundances instead of largely presence/absence data on character states.

This makes seriation, in our view, the method of choice for “mesoscale” problems and questions.

Behavioral Modernity and the Cultural Transmission of Structured Information: The Semantic Axelrod Model

ABSTRACT Cultural transmission models are coming to the fore in explaining increases in the Paleolithic toolkit richness and diversity. During the later Paleolithic, technologies increase not only in terms of diversity but also in their complexity and interdependence. As [Mesoudi et al. \(2008\)](#) have shown, selection broadly favors social learning of information that is hierarchical and structured. We believe that teaching provides the necessary scaffolding for transmission of more complex cultural traits. Here, we introduce an extension of the Axelrod ([1997](#)) model of cultural differentiation in which traits have prerequisite relationships, and where social learning is dependent upon the ordering of those prerequisites. We examine the resulting structure of cultural repertoires as learning environments range from largely unstructured imitation, to structured teaching of necessary prerequisites, and we find that in combination with individual learning and innovation, high probabilities of teaching prerequisites leads to richer cultural repertoires. Our results point to ways in which we can build more comprehensive explanations of the archaeological record of the Paleolithic as well as

other cases of technological change..

SOURCE Published in *Learning Strategies and Cultural Evolution During The Paleolithic*, edited by Alex Mesoudi and Kenichi Aoki, 2015, in the series *Replacement of Neanderthals By Modern Humans*, Springer. Co-authored with Carl P. Lipo.

7.1 Introduction

Although humans and our hominid ancestors have been cultural animals throughout our evolutionary history, an important change occurred in our lineage during the Middle and Upper Paleolithic. For millennia our ancestors manufactured relatively small toolkits and their material culture was remarkably similar across continental distances and over many generations. Beginning in the Middle Paleolithic and continuing through the Upper Paleolithic, the archaeological record reflects an explosion in our cultural repertoire. Over tens of thousands of years, artifactual toolkits shift from sets of relatively few objects with multiple uses to large collections of functionally-specialized tools that, employed increasingly complex technologies and that were manufactured from an enriched range of materials. The changes in artifacts suggest that human solutions to the problems of everyday life became regionalized and differentiated. Further, the economic basis of our lives began to broaden and also, in many areas, to become specialized ([Bar-Yosef, 2002](#); [d’Errico and Stringer, 2011](#); [Straus, 2005](#)).

While early researchers believed that the Upper Paleolithic resulted from a singular “revolution” in human evolution leading to behaviorally modern homo sapiens, this view is held by a minority of paleoanthropologists and archaeologists today (e.g., [Klein, 2009](#)). Careful examination of the Middle Paleolithic archaeological record especially in Africa and the Near East suggests that this change in behavior did not occur as a single distinct event, instead occurring over a long period of time since much of the enriched material culture we later characterize as the “Upper Paleolithic” had precursors. In addition, this change now appears to be patchy and fitful, with modern features appearing and

frequently being lost again (Bouzouggar et al., 2007; d’Errico and Henshilwood, 2007; d’Errico and Stringer, 2011; Straus, 2005; McBrearty and Brooks, 2000; McBrearty, 2007). Nor does behavioral modernity map neatly to biological taxa and their movements, given that evidence for the precursors of fully modern behavior is abundant in deposits associated with Neanderthals in addition to modern *Homo sapiens* (Villa and Roebroeks, 2014).

The “learning hypothesis” studied in this series of volumes makes the plausible claim that behavioral modernity is the product of cumulative changes in the way cultural information was acquired and retained across generations (Nishiaki et al., 2013), thus providing a potential explanation for the slow evolution of “modern” features, its patchiness in space and time, and the lack of a neat mapping between hominin taxonomy and material culture. In short, according to the learning hypothesis, behavioral modernity arose through a change or changes in the way social learning operated within hominin groups, with those groups adopting richer modes of cultural learning surviving and spreading compared to those who retained simpler forms of social learning.

Within the umbrella of the learning hypothesis, there are many ways in which social learning and thus intergenerational cultural transmission could have changed, and an increasing amount of research is focused upon formulating and testing different models. One class of studies is focused upon factors exogenous to the learning or imitation process itself. Shennan (2000; 2001) proposed that population size has a powerful effect on diversity within cultural transmission processes, which Henrich showed in the case of toolkit element loss during a Tasmanian population bottleneck (Henrich, 2004). In a similar line of reasoning, Kuhn (2013) argues that low population size and density put Neanderthals in a situation where innovations spread slowly and ultimately led to their demise relative to modern humans. Furthermore, a growing set of experimental studies clearly show a relationship between accumulation of complex cultural traits and the number of cultural “models” from whom individuals can learn (Muthukrishna et al., 2014; Derex et al., 2013; Kempe and Mesoudi, 2014). Not all studies have shown a strong association between population size and cultural diversity, however. Collard and colleagues, find little association in a linked series of comparative studies (Collard et al.,

2011, 2013a,b,c). Finally, in his analysis of the overall evolutionary rate, Aoki (2013) found that innovation rates were more important than population size to determining the rate of evolution in a population.

To us, this body of work indicates that while population size is an important parameter in mathematical models, it may be better understood as a second-order effect in the real world, interacting with a myriad of other factors and thus often dominated by those factors. Another important factor is the structure of bands or demes into larger regional metapopulations. Network topology, for example, is known to have a substantial effect upon contagion or diffusion processes (e.g., Castellano et al., 2009; Smilkov and Kocarev, 2012). Thus, it is likely that regional structure has critical effects on the outcomes we can expect from a single social “learning rule.” Along these lines, Premo (2012) has examined whether metapopulation dynamics that include local extinction and recolonization might provide an improved account for the retention and expansion of diversity.

A second group of studies has focused upon endogeneous changes to social learning processes. Many authors in this volume series, for example, have looked at aspects of the way individuals learn skills and acquire information (Aoki, 2013; Nishiaki et al., 2013). We know that learning and teaching styles vary across human groups, and formal modeling efforts are beginning to make clear that such variation has evolutionary consequences that might lead to a rapid expansion of the human cultural repertoire (Nakahashi, 2013). Those populations which increased the amount or effectiveness of teaching would have a fitness advantage over those who relied upon imitation and “natural pedagogy” in passing along technological and foraging knowledge (Csibra and Gergely, 2011; Fogarty et al., 2011; Terashima, 2013). Demography and population structure would then play an important role in reinforcing the fitness differences which different learning strategies would create, as pointed out by Kuhn (2013).

Ultimately, a full “learning explanation” for behavioral modernity will be multifaceted, including demographic and spatial changes as well as changes to the mechanisms of social learning and technological innovation themselves. Sterelny (2012, p.61) sums up this kind of multifactorial approach

to behavioral modernity well:

...the cultural learning characteristic of the Upper Paleolithic transition and later periods of human culture—social transmission with both a large bandwidth and sufficient accuracy for incremental improvement—requires individual cognitive adaptations for cultural learning, highly structured learning environments, and population structures that both buffer existing resources effectively and support enough specialization to generate a supply of innovation.

In research designed to explore how the structure of a learning environment affects the results of social learning, Creanza and colleagues (2013), Aoki (2013), Nakahashi (2013), and Castro and colleagues (2014) developed models that examine how explicit teaching (as opposed to simple imitation) affects the overall evolutionary rate or cultural diversity in a population. Castro et al., for example, find that cumulative cultural transmission requires active teaching in order to achieve fidelity across generations. Our work in this chapter follows these authors, focusing on the nature of transmitted information itself and the effects of teaching upon the richness of structured technological knowledge.

In particular, we suggest that when knowledge is structured such that skills and information must be learned in sequences, high fidelity learning environments are critical to evolving ever-richer cultural repertoires, of the type seen in behaviorally modern assemblages. To formalize this idea, we construct a model which:

- Represents cultural traits as hierarchically structured, in order to study increases in complexity,
- Has a learning rule sensitive to the order in which cultural traits are acquired, with multiple levels of fidelity, and
- Has a mechanism (such as homophily) that allows cultural differentiation endogenous to the model.

As we alter the “learning environment” in our models from less to more frequent teaching of traits and their prerequisites, we expect to see greater diversity, larger structured sets of traits persisting in the population, and greater differentiation of the population into “different” cultural configurations. We also expect that individual innovation, independent of the social learning context, will play a role in the accumulation of cultural complexity by allowing a population to explore increasingly large spaces of technological design possibilities; this expectation is concordant with Aoki’s (2013) result in Volume I of this series.

In this chapter, we introduce a simulation model which combines a hierarchical trait space capable of expressing dependencies or semantic relationships between skills and information (Mesoudi et al., 2008), and a modified version of Robert Axelrod’s (1997) homophilic social learning model which allows us to examine the conditions under which evolution in a hierarchical design space leads to cultural differentiation. After describing the model, we study its dynamics and provide an initial assessment of its suitability for studying the onset of behavioral modernity in the later Paleolithic. Models like this begin to move beyond diffusion dynamics, bringing the actual meaning and relations of traits into the modeling process. Hence, we call these “semantic Axelrod” models, and believe that such models form a platform for formalizing the type of multi-factor hypotheses necessary to examine major transitions in human evolution, such as “behavioral modernity.”

7.2 The Semantic Axelrod Model for Trait Prerequisites

Much of our technical knowledge, whether of stone tool manufacture, throwing clay pots, or computer repair, is built from simple tasks, bits of background knowledge, and step-by-step procedures (Neff, 1992; Schiffer and Skibo, 1987). These pieces of cultural information are not simply a set of alternative options, which can be mixed and matched in any combination. Instead, there are dependencies and relationships between items which affect how skills and information are learned and passed on between individuals. Some items will be related in time, as steps in a process. Others will

be related by subsumption: arrowheads are a subclass of bifacial stone tools, and require many of the same production techniques as bifaces used in other projectiles. Still others will be related as sets of alternatives: choices of surface treatment for a given ceramic paste, given the firing regime selected, for example. To date, most archaeological models of tool production have focused upon temporal relations in the construction of an artifact, as in “sequence models” or “chaîne opératoire,” but it is important to remember that other representations are possible, including trees and more general graphs to capture relations of use, reworking, or discard (Bamforth and Finlay, 2008; Bleed, 2008; Ferguson, 2008; Högberg, 2008; Bleed, 2001, 2002; Schiffer and Skibo, 1987; Stout, 2002).

Given conscious reflection, we describe and organize our knowledge and skills in many ways, but it is common (especially while learning a new skill) to think of a complex process as a “script” or “recipe” (Schank and Abelson, 1977). Experts in a task or field may not represent their knowledge this way, having internalized such structures below the conscious level. Experts will often know more than one way to accomplish any given goal, and be able to repurpose and recombine methods and tools, as opposed to the simpler, more linear or tree-based recipes of the novice or student (e.g., Bleed, 2008, 2002; Stout, 2002). Nevertheless, it is common to teach or learn new information and skills in a stepwise manner.

In this chapter, we focus not on the execution steps of a recipe (and thus not on sequence models), but the relations between skills and information *during the learning process*. In specific, we focus upon the *prerequisite* relationships that exist between cultural traits, since the ordered dependencies between skills and information form one of the structures within social learning occurs during development (and into adulthood). Some pieces of information or skills must be in place before a person can effectively learn or practice others. Examples from our own childhoods abound: one needed to understand addition and subtraction and multiplication before learning long division; in order to make soup, we need to understand how to simmer rather than boil, how to chop and slice, what ingredients might be combined, and so on. The fact that knowledge and skills build upon one another make prerequisite relations between cultural traits ubiquitous. In this chapter, we represent

prerequisite relations as trees in the graph-theoretic sense ([Diestel, 2010](#)), replacing the “nominal scale” structure of “locus/allele” models or paradigmatic classifications and some typologies ([Dunnell, 1971](#)), but we emphasize that the tree models we discuss here are still classifications and thus analytic tools, designed to allow us to measure variation in the archaeological record, not reconstruct emic models of Paleolithic technologies.

Our model also requires a way of representing a changing learning environment, in ways that create higher fidelity and greater possibility for building cumulative knowledge. In real learning environments, there are many possibilities, but deliberate teaching and apprentice learning are repeatedly seen across human groups as ways that naive individuals can reliably learn the complex skills and information needed for foraging, artifact production and maintenance, and navigating an increasingly rich social world. The point of structuring the learning environment with teaching and/or apprenticeship is to give the learner skilled models to imitate, shortcut trial and error when acquiring a skill, provide a reference for needed information, and to guide individuals to put their information and skills together into appropriate sequences to accomplish an overall goal. Apprenticeship and formalized teaching provide a social learning “scaffold,” helping to lower the amount of individual trial and error learning needed to master a body of material ([Wimsatt and Griesemer, 2007](#); [Wimsatt, 2007](#)).

Within a standard discrete-time simulation model of a social learning process, we can model this type of learning environment with the following modifications:

1. Represent the order in which skills and information need to be acquired as a series of trees, with vertices representing traits (either a skill or piece of information), and edges the prerequisite relations between them.
2. Disallowing individuals the ability to copy traits from a cultural model for which they do not have necessary background or prerequisites, given the relations in the applicable tree model.
3. Creating a probability that individuals, if disallowed a trait, can be taught one of the needed prerequisites instead by that cultural model, leading to the potential accumulation of fuller

knowledge and skills over time.

By changing the probability that individuals learn a missing prerequisite trait, we can “tune” the learning environment. Low probabilities might correspond, for example, to a learning environment where individuals can observe others executing a production step, but are given little or no instruction or guidance on what they need to know in order to successfully master it. High probabilities of learning prerequisites would correspond, on the other hand, to environments where individuals receive instruction, or work together with a more skilled individual who guides them toward learning the information and skills they lack. In the next section, we discuss our model of trait relationships and the learning environment in more detail.

7.2.1 Representation of Traits And Their Prerequisites

In order to represent the “prerequisite” relations between a number of cultural traits, we organize the traits into trees¹, where nodes higher in the tree represent knowledge, skills, or concepts which are necessary for traits further down the tree. Let us consider the different skills and information necessary for the construction of a single artifact, say a dart thrown by an atlatl. An artisan will possess information about different raw materials, an understanding of what materials are suitable for specific purposes, skills and information concerning the knapping of different types of bifaces, methods of hafting bifaces into different kinds of shafts, and so on. Stout (2011) organized such knowledge into “action hierarchies,” which represent sequences of actions, sets of choices, and optional elements for the construction of a class of stone tools, drawing the representation from Moore’s (2010) graphical notation.

We should emphasize that employing tree structures to represent learning dependencies is a modeling choice. Other choices may be sensible as well. General graphs could represent webs of relations

¹A tree is a graph with no cycles or loops. That is, a tree is a connected graph on n vertices that possesses at most $n - 1$ edges (Diestel, 2010). Furthermore, in this chapter we are concerned with *rooted* trees, in which one vertex is distinguished as the “origin” of the tree, giving rise to a hierarchical structure.

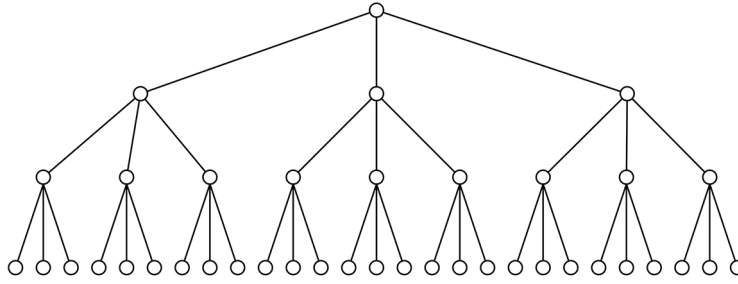


Figure 7.1: A single trait tree, represented by a balanced tree with branching factor 3 and depth factor 3, order 40. In our model, nodes higher in the tree represent prerequisites for nodes lower down the tree. Each instance of the model will have several or many of these trees in the design space.

between concepts or skills, and multigraphs (replacing adjacency matrices with tensors) can represent different types of relations in a single structure (Nickel et al., 2011). For purposes of the present chapter, we are interested in the order in which people usually *learn* skills and information, rather than the order in which steps are executed. The difference is potentially significant, in that two adjacent steps in a sequence might involve very different information, tools, or skills, which can be learned in parallel without dependencies. Because, in our model, traits cannot be learned unless an individual possesses the necessary prerequisites, we introduce the idea of a “learning hierarchy,” which is a division of Stout’s action hierarchy into components which are learned with ordered dependencies, and independent components represented in separate trees. For example, one might learn about the sources of good lithic raw materials, independent of learning how to perform different percussion techniques. In our model, each of these independent areas is represented by a separate tree of traits.

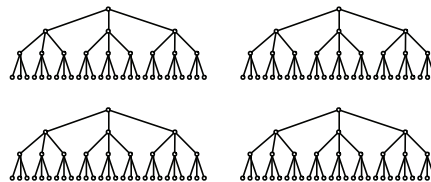


Figure 7.2: A design space composed of 4 independent trees, each tree with branching factor 3 and depth factor 3, order 40. We also studied larger design spaces with 16 independent trees, and with larger branching and depth factors.

In each simulation model, we begin with a trait or “design space” that incorporates several inde-

pendent sets of traits (O'Brien et al., 2010). The overall design space of a simulation model is thus a forest², composed of several trees (Figure 7.2). For each tree in a learning hierarchy, we employ balanced trees which have the same number of nodes at each level, to provide a simplified model of a design space with which to begin our exploration of this class of social learning model, although real design spaces are undoubtedly more complex in their geometry. Each tree in our model is specified by a branching factor r and depth h . As a result, each trait tree in the design space has $\sum_{i=0}^h r^i$ traits.

The tree depicted in Figure 7.1 thus has 40 vertices, for example. In this chapter, we examine both small (4 trees) and larger (16 trees) design spaces, to see how learning may differ in problems involving design spaces of different size and complexity. We examine trees with combinations of branching and depth factors of 3 and 5. Thus, a design space with 4 trees with branching and depth factors of 3 (as in Figure 7.1) would have 160 traits, whereas a design space with 16 trees of branching and depth factors of 5 would have a total of 62,496 traits.³ Even the small design spaces we consider here create a large space for cultural change and differentiation, given the number of possible trees one can construct on even 40 vertices.⁴ In the experiments reported here, the overall size of the design space remains constant over time, which is a simplifying assumption as we develop this class of structured information models. In future work, we will explore the role of invention in episodically creating large new regions of design space for the evolving population to explore.

Given the total “design space” represented by a forest of trait trees, each individual in our model is initialized with a small number of “initial” traits. Initial traits are chosen randomly but heavily weighted towards the roots of the trees to represent the fact that our knowledge starts out basic and sparse. In general, all of the design spaces modeled here are larger than populations will explore

²A forest is a graph composed of multiple components, each of which is a tree.

³We initially chose 6 as the limit on branching and depth factors, but found that we cannot calculate certain symmetry statistics, such as the size of the automorphism group, on trees that large using existing tools. Even a tree with $r = 5, h = 6$ has over 10^{1623} possible symmetries, and an attempt to calculate the symmetries for $r = 6, h = 6$ did not complete given the memory limits of the computers we had available.

⁴If we consider each trait to be unique and non-interchangeable, the number of unique trees with unique vertex labels is n^{n-2} by Cayley's theorem (Diestel, 2010). For example, for each trait tree of 40 vertices, there are roughly 10^{60} possible trees. Even if we consider traits to be interchangeable (e.g., we look at the abstract topology of trees rather than the details of individual traits), there are *at least* 10^{16} possible unlabelled rooted trees on 40 vertices (using Otter's (1948) approximation).

within the bounds of a simulation run. In the next sections we describe the social learning model, modified from Robert Axelrod's original, by which each simulated population evolves within this tree-structured design space, and will return to the specifics of how an initial culture repertoire is chosen.

7.2.2 The Axelrod Model of Social Learning and Differentiation

Robert Axelrod (1997) formulated a model aimed at studying the conditions under which simple learning rules could lead to cultural differentiation, rather than a single fixed state (which is the result of simpler neutral or diffusion models). This makes it useful as a starting point for understanding phenomena such as behavioral modernity, in our view. Axelrod's model combines social learning, in the form of random copying, a spatial structure to interaction, in the form of localized copying of neighbors on a lattice, and the tendency to interact most strongly with those to whom we are already culturally similar (homophily). The model displays a rich and interesting set of behaviors, and has been extensively studied by social scientists and physicists (Castellano et al., 2009). First we review the basic model, and in the following section our modified algorithm.

7.2.2.1 Axelrod's Original Model

The original model locates N individuals on the nodes of a regular lattice or grid, but various network structures have also been studied. Each individual is endowed with F integer variables $(\sigma_1, \dots, \sigma_F)$, that can each assume q values. In the original model, each variable is a "cultural feature" each of which can assume q "traits." In each step, a randomly chosen individual i and a random neighbor j are selected, and "interact" with probability equal to the overlap between their cultural repertoire. Overlap, in the basic model, is simply the fraction of features for which i and j possess the same trait value:

$$p(i, j) = \frac{1}{F} \sum_{f=1}^F \delta_{\sigma_f(i)\sigma_f(j)} \quad (7.1)$$

where $\delta_{i,j}$ is Kronecker's delta function, taking the value 1 when its two arguments are equal and 0 otherwise. When individuals interact, the focal individual i takes the trait value of its neighbor for one of the features where the two individuals differ.

Interaction has no effect when two individuals already possess identical cultural repertoires, and there is no probability of interaction if individuals have no traits in common. This eventually causes the model to reach an absorbing state where no further changes are possible. Instances of the model are initialized with a random distribution of traits among individuals, and left to update until the steady state is reached. The evolution of the population leads to two classes of absorbing states: (a) a “monocultural” state in which all individuals share the same set of variables, and (b) a “polycultural” state in which subpopulations exist which share the same set of variables within the group, and are completely different from their neighbors.

Which of the two results is reached, and the statistical character of “polycultural” states when they exist, depends mainly upon the number of traits possible q for each cultural feature. For small values of q , individuals share many traits with their neighbors, interactions are thus frequent, and one domain comprising a single set of traits will grow to become fixed within the entire population. In contrast, when the value of q is high, individuals start out sharing very few traits, with interactions that are correspondingly less frequent. Regions of uniform cultural variation do grow, but as they do, sets of individuals who share no traits at all (and thus do not interaction) grow as well, and often prevent any single regional culture from expanding to fix within the population.

Many variants of the basic Axelrod model have been studied, including the addition of “drift” via the introduction of copying error, situating agents on different types of complex networks, the addition of an external “field” to simulate the effects of mass media, and copying that obeys a “conformist” or majoritarian rule by selecting the most common trait among the neighbor set ([Castellano et al., 2000](#); [De Sanctis and Galla, 2009](#); [Flache and Macy, 2006](#); [Gonzalez-Avella et al., 2007b,a](#); [González-](#)

[Avella et al., 2005, 2006](#); [Klemm et al., 2003a,b, 2005](#); [Lanchier et al., 2010](#); [Lanchier, 2012](#)). In general, modifications of the basic model can reduce the tendency of the model to produce polycultural solutions, or change the time scale or location of the critical point.

7.2.2.2 Semantic Extensions to the Axelrod Model

We begin each simulation with N (100, 225, or 400) agents, arranged on a square grid. A design space is created, with some number of trait trees (4 or 16), with uniform branching factors and depth factors (3 or 5). An example of such a tree is shown in panel A of Figure 7.3. Initial traits (and their prerequisites) are chosen randomly across the configured number of trait trees, as follows. For each individual, we select a random number t between 1 and 4, and repeat the trait selection process t times for that individual. In each selection, we choose a random tree in the design space, and then select a depth in the tree for the trait, given by $d \sim \text{Poisson}(0.5)$. This biases trait selection towards the root of the tree, as one would expect in young or inexperienced individuals. We then walk d steps into the tree, making uniform random selections for the children of each vertex. The path of vertices thus constructed is added to the individual's trait set, giving them an initial trait and its necessary prerequisites. One such initial trait is shown in Panel B of Figure 7.3. Given that individuals begin with a small number of initial traits (between 1 and 4, selected randomly), and their prerequisites, the initial trait endowment of an individual is between 1 and $4h$, where h is the maximum depth of the design space (either 3 or 5 in the experiments reported here).⁵

Once the population is initialized, the simulation runs a discrete approximation to a continuous-time model. In other words, only one agent changes at each elemental time step, as in the original Axelrod model and the Moran model of population genetics and its cultural version ([Aoki et al., 2011](#); [Moran, 1962, 1958](#)). At each step, an agent (A) is chosen at random, and a random neighbor of A is then selected (agent B). Their probability of interaction is given by the overlap of trait sets, which

⁵At maximum, this yields some individuals who begin the simulation with up to 20 traits. The median number of traits in samples taken after 6–10 million time steps is considerably higher—259 traits per cultural configuration or region. Thus, cultural repertoires in the simulation grow through copying and innovation, as expected.

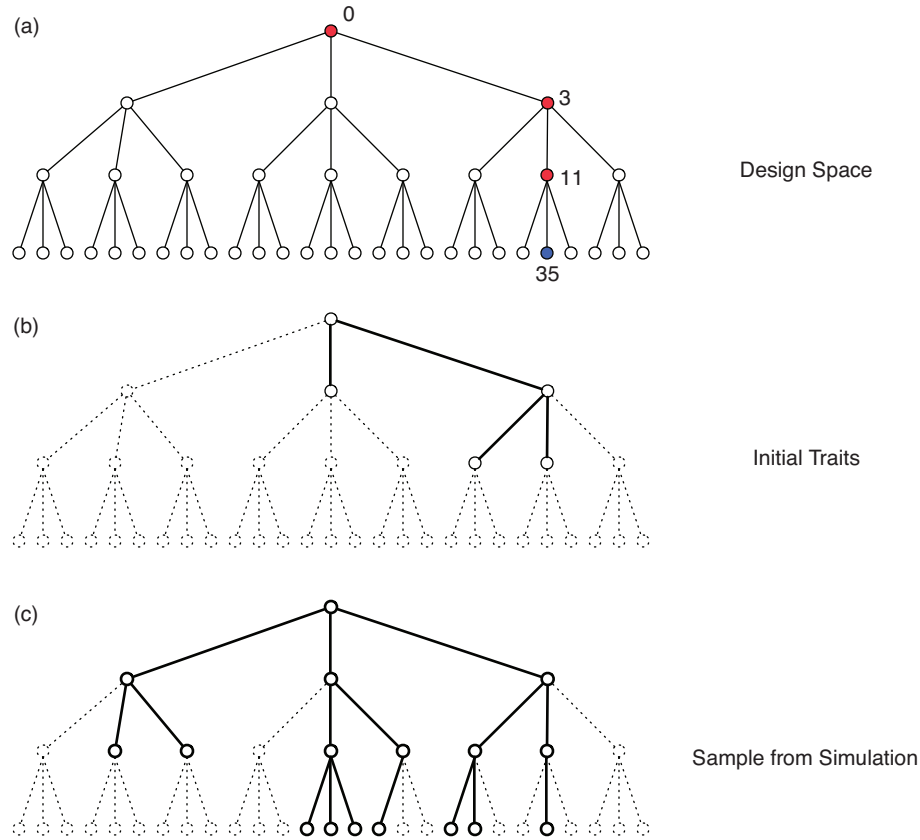


Figure 7.3: Illustration of a design space composed of a single trait tree, along with a random initial trait chosen from the design space, and a final sample from a simulation run, showing the evolution of traits within the design space. Also shown in the top panel are the “prerequisites” for a cultural trait (35), as an example.

is most simply calculated as the Jaccard overlap between the set of tree vertices each possesses, thus replacing Equation 7.1 with:

$$J(A, B) = \frac{|V(A) \cap V(B)|}{|V(A) \cup V(B)|} \quad (7.2)$$

where $V(i)$ represents the vertex list for trait trees held by individual i in the population.

If the agents end up interacting, agent A observes the traits currently possessed by B , and selects a trait (T) that it does not already possess to learn. If agent A has the necessary prerequisite traits for the selected trait, it can learn trait T . If not, there is a probability $\mathbb{P}(I)$ that B can teach A a necessary

prerequisite for T instead. This simulates the process of agent B structuring the learning environment of A through formal instruction or apprenticeship, for example. If such a prerequisite learning event occurs given $\mathbb{P}(1)$, agent A learns the most fundamental of T's prerequisites that it does not already possess. For example, agent A might require the trait closest to T (e.g., trait 11 in Figure 7.3, if the original trait targeted was 35).

Additionally, at each time step, there is a probability $\mathbb{P}(m)$ that one random individual in the population will learn a new trait (and necessary prerequisites) that it does not already possess. For example, if an innovation event occurs and an agent discovers trait 35 by individual trial and error learning, we assume that the agent also discovered traits 0, 3, and 11. Thus innovation can introduce one trait to the population, or a linked set depending upon its prerequisites and what the innovating individual already “knows.” This model of innovation simulates an ongoing process of individual learning unconnected to social learning or teaching within the population. Because this functions much like “infinite-alleles mutation” in the classical Wright-Fisher neutral models (Ewens, 2004), or like noise terms in Axelrod, Ising, or Potts models (Castellano et al., 2009), we will refer to this as the “global innovation rate” in this chapter.

One of the editors noted that this model of innovation may not be as realistic as an alternative, where random innovations would be “discoverable” only with the correct prerequisites in place. We believe that innovation in the face of skill or knowledge prerequisites is continuous between these two models. Occasionally one will discover a new piece of knowledge or develop a skill, having learned surrounding and related knowledge. In other situations, individuals may learn sequences and sets of information or skills by trial and error and “tinkering.” The “size” of innovations that can be learned purely by individual trial and error should thus vary between these extremes, biased towards the “small” end of the range. Our selection of an innovation model where individuals discover a trait and its prerequisites thus potentially overestimates the effect of individual learning, but it made certain graph operations easier, and can be relaxed in future models.

Each simulation run lasts 10^7 steps, which yields between 10^4 and 10^5 copying events per indi-

vidual, depending upon population size.⁶ Since we do not explicitly model the interaction between cultural transmission and biological reproduction here, we can interpret the model as representing either fine-grained learning within individuals over the course of their lifetimes, or long-term cultural evolution within a fixed size population where we are not modeling fitness. We felt this simplification was appropriate in a pilot study exploring structured information models, but a more detailed study would include dynamics on two time scales: developmental learning and evolutionary dynamics given birth and death. Samples are taken beginning at 6 million steps, and sampling at an interval of 1 million steps, and record the trait trees seen in the population. An example of such a sampled tree is shown in Panel C of Figure 7.3. For reference, the full algorithm for each copying step is given in the Appendix as Algorithm 7.1.

7.3 Measuring Cultural Diversity and the Results of Structured Learning

Each sample from a simulation run is composed of the distinct sets of trait trees possessed by individuals in the population, along with summary statistics. If a simulation run converges to a monocultural solution, the sample will have one set of trait trees, which are shared across the entire population. In other cases, there will be clusters of cultural configurations which might be unique to a single individual, or shared by some number of agents. Each cluster will be composed of some number of trait trees (typically, the number configured for the simulation run: 4 or 16, but perhaps a subset), and each trait tree will be the result of many agents learning traits and their prerequisites socially, and for runs with a non-zero mutation rate, by individual learning or innovation. Each cluster will thus have some number of traits, typically higher (often much higher) than the initial endowment given to the population.

⁶100,000 was chosen as a compromise for running large batches of simulations in parallel. Some simulation runs, especially in small design spaces with very high prerequisite learning rates, can converge to a monocultural solution and quasi-stable equilibrium quite quickly; in the largest design spaces and low learning rates, convergence may never occur even though the process is well-mixed. However, the processes have reached a quasi-stable equilibrium, verified by examining samples at different times for secular trends in median and mean values, which were not found.

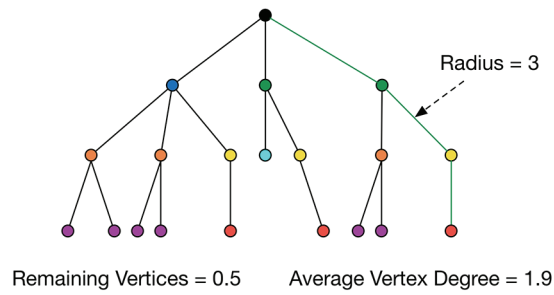


Figure 7.4: An example set of traits at the conclusion of a simulation run, extracted from a simulation with branching factor 3 and depth factor 3, and a single trait tree as the trait space. The remaining density of vertices, mean vertex degree, and radius of the tree are noted. Vertex colors denote “structural equivalence” classes or “orbit structure,” as measured by adjacency patterns, and is one measure of the symmetries present in the tree.

From the sampled trait trees, we calculate summary statistics as follows. The ratio of the number of traits in the sample to the full design space size (or “remaining density” of traits) is one measure of trait richness. The radius of a rooted tree is the number of edges in the path from root to the furthest edge. The average radius of trees in a sample (or its ratio to the depth of the design space) is another richness measure, aimed at measuring whether knowledge with multiple prerequisites is being learned within the simulated population. Similarly, in the original design space, the branching factor describes how many children each node in the tree started with, so measuring the average vertex degree gives us a rough measure of how broad a cultural repertoire is. Each of these measures is illustrated in Figure 7.4 for an example tree selected from our data.

In addition to these simple numerical measures comparing final trees to the original design space, it is useful to measure something about the overall “shape” of the trees themselves. One way of formalizing this notion is to examine the *symmetries* of the final trait trees. Examining Figure 7.4, if we ignore the exact identities of traits for the moment, it is apparent that there are repeating patterns. For example, the left-most branches each terminate in a pair of leaves. This pattern is repeated on the second right-most branch. These types of repeating patterns are computationally expensive to search for in large sets of trees, but we can summarize them by considering trait trees as algebraic objects and examining their *automorphisms*.

An automorphism is a function which maps an object to itself, in such a way that the structure of the object is preserved (Rotman, 1995). Graph automorphisms map vertices in a graph to each other, preserving properties such as the adjacency pattern of edges. The six vertices which mark the repeating pattern of leaf-pairs in Figure 7.4 are an automorphism of the tree, and thus are symmetries we can measure. An overall measure of “how symmetrical” (or “how many interchangeable patterns”) there are in a graph possesses given by the total number of automorphisms found, called the size of the automorphism group or $|Aut(G)|$ (Godsil and Royle, 2001). A tree with no repeating patterns will thus have an automorphism group size of 1, indicating that the only symmetry is the entire tree itself. A balanced tree with branching and depth factors of 3, as depicted in Figure 7.1, has approximately 1.3×10^{10} automorphisms. The more repeating patterns there are in trait trees, the more automorphisms they will possess.

Because group sizes grow quickly and the accuracy of performing calculations with truly astronomical numbers is low, another possible measure of the symmetries present is to count the *classes* of equivalences into which vertices fall. The *orbits* of the automorphism group are the sets of vertices which are interchangeable by some permutation that preserves structure. For example, the graph in Figure 7.1 has five orbits, with each vertex at a given level interchangeable (in a structural sense). Similarly, the six leaf vertices that are part of pairs in Figure 7.4 are part of the same orbit; in this illustration, each orbit is given a different color to highlight their equivalence. For each cultural region found when sampling a simulation, we calculate the size of the automorphism group and the number and multiplicity (frequency) of orbits. For this analysis, we employ the *nauty* + *Traces* software by Brendan McKay and Adolfo Piperno (McKay and Piperno, 2014).⁷

⁷Nauty+Traces can be downloaded at <http://pallini.di.uniroma1.it/>. We employed version 2.5r7 for this research.

7.4 Experiments

Given a modified Axelrod model on a tree-structured trait space, we expect to see greater cultural diversity, differentiation among groups of individuals, and larger sets of traits as the “learning environment” is tuned from a low to high probability of teaching and learning among individuals. We also expect that individual innovation, independent of the social learning context, will increase the amount of the technological design space that a population explores, which leads to enhanced opportunities for differentiation even through simple random copying. Here we measure cultural differentiation by the number of clusters of individuals who share the same trait trees when we sample the population.

Second, we looked at whether highly structured learning environments, represented here by higher probabilities of naive individuals gaining the prerequisites for the skills and information they encounter with peers, led to deeper and richer cultural repertoires. We explore a number of ways of measure the richness of a cultural repertoire in a model with structured relations between traits, through the use of graph properties and symmetry measures. The measures used are those described above: the tree radius (or depth), mean vertex degree, the fraction of remaining vertices, and the size of the automorphism group of sampled trait forests. Finally, we began to examine how the structured learning environment might interact with demography, by simulating the same parameters across two sizes of population.

For this chapter, we examined populations of size 100, 225 and 400, to begin to examine the effects of population size. For these populations, we examined design spaces that were small (4 trait trees) and large (16 trait trees). Within each size, we further examined combinations of branching factor and depth factor with values of 3 and 5, thus yielding 8 total sizes of design space (Table 7.1).

Branching Factor	Depth Factor	Number of Trait Trees	Size of Design Space
3	3	4	160
5	3	4	624
3	5	4	1456
5	5	4	15624
3	3	16	640
5	3	16	2496
3	5	16	5824
5	5	16	62496

Table 7.1: Size of design space for different trait tree configurations

Further, we examined three levels of global mutation or innovation rate: zero, or no mutation, and 0.00005 and 0.0001. Such rates created a constant supply of new innovations, but several orders of magnitude less frequent than copying and prerequisite learning events. The full set of parameters are given in Table 7.2. In this pilot study, for each combination of all of the above parameters, we performed 25 replications. With 5 samples per simulation run, this yielded 10,963,691 samples of cultural regions.

Simulation Parameter	Value or Values
Population rate at which new traits arise by individual learning	0.0, 5e-05, 0.0001
Maximum number of initial traits (not including their prerequisites) each individual is endowed with	4
Number of distinct trees of traits and prerequisites	4, 16
Population sizes	100, 225, 400
Replicate simulation runs at each parameter combination	25
Maximum time after which a simulation is sampled and terminated	10000000
Individual probability for being taught a missing prerequisite	0.05, 0.1, 0.2, 0.3, 0.4, 0.5, 0.6, 0.7, 0.8, 0.9
Number of branches at each level of a trait tree	3, 5
Depth of traits in each trait tree	3, 5

Table 7.2: Parameter space for simulations described in this chapter

7.5 Results

We begin by noting that compared to the original Axelrod model, or neutral and biased copying models, the dynamics of our semantic Axelrod model are highly variable. A very wide range of outcomes is possible for each parameter combination, especially when the size of the design space is large. Some variables, such as the average vertex degree of sampled trait trees, are strongly overlapping across all learning rates and do not appear diagnostic of different learning environments, at least in these initial experiments. Given the large amount of variability in the dynamics, larger numbers of replications would be useful, although this is computationally quite expensive at present.⁸ That said, several features of the data are strongly suggestive that hierarchical trait models have potential in modeling cumulative technological evolution, making the computational expense worthwhile.

7.5.1 Cultural Diversity

Variation among individuals is foundational to evolutionary processes, and is the raw material from which differentiation between regions and cultural groups is constructed. Figure 7.5 depicts the number of cultural configurations (i.e., trait trees) in a population of size 100, for the smallest trait space with only 160 total traits, and relatively high levels of individual innovation. For example, in the left-most panel the large peak just above zero indicates that most simulated populations are characterized by one or a few sets of trait trees. Five learning rates are depicted, increasing from left to right across the panels. At the very lowest rate of learning fidelity, with only a 10% chance of being taught a needed prerequisite for knowledge being copied, most of the populations simulated share a single set of traits, and even individual innovation does not drive significant exploration of the space of structured traits. With increased fidelity in teaching needed prerequisites, however, simulated populations begin exhibiting marked differentiation, with individuals possessing more unique configurations of

⁸The simulations reported here ran on a cluster of 6 compute-optimized “extra large” Linux instances on Amazon’s EC2 computing cloud, for a total of 17 days of wall clock time and 2075 CPU hours. We plan further optimizations to the simulation code to make larger samples economically feasible.

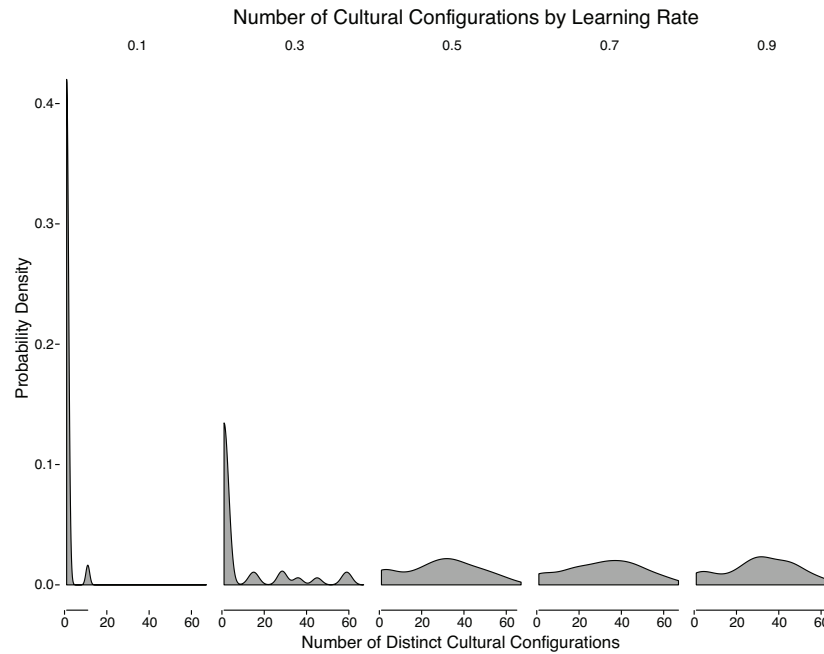


Figure 7.5: Number of cultural configurations in simulations with the smallest trait space (160 total traits in 4 trees), and a high individual innovation rate (10^{-4}).

traits from the overall design space.

Looking at the data from another perspective, we can hold the fidelity of learning constant (say, at a 40% chance of being taught a needed prerequisite), with the same global innovation rate (10^{-4}) as Figure 7.5, and examine the effect of different size design spaces (Figure 7.6). In general, populations exhibit greater differentiation between individuals as the design space gets larger, as prerequisite learning helps individuals acquire adjacent traits, and individual innovation randomly explores more distant portions of the design space.

Given the structure of the Axelrod model, with the strong tendency towards cultural uniformity given homophily, all simulated populations converged to a single cultural configuration in the absence of a global innovation rate. This highlights the importance of various “innovation” and “invention” processes in the creation and maintenance of cultural differentiation and diversity (Eerkens and Lipo, 2005; O’Brien and Shennan, 2010), and suggest that highly conservative cultural repertoires, such as those posited to precede behavioral modernity in hominin populations, occur whenever individuals

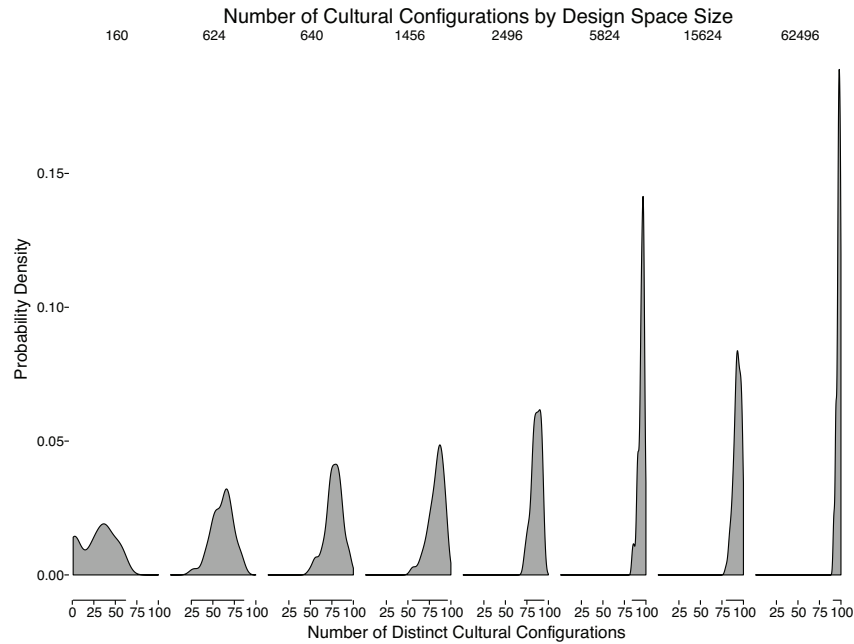


Figure 7.6: Number of cultural configurations in simulations with an intermediate learning rate (0.4), across different sizes of trait space.

engage in social learning in small technological design spaces, in the absence of strong and regular individual innovation.

7.5.2 Trait Richness and Knowledge Depth

Cumulative evolution of technology is represented in our model by the population learning its way *down* the trees which compose the design space. Possession of traits deeper in the trees represents skills or information which is more specific, possessing more prerequisites. Thus, we expect that the depth (or “radius”, see Figure 7.4) of trees would increase with the prerequisite learning rate, representing a learning environment which is structured to ensure such acquisition.

Figure 7.7 gives the *normalized* mean radius of cultural regions, broken out by the prerequisite learning rate along the horizontal axis, and each group of 3 boxplots displays the differing global innovation rates studied. Radii are normalized to the depth of their design space, to facilitate comparison. The results indicate that essentially two regimes exist: shorter trees, which do not grow much beyond

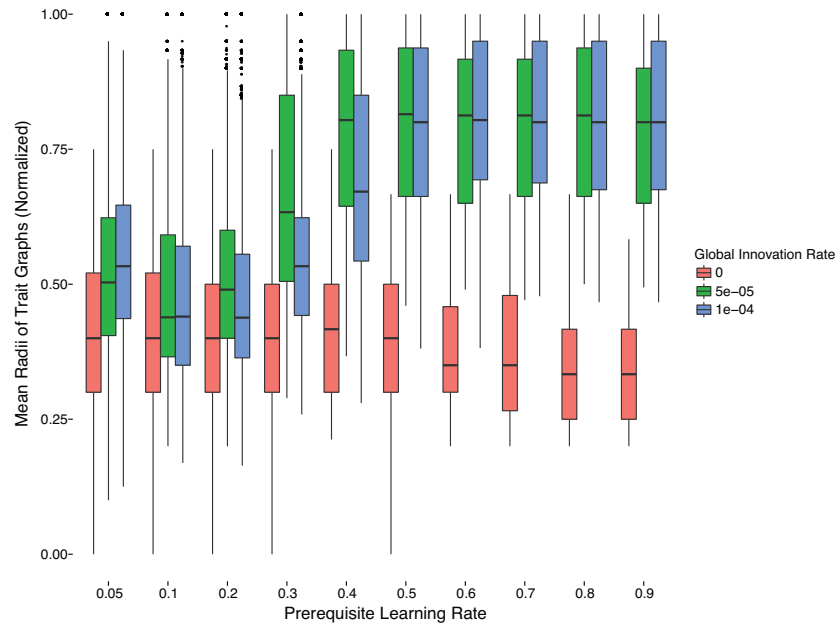


Figure 7.7: Mean depth of trait sets, by prerequisite learning rate and global innovation rate, for population size 100.

their initialized size, and larger trees. The mean radius has an asymptote just above 0.75, achieved with the prerequisite learning rate is approximately 0.4 or higher. Further increases do not seem to matter. Additionally, the difference between the two global innovation rates is small—what matters most in terms of qualitative behavior is the presence of global innovation outside the teaching or learning of prerequisites themselves.

7.5.3 Population Size

Earlier, we mentioned that population size does not seem to be a primary factor in explaining the measured diversity in cultural transmission models, except perhaps in bottleneck situations like the one Henrich analyzes in Tasmania (2004). Instead, population size may have an interaction effect with other factors, yielding smaller second-order effects. We examined the effect of population size in the research reported here, repeating the entire set of simulation runs for populations of 100, 225,

and 400.⁹

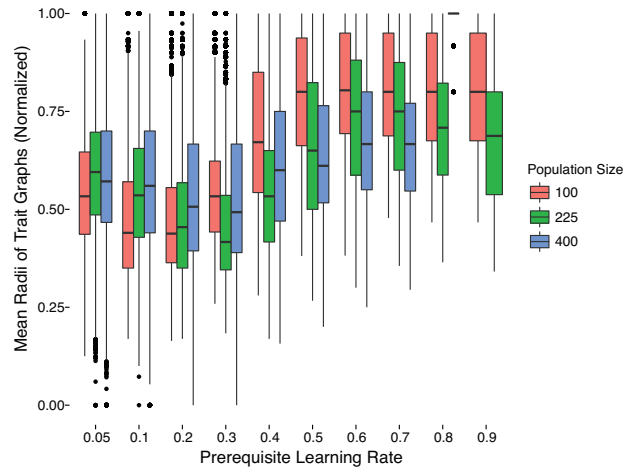


Figure 7.8: Mean depth of trait sets, by prerequisite learning rate and population sizes of 100, 225 and 400.

Figure 7.8 displays the relationship between mean radius (or depth) of the cultural traits in each cultural sample, as in Figure 7.7 above, but the boxplots are instead colored by population size. At least over a range of group or deme sizes likely to be relevant to Paleolithic archaeology, population size makes no difference to the qualitative behavior of the model. There is, however, a very slight decrease in mean radius of trait sets with larger population size, which is likely a consequence of a larger population spreading out over the trait space.

7.5.4 Trait Tree Symmetries

Finally, we examined the algebraic properties of the trait trees composing cultural regions, examining both the number of vertex equivalence classes (orbits) and the size of the automorphism group of the trait forests. We examined the raw metrics, and versions normalized by the size of the maximally symmetric forest with the same number of traits, branching factor, and depth factor. The latter proved

⁹We should note that learning rates of 0.8 and 0.9 for population size 400 were cut short due to budget constraints, but this does not appear to affect the pattern in our dataset.

difficult and led to serious overflow problems even with 64 bit arithmetic, so we focus here on the raw automorphism group size.

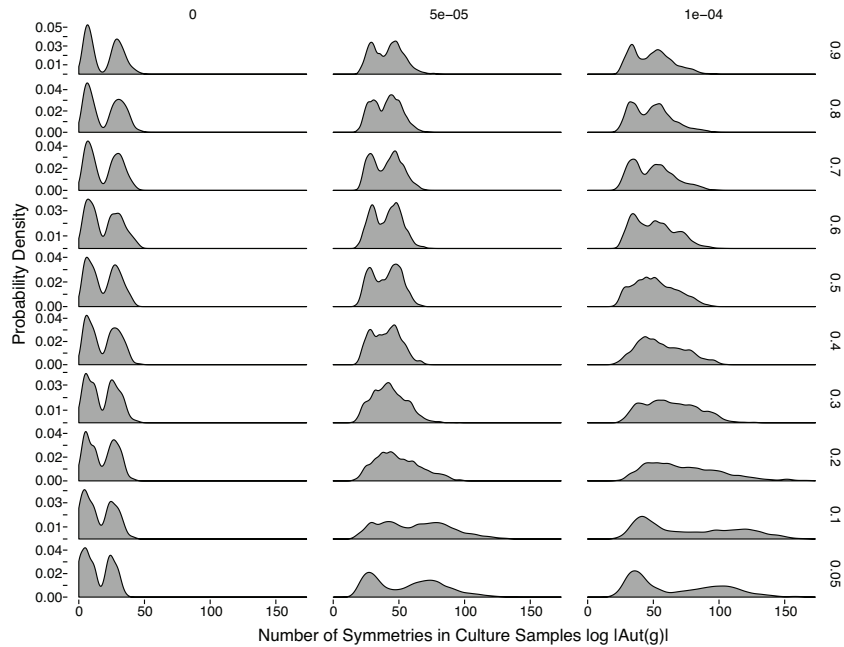


Figure 7.9: Number of symmetries in trait tree samples, measured as the log of the order of the automorphism group of the trait graphs, broken down by prerequisite learning rate (rows) and global innovation rate (columns).

The logarithm of the automorphism group size does hint at interesting structure (Figure 7.9). In the presence of mutation, the learning of prerequisites narrows the range of variability for the automorphism group size, and at higher learning rates renders the distribution multimodal. The modality arises because of the different combinations of branching factor and depth factor we employed for design spaces—i.e., some design spaces are “wide” and some are “narrow,” while also being “shallow” or “deep.” This gives rise to different modes in the measured symmetries, but overall the reduction in variability in symmetry is the most important qualitative effect seen in our data.

We do not fully understand the “shapes” of cultural regions to which the model appears to converge, but it appears that there is a tendency for trait graphs to converge towards shapes which have moderate numbers of symmetries. This graph is on a logarithmic scale, so a peak at 50 along the

horizontal axis corresponds to a trait graph with approximately 5×10^{21} symmetries. This is a fairly small number, compared to the original design spaces, which have symmetries ranging from approximately 10^{41} to 10^{6496} . Thus, the geometry of cultural traits in our hierarchical design spaces are fairly asymmetric and represent small and very specific segments of the total design space.

Further analysis of trait graph “shapes” is needed to tell whether there are repeating patterns or graph “motifs” which characterize a social learning model in a graph-structured trait space. The results here are suggestive of such a phenomenon, but inconclusive given just the bulk algebraic properties of cultural regions, since the size of the automorphism group (or the number of orbits) tells only *how many* symmetries there are, not what types of symmetries exist. The next step in our analysis of shape is to pursue a geometric decomposition of the graph following Ben MacArthur and Rubén Sánchez-García’s (2008) work on the symmetries of complex networks.

7.6 Discussion

The “semantic Axelrod” model described here specifically addresses social learning of knowledge with “prerequisite” structure, and a learning environment which is tunable from low to high fidelity, simulating the intensity with which “teaching” occurs in addition to imitative copying. The model displays a characteristic increase in the cultural repertoires of individuals, as they learn in environments of higher fidelity. At the individual level, an increase in higher fidelity learning within structured information environments both creates path-dependency in what is learned, and increases the chances for specialization among individuals. Hominin populations in which complex knowledge is taught systematically along with prerequisites will accumulate and retain skills and technology faster and to a greater extent than those groups which rely upon natural pedagogy and imitation for social learning.

Previous research had established the importance of teaching and learning environments for cumulative cultural evolution and cultural diversity (Aoki, 2013; Castro and Toro, 2014; Creanza et al.,

2013; Nakahashi, 2013). Our contribution in this paper is a model capable of connecting the fact of teaching with the actual structure and content of cultural knowledge. Such models, we believe, are important in explaining the explosion of cumulative material culture that accompanies behavioral modernity. The model described here only makes a start on modeling the additive and recombinative complexity of real technologies, but it does display accumulated depth of “knowledge” or “skills,” as represented by the radius or depth of trait trees. In combination with realistic models of technology—such as the production sequences studied by experts on stone tools—we believe that empirically sufficient models of the evolution of specific technologies are possible and within reach.

Several areas suggest themselves for future research in structured information or “semantic” cultural transmission models. Some we are pursuing, others remain open questions and we invite collaboration towards their solution.

- Regional scale cultural differentiation given a metapopulation embedding of the basic model.
- Additional trait relations (e.g., class subsumption, functional equivalencies).
- Realistic technology models for key artifact classes (e.g., bifaces, scrapers, pottery).
- Incorporation of trait fitness in order to study directional change.

Models of the class introduced here are “thicker” descriptions of how humans acquire skills and information in real learning environments, and thus complement existing models which describe the conditions under which teaching and structured learning might evolve and spread. We believe models of this type make a needed “downpayment” on cultural transmission models which can substantively incorporate specialties such as archaeometry, the technological analysis of lithics and pottery (Tostevin, 2012), and studies of how innovation occurs in various tool classes (e.g., O’Brien and Shennan, 2010). Bringing cultural transmission modeling together with the details of technologies will be a crucial component in multifactor evolutionary explanations for the complex of changes seen in modern *Homo sapiens* and some Neanderthal populations in the later Paleolithic.

7.7 Acknowledgements

The authors wish to thank Briggs Buchanan and Mark Collard for the invitation to participate in the symposium “Current Research in Evolutionary Archaeology,” at the 79th Annual Meeting of the Society for American Archaeology in Austin, TX. A summary of this research was presented in that session, and Alex Mesoudi provided valuable comments on an early post-conference draft. Kenichi Aoki and an anonymous reviewer provided feedback prior to publication, and although we did not take all of their suggestions, the comments led to a number of improvements. Madsen wishes to thank Frédéric Chapoton of the Institut Camille Jordan for answering a question about the maximal automorphism group of trees.

7.8 Appendices

7.8.1 Algorithm Description

Algorithm [7.1](#) describes the “semantic” Axelrod model variant studied in this chapter. Within the algorithm, there are several functions which find traits with particular properties. Some, like `GetTraitUniquetoFocal()`, are fairly simple set operations but were abbreviated to clarify the notation.

Algorithm 7.1

Require: innovrate is the population rate at which individuals randomly learn a trait
Require: learningrate is the probability of learning a missing prerequisite during a learning interaction

```

1: focal  $\leftarrow$  GetRandomAgent()
2: neighbor  $\leftarrow$  GetRandomNeighbor(focal)
3: if focal = neighbor  $\vee$  focal  $\cap$  neighbor =  $\emptyset$   $\vee$  neighbor  $\subsetneq$  focal then
4:   exit { No interaction is possible, move on to next agent }
5: end if
6: prob  $\leftarrow$  (focal  $\cup$  neighbor  $-$  focal  $\cap$  neighbor) / focal  $\cup$  neighbor
7: if RandomUniform() < prob then
8:   differing  $\leftarrow$  neighbor  $\setminus$  focal
9:   newtrait  $\leftarrow$  GetRandomChoice(differing)
10:  if hasPrerequisiteForTrait(focal, newtrait) = True then
11:    replace  $\leftarrow$  GetTraitUniquetoFocal(focal, neighbor)
12:    focal  $\leftarrow$  focal  $\setminus$  replace
13:    focal  $\leftarrow$  focal  $\cup$  newtrait
14:  else
15:    if RandomUniform() < learningrate then
16:      prereq  $\leftarrow$  GetDeepestMissingPrerequisite(newtrait, focal)
17:      focal  $\leftarrow$  focal  $\cup$  prereq
18:    end if
19:  end if
20: end if
21: if RandomUniform() < innovrate then
22:   focal3  $\leftarrow$  GetRandomAgent()
23:   innovation  $\leftarrow$  GetRandomTraitNotInFocal(focal3)
24:   focal3  $\leftarrow$  focal3  $\cup$  innovation
25: end if

```

GetDeepestMissingPrerequisite() is a procedure which takes the trait set of an individual, and a trait for which the individual is known to be missing necessary prerequisites, and returns the “most basic” missing prerequisite for that trait (i.e., closest to the root). This is done by finding the path which connects the root and desired trait, and walking its vertices from the root downward, checking to see if each vertex is part of the individual’s trait set. The first trait not found in the individual’s repertoire is returned.

7.8.2 Availability of Software and Analysis Code

The simulation software used in this chapter is available under an open-source license at Mark Madsen's GitHub repository <https://github.com/mmadsen/axelrod-ct>. Required libraries and software are listed in the source archive itself, and include Python 2.7 and the open-source MongoDB database engine to store simulation output.

The codebase consists of a set of library modules which implement the shared and unique aspects of each model, unit tests to verify the basic functionality of the code, and scripts which execute each model. The **axelrod-ct** repository contains three models:

- An implementation of the original Axelrod model using the **axelrod-ct** libraries.
- A basic model with an “extensible” trait space but no relations between traits.
- A “semantic” Axelrod model with tree-structured trait space representing prerequisite relationships between traits.

Stepwise extension from the original Axelrod to the semantic models on the same code library allowed a degree of verification, which is difficult in a situation where there is no existing mathematical theory against which to compare the code implementation (Committee on Mathematical Foundations of Verification Validation and Uncertainty Quantification, National Research Council, 2012).

The analysis and final dataset reported here are available, along with the source of this paper and associated presentations, in an associated GitHub repository: <https://github.com/mmadsen/madsenlipo2014>. Statistical analyses of the final dataset were performed in R, rendering our results reproducible given simulated data from the “axelrod-ct” software linked above.

Part III

Discussion and Conclusions

Directions for Future Research

OVERVIEW Lorem ipsum dolor sit amet, consectetur adipiscing elit. Ut purus elit, vestibulum ut, placerat ac, adipiscing vitae, felis. Curabitur dictum gravida mauris. Nam arcu libero, nonummy eget, consectetur id, vulputate a, magna. Donec vehicula augue eu neque. Pellentesque habitant morbi tristique senectus et netus et malesuada fames ac turpis egestas. Mauris ut leo. Cras viverra metus rhoncus sem. Nulla et lectus vestibulum urna fringilla ultrices. Phasellus eu tellus sit amet tortor gravida placerat. Integer sapien est, iaculis in, pretium quis, viverra ac, nunc. Praesent eget sem vel leo ultrices bibendum. Aenean faucibus. Morbi dolor nulla, malesuada eu, pulvinar at, mollis ac, nulla. Curabitur auctor semper nulla. Donec varius orci eget risus. Duis nibh mi, congue eu, accumsan eleifend, sagittis quis, diam. Duis eget orci sit amet orci dignissim rutrum.

CONTENTS Nam dui ligula, fringilla a, euismod sodales, sollicitudin vel, wisi. Morbi auctor lorem non justo. Nam lacus libero, pretium at, lobortis vitae, ultricies et, tellus. Donec aliquet, tortor sed accumsan bibendum, erat ligula aliquet magna, vitae ornare odio metus a mi. Morbi ac orci et nisl hendrerit mollis. Suspendisse ut massa. Cras nec ante. Pellentesque a nulla. Cum sociis natoque penatibus et magnis dis parturient montes, nascetur ridiculus mus. Aliquam tincidunt urna. Nulla ullamcorper vestibulum turpis. Pellentesque cursus luctus mauris.

Conclusion

OVERVIEW Lorem ipsum dolor sit amet, consectetur adipiscing elit. Ut purus elit, vestibulum ut, placerat ac, adipiscing vitae, felis. Curabitur dictum gravida mauris. Nam arcu libero, nonummy eget, consectetur id, vulputate a, magna. Donec vehicula augue eu neque. Pellentesque habitant morbi tristique senectus et netus et malesuada fames ac turpis egestas. Mauris ut leo. Cras viverra metus rhoncus sem. Nulla et lectus vestibulum urna fringilla ultrices. Phasellus eu tellus sit amet tortor gravida placerat. Integer sapien est, iaculis in, pretium quis, viverra ac, nunc. Praesent eget sem vel leo ultrices bibendum. Aenean faucibus. Morbi dolor nulla, malesuada eu, pulvinar at, mollis ac, nulla. Curabitur auctor semper nulla. Donec varius orci eget risus. Duis nibh mi, congue eu, accumsan eleifend, sagittis quis, diam. Duis eget orci sit amet orci dignissim rutrum.

CONTENTS Nam dui ligula, fringilla a, euismod sodales, sollicitudin vel, wisi. Morbi auctor lorem non justo. Nam lacus libero, pretium at, lobortis vitae, ultricies et, tellus. Donec aliquet, tortor sed accumsan bibendum, erat ligula aliquet magna, vitae ornare odio metus a mi. Morbi ac orci et nisl hendrerit mollis. Suspendisse ut massa. Cras nec ante. Pellentesque a nulla. Cum sociis natoque penatibus et magnis dis parturient montes, nascetur ridiculus mus. Aliquam tincidunt urna. Nulla ullamcorper vestibulum turpis. Pellentesque cursus luctus mauris.

Bibliography

- Abramowitz, M. and Stegun, L. 1965. *Handbook of Mathematical Functions*. Dover, New York.
- Alexey Natekin, A. K. 2013. Gradient boosting machines, a tutorial. *Frontiers in Neurorobotics*, 7:21.
- Altman, D. G. 1991. *Practical statistics for medical research*. CRC Press.
- Ammerman, A. J. and Cavalli-Sforza, L. L. 1971. Measuring the rate of spread of early farming in europe. *Man*, pages 674–688.
- Antos, A., Devroye, L., and Györfi, L. 1999. Lower bounds for Bayes error estimation. *Pattern Analysis and Machine Intelligence, IEEE Transactions on*, 21(7):643–645.
- Aoki, K. 2013. Determinants of cultural evolutionary rates. In Akazawa, T., Nishiaki, Y., and Aoki, K., editors, *Dynamics of Learning in Neanderthals and Modern Humans Volume 1*, Replacement of Neanderthals by Modern Humans Series, pages 199–210. Springer Japan.
- Aoki, K., Lehmann, L., and Feldman, M. W. 2011. Rates of cultural change and patterns of cultural accumulation in stochastic models of social transmission. *Theoretical population biology*, 79(4):192–202.
- Aronica, G., Hankin, B., and Beven, K. 1998. Uncertainty and equifinality in calibrating distributed roughness coefficients in a flood propagation model with limited data. *Advances in Water Resources*, 22(4):349–365.
- Arrow, K. 2009. Some developments in economic theory since 1940: An eyewitness account. *Annual Review of Economics*, 1(1):1–16.

- Ascher, M. and Ascher, R. 1963. Chronological ordering by computer. *American Anthropologist*, 65(5):1045–1052.
- Axelrod, R. 1997. The dissemination of culture: A model with local convergence and global polarization. *Journal of conflict resolution*, 41(2):203–226.
- Bailey, G. 1981. Concepts, time-scales and explanations in economic prehistory. *Economic Archaeology: towards an integration of ecological and social approaches*, pages 97–118.
- Bailey, G. 2007. Time perspectives, palimpsests and the archaeology of time. *Journal of Anthropological Archaeology*, 26(2):198–223.
- Bamforth, D. B. and Finlay, N. 2008. Introduction: Archaeological Approaches to Lithic Production Skill and Craft Learning. *Journal of Archaeological Method and Theory*, 15(1):1–27.
- Bar-Yosef, O. 2002. The upper paleolithic revolution. *Annual Review of Anthropology*, pages 363–393.
- Beals, R., Brainerd, G., Smith, W., Hack, J., and Jones, V. 1945. *Archaeological Studies in the Northeast Arizona*. University of California press.
- Bentley, R. 2007a. Fashion versus reason-then and now. *Antiquity*, 81(314):1071–1073.
- Bentley, R. 2007b. Fashion versus reason-then and now. *ANTIQUITY-OXFORD-*, 81(314):1071.
- Bentley, R., Hahn, M., and Shennan, S. 2004. Random drift and culture change. *Proceedings of the Royal Society of London. Series B: Biological Sciences*, 271(1547):1443.
- Bentley, R., Lipo, C., Herzog, H., and Hahn, M. 2007. Regular rates of popular culture change reflect random copying. *Evolution and Human Behavior*, 28(3):151–158.
- Bentley, R., Madsen, M., and Ormerod, P. 2009. Physical space and long-tail markets. *Physica A: Statistical Mechanics and its Applications*, 388(5):691–696.
- Bentley, R. A. and Shennan, S. J. 2003. Cultural transmission and stochastic network growth. *American Antiquity*, 68(3):459–485.
- Bettinger, R. and Eerkens, J. 1999. Point typologies, cultural transmission, and the spread of bow-and-arrow technology in the prehistoric great basin. *American Antiquity*, 64(2):231–242.

- Beven, K. 2006. A manifesto for the equifinality thesis. *Journal of Hydrology*, 320(1-2):18–36.
- Binford, L. 1981. Behavioral archaeology and the “pompeii premise”. *Journal of Anthropological Research*, pages 195–208.
- Bleed, P. 2001. Trees or chains, links or branches: conceptual alternatives for consideration of stone tool production and other sequential activities. *Journal of Archaeological Method and Theory*, 8(1):101–127.
- Bleed, P. 2002. Obviously sequential, but continuous or staged? refits and cognition in three late paleolithic assemblages from japan. *Journal of Anthropological Archaeology*, 21(3):329–343.
- Bleed, P. 2008. Skill Matters. *Journal of Archaeological Method and Theory*, 15(1):154–166.
- Bluhm, E. 1951. Ceramic sequence in central basin and hopewell sites in central illinois. *American Antiquity*, 16:301–312.
- Bonham, S. G., Haywood, A. M., Lunt, D. J., Collins, M., and Salzmann, U. 2009. El Niño-Southern Oscillation, Pliocene climate and equifinality. *Philosophical Transactions of the Royal Society A: Mathematical, Physical and Engineering Sciences*, 367(1886):127–156.
- Bordaz, V. v. H. and Bordaz, J. 1970. A computer pattern recognition method of classification and seriation applied to archaeological material. In Gardin, J.-C., editor, *Archéologie et Calculateurs*, pages 229–244. Centre National de la Recherche Scientifique.
- Bouzouggar, A., Barton, N., Vanhaeren, M., d’Errico, F., Collcutt, S., Higham, T., Hodge, E., Parfitt, S., Rhodes, E., Schwenninger, J.-L., et al. 2007. 82,000-year-old shell beads from north africa and implications for the origins of modern human behavior. *Proceedings of the National Academy of Sciences*, 104(24):9964–9969.
- Boyd, R. and Richerson, P. 1985a. *Culture and the Evolutionary Process*. University of Chicago Press, Chicago.
- Boyd, R. and Richerson, P. 1985b. *Culture and the Evolutionary Process*. University of Chicago Press, Chicago.

- Brainerd, G. W. 1951. The place of chronological ordering in archaeological analysis. *American Antiquity*, 16:301–312.
- Breiman, L. 2001. Random forests. *Machine learning*, 45(1):5–32.
- Castellano, C., Fortunato, S., and Loreto, V. 2009. Statistical physics of social dynamics. *Reviews of modern physics*, 81(2):591.
- Castellano, C., Marsili, M., and Vespignani, A. 2000. Nonequilibrium phase transition in a model for social influence. *Physical Review Letters*, 85(16):3536.
- Castro, L. and Toro, M. A. 2014. Cumulative cultural evolution: The role of teaching. *Journal of Theoretical Biology*, 347(0):74 – 83.
- Cavalli-Sforza, L. and Feldman, M. 1973a. Cultural versus biological inheritance: phenotypic transmission from parents to children.(a theory of the effect of parental phenotypes on children's phenotypes). *American Journal of Human Genetics*, 25(6):618–637.
- Cavalli-Sforza, L. and Feldman, M. 1973b. Models for cultural inheritance. I. Group mean and within group variation. *Theor. Popul. Biol.:(United States)*, 4(1).
- Cavalli-Sforza, L. and Feldman, M. W. 1981a. *Cultural Transmission and Evolution: A Quantitative Approach*. Princeton University Press, Princeton.
- Cavalli-Sforza, L. and Feldman, M. W. 1981b. *Cultural Transmission and Evolution: A Quantitative Approach*. Princeton University Press, Princeton.
- Cicchetti, D. and Rogosch, F. A. 1996. Equifinality and multifinality in developmental psychopathology. *Development and Psychopathology*, 8(04):597–600.
- Collard, M., Buchanan, B., Morin, J., and Costopoulos, A. 2011. What drives the evolution of hunter–gatherer subsistence technology? a reanalysis of the risk hypothesis with data from the pacific northwest. *Philosophical Transactions of the Royal Society B: Biological Sciences*, 366(1567):1129–1138.
- Collard, M., Buchanan, B., and OBrien, M. J. 2013a. Population size as an explanation for patterns in

- the paleolithic archaeological record. *Current Anthropology*, 54(S8):S388–S396.
- Collard, M., Buchanan, B., O'Brien, M. J., and Scholnick, J. 2013b. Risk, mobility or population size? drivers of technological richness among contact-period western north american hunter–gatherers. *Philosophical Transactions of the Royal Society B: Biological Sciences*, 368(1630):20120412.
- Collard, M., Ruttle, A., Buchanan, B., and O'Brien, M. J. 2013c. Population size and cultural evolution in nonindustrial food-producing societies. *PloS one*, 8(9):e72628.
- Committee on Mathematical Foundations of Verification Validation and Uncertainty Quantification, National Research Council 2012. *Assessing the Reliability of Complex Models: Mathematical and Statistical Foundations of Verification, Validation, and Uncertainty Quantification*. The National Academies Press.
- Craytor, W. B. and Johnson, L. 1968. *Refinements in computerized item seriation*. Museum of Natural History, University of Oregon.
- Creanza, N., Fogarty, L., and Feldman, M. 2013. Exploring cultural niche construction from the paleolithic to modern hunter-gatherers. In Akazawa, T., Nishiaki, Y., and Aoki, K., editors, *Dynamics of Learning in Neanderthals and Modern Humans Volume 1*, Replacement of Neanderthals by Modern Humans Series, pages 211–228. Springer Japan.
- Crema, E. R., Edinborough, K., Kerig, T., and Shennan, S. J. 2014. An Approximate Bayesian Computation approach for inferring patterns of cultural evolutionary change. *Journal of Archaeological Science*.
- Crow, J. and Kimura, M. 1970. *An Introduction to Population Genetics Theory*. New York, Harper & Row.
- Csibra, G. and Gergely, G. 2011. Natural pedagogy as evolutionary adaptation. *Philosophical Transactions of the Royal Society B: Biological Sciences*, 366(1567):1149–1157.
- Csilléry, K., Blum, M. G. B., Gaggiotti, O. E., and François, O. 2010. Approximate Bayesian Computation (ABC) in practice. *Trends in Ecology & Evolution*, 25(7):410–418.

- Culling, W. E. H. 1987. Equifinality: Modern Approaches to Dynamical Systems and Their Potential for Geographical Thought. *Transactions of the Institute of British Geographers*, 12(1):57.
- De Sanctis, L. and Galla, T. 2009. Effects of noise and confidence thresholds in nominal and metric axelrod dynamics of social influence. *Physical Review E*, 79(4):046108.
- Deetz, J. and Dethlefsen, E. S. 1965. The Doppler-effect and archaeology: a consideration of the spatial aspects of seriation. *Southwestern Journal of Anthropology*, 21:196–206.
- Deetz, J. and Dethlefsen, E. S. 1971. Some social aspects of new england colonial mortuary art. *Memoirs of the Society for American Archaeology*, 25:30–38.
- Dempsey, P. and Baumhoff, M. 1963. The statistical use of artifact distributions to establish chronological sequence. *American Antiquity*, pages 496–509.
- Derex, M., Beugin, M.-P., Godelle, B., and Raymond, M. 2013. Experimental evidence for the influence of group size on cultural complexity. *Nature*, 503(7476):389–391.
- d’Errico, F. and Henshilwood, C. S. 2007. Additional evidence for bone technology in the southern african middle stone age. *Journal of Human Evolution*, 52(2):142–163.
- d’Errico, F. and Stringer, C. B. 2011. Evolution, revolution or saltation scenario for the emergence of modern cultures? *Philosophical Transactions of the Royal Society B: Biological Sciences*, 366(1567):1060–1069.
- Devijver, P. A. and Kittler, J. 1982. *Pattern recognition: A statistical approach*, volume 761. Prentice-Hall London.
- Diestel, R. 2010. *Graph Theory, 4th Edition*. Springer-Verlag, Heidelberg.
- Dobbin, K. K. 2009. A method for constructing a confidence bound for the actual error rate of a prediction rule in high dimensions. *Biostatistics (Oxford, England)*, 10(2):282–296.
- Dunnell, R. 1981. *Seriation, groups, and measurements*, pages 67–90. Union International de Ciencias Prehistoricas y Protohistoricas, Mexico, DF.
- Dunnell, R. C. 1970. Seriation method and its evaluation. *American Antiquity*, 35(3):305–319.

- Dunnell, R. C. 1971. *Systematics in prehistory*. Free Press, New York.
- Dunnell, R. C. 1978a. Style and function: A fundamental dichotomy. *American Antiquity*, 43(2):192–202.
- Dunnell, R. C. 1978b. Style and function: a fundamental dichotomy. *American Antiquity*, 43:192–202.
- Durrett, R. 2008. *Probability models for DNA Sequence Evolution*. New York, Springer, 2nd edition edition.
- Eerkens, J. and Lipo, C. 2005. Cultural transmission, copying errors, and the generation of variation in material culture and the archaeological record. *Journal of Anthropological Archaeology*, 24(4):316–334.
- Eerkens, J. and Lipo, C. P. 2007. Cultural transmission theory and the archaeological record: Providing context to understanding variation and temporal changes in material culture. *Journal of Archaeological Research*, 15:239–274.
- Evans, C. 1955. *A ceramic study of Virginia Archaeology*. BAE Bulletin 160, Washington.
- Evans, T. S. and Giometto, A. 2011. Turnover rate of popularity charts in neutral models. *arXiv.org*, <http://arxiv.org/abs/1105.4044>.
- Ewens, W. 1964. The maintenance of alleles by mutation. *Genetics*, 50(5):891–898.
- Ewens, W. 1972. The sampling theory of selectively neutral alleles. *Theoretical Population Biology*, 3(1):87–112.
- Ewens, W. 1974. A note on the sampling theory for infinite alleles and infinite sites models. *Theoretical Population Biology*, 6(2):143–148.
- Ewens, W. and Gillespie, J. 1974. Some simulation results for the neutral allele model, with interpretations. *Theoretical Population Biology*, 6(1):35–57.
- Ewens, W. J. 2004. *Mathematical Population Genetics, Volume 1: Theoretical Introduction*. New York, Springer, 2nd edition.

- Ferguson, J. R. 2008. The When, Where, and How of Novices in Craft Production. *Journal of Archaeological Method and Theory*, 15(1):51–67.
- Flache, A. and Macy, M. W. 2006. What sustains cultural diversity and what undermines it? axelrod and beyond. *arXiv preprint physics/0604201*.
- Fogarty, L., Strimling, P., and Laland, K. N. 2011. The evolution of teaching. *Evolution*, 65(10):2760–2770.
- Ford, J. A. 1935. *Ceramic Decoration Sequence at an Old Indian Village Site near Sicily Island, Louisiana*. Dept. Conservation, Louisiana Geological Survey, New Orleans.
- Ford, J. A. 1938. A chronological method applicable to the southeast. *American Antiquity*, 3:260–264.
- Ford, J. A. 1949. *Cultural dating of prehistoric sites in Viru Valley, Peru*, volume 43 of *Anthropological Papers*. American Museum of Natural History, New York.
- Ford, J. A. 1962. *A Quantitative Method for Deriving Cultural Chronology*. Technical Manual, No. 1. Pan American Union.
- Freund, Y. 1995. Boosting a weak learning algorithm by majority. *Information and computation*, 121(2):256–285.
- Freund, Y., Schapire, R., and Abe, N. 1999. A short introduction to boosting. *Journal-Japanese Society For Artificial Intelligence*, 14(771-780):1612.
- Friedman, J. H. 2001. Greedy function approximation: a gradient boosting machine. *Annals of Statistics*, pages 1189–1232.
- Fu, Y.-X. and Li, W.-H. 1993. Statistical tests of neutrality of mutations. *Genetics*, 133(3):693–709.
- Fukunaga, K. 1990. *Introduction to statistical pattern recognition*. Academic press.
- Gardin, J.-C. 1970. A computer pattern recognition method of classification and seriation applied to archaeological material. *Archaeologie et Calculateurs*:229–244.
- Godsil, C. D. and Royle, G. 2001. *Algebraic graph theory*, volume 8. Springer New York.
- Gonzalez-Avella, J., Cosenza, M., and Klemm, K. 2007a. Information feedback and mass media

- effects in cultural dynamics. *Journal of Artificial Societies and Social Simulation*.
- Gonzalez-Avella, J., Eguiluz, V., and San Miguel, M. 2007b. Homophily, Cultural Drift, and the Co-Evolution of Cultural Groups. *Journal of Conflict Resolution*.
- González-Avella, J. C., Cosenza, M. G., and Tucci, K. 2005. Nonequilibrium transition induced by mass media in a model for social influence. *Physical Review E*, 72(6):065102.
- González-Avella, J. C., Eguíluz, V. M., Cosenza, M. G., Klemm, K., Herrera, J., and San Miguel, M. 2006. Local versus global interactions in nonequilibrium transitions: A model of social dynamics. *Physical Review E*, 73(4):046119.
- Grayson, D. and Delpech, F. 1998. Changing diet breadth in the early upper paleolithic of southwestern france. *Journal of Archaeological Science*, 25:1119–1129.
- Hahn, M. W. and Bentley, R. A. 2003. Drift as a mechanism for cultural change: an example from baby names. *Proceedings of the Royal Society Biology Letters B*, 270:S120–S123.
- Hastie, T., Tibshirani, R., Friedman, J., Hastie, T., Friedman, J., and Tibshirani, R. 2009. *The elements of statistical learning*, volume 2. Springer.
- Henrich, J. 2004. Cultural group selection, coevolutionary processes and large-scale cooperation. *Journal of Economic Behavior and Organization*.
- Henrich, J. 2006. Understanding cultural evolutionary models: A reply to read's critique. *American Antiquity*, 71:771–782.
- Henrich, J. and Boyd, R. 1998. The Evolution of Conformist Transmission and the Emergence of Between-Group Differences. *Evolution and Human Behavior*, 19(4):215–241.
- Henrich, J. and Boyd, R. 2004. Demography and cultural evolution: how adaptive cultural processes can produce maladaptive losses: the tasmanian case. *American Antiquity*, 69:197–214.
- Herzog, H. A., Bentley, R. A., and Hahn, M. W. 2004. Random drift and large shifts in popularity of dog breeds. *Proceedings of the Royal Society of London Series B-Biological Sciences*, 271:S353–S356. Suppl. 5.

- Högberg, A. 2008. Playing with Flint: Tracing a Child's Imitation of Adult Work in a Lithic Assemblage. *Journal of Archaeological Method and Theory*, 15(1):112–131.
- Holme, P. and Saramäki, J. 2012. Temporal networks. *Physics reports*, 519(3):97–125.
- Jordan, P. and Shennan, S. 2003. Cultural transmission, language, and basketry traditions amongst the california indians. *Journal of Anthropological Archaeology*, 22(1):42–74. TY - JOUR.
- Kadane, J. B. 1971. *Chronological Ordering of Archeological Deposits by the Minimum Path Length Method*. Center for Naval Analyses, Arlington, VA.
- Kandler, A. and Shennan, S. 2013. A non-equilibrium neutral model for analysing cultural change. *Journal of theoretical biology*, 330:18–25.
- Kandler, A. and Shennan, S. 2015. A generative inference framework for analysing patterns of cultural change in sparse population data with evidence for fashion trends in lbk culture. *Journal of The Royal Society Interface*, 12(113).
- Keeling, M. 2005. The implications of network structure for epidemic dynamics. *Theoretical Population Biology*, 67(1):1–8.
- Keeling, M. and Rohani, P. 2007. *Modeling infectious diseases in humans and animals*. Princeton, Princeton University Press.
- Kempe, M. and Mesoudi, A. 2014. An experimental demonstration of the effect of group size on cultural accumulation. *Evolution and Human Behavior*.
- Kendall, D. G. 1963. A statistical approach to flinders petrie's sequence dating. *Bulletin of the International Statistical Institute*, 40:657–680.
- Kendall, D. G. 1969. Some problems and methods in statistical archaeology. *World Archaeology*, 1:68–76.
- Kendall, D. G. 1970. A mathematical approach to seriation. *Philosophical Transactions of the Royal Society, Series A, Mathematical and Physical Sciences*, 269:125–135.
- Kendall, D. G. a. 1971. Seriation from abundance matrices. *Zeitschrift für Wahrscheinlichkeitstheorie*

- und Verwandte Gebiete*, pages 214–252.
- Kendall, M. and Hill, A. 1953. The analysis of economic time-series-part i: Prices. *Journal of the Royal Statistical Society. Series A (General)*, 116(1):11–34.
- Kidder, A. V. 1917. A design sequence from new mexico. *Proceedings of the National Academy of Sciences*, 3:369–370.
- Kim, J.-H. 2009. Estimating classification error rate: Repeated cross-validation, repeated hold-out and bootstrap. *Computational Statistics & Data Analysis*, 53(11):3735–3745.
- Kimura, M. and Crow, J. 1964. The number of alleles that can be maintained in a finite population. *Genetics*, 49(4):725.
- Kingman, J. 1977. The population structure associated with the ewens sampling formula. *Theoretical Population Biology*, 11(2):274–283.
- Klein, R. G. 2009. *The human career: human biological and cultural origins*. University of Chicago Press.
- Klemm, K., Eguíluz, V., Toral, R., and Miguel, M. 2003a. Global culture: A noise-induced transition in finite systems. *Physical Review E*.
- Klemm, K., Eguíluz, V., Toral, R., and San Miguel, M. 2003b. Nonequilibrium transitions in complex networks: A model of social interaction. *Physical Review E*.
- Klemm, K., Eguíluz, V., Toral, R., and Miguel, M. 2005. Globalization, polarization and cultural drift. *Journal of Economic Dynamics and Control*.
- Kohler, T. A., VanBuskirk, S., and Ruscavage-Barz, S. 2004a. Vessels and villages: evidence for conformist transmission in early village aggregations on the pajarito plateau, new mexico. *Journal of Anthropological Archaeology*, 23(1):100–118.
- Kohler, T. A., VanBuskirk, S., and Ruscavage-Barz, S. 2004b. Vessels and villages: evidence for conformist transmission in early village aggregations on the pajarito plateau, new mexico. *Journal of Anthropological Archaeology*, 23(1):100–118.

- Krieger, A. D. 1944. The typological concept. *American Antiquity*, 3:271–288.
- Kroeber, A. 1916. *Zuni Potsherds*. Anthropological Paper, No. 18, Part 1. American Museum of Natural History, New York.
- Kroeber, A. 1937. Diffusion. *The Encyclopedia of Social Science*, II, pages 137–142.
- Kroeber, A. L. 1923. *Cultural Patterns and Processes*. Harbinger, New York.
- Kuhn, M. 2008. Building predictive models in r using the caret package. *Journal of Statistical Software*, 28(5):1–26.
- Kuhn, M. and Johnson, K. 2013. *Applied predictive modeling*. Springer.
- Kuhn, S. 2013. Cultural transmission, institutional continuity and the persistence of the mousterian. In Akazawa, T., Nishiaki, Y., and Aoki, K., editors, *Dynamics of Learning in Neanderthals and Modern Humans Volume 1*, Replacement of Neanderthals by Modern Humans Series, pages 105–113. Springer Japan.
- Kuzara, R. S., Mead, G. R., and Dixon, K. A. 1966. Seriation of anthropological data: A computer program for matrix-ordering. *American Anthropologist*, 68(6):1442–1455.
- Lanchier, N. 2012. The Axelrod model for the dissemination of culture revisited. *The Annals of Applied Probability*, 22(2):860–880.
- Lanchier, N., Deijfen, M., Häggström, O., and Connor, S. 2010. Opinion dynamics with confidence threshold: an alternative to the Axelrod model. *Alea*.
- Landau, D. and Binder, K. 2005. *A Guide to Monte Carlo Simulations In Statistical Physics*. Cambridge, Cambridge Univ Press.
- Lewontin, R. 1974. *The Genetic Basis of Evolutionary Change*. Columbia University Press.
- Lipo, C. 2005. The resolution of cultural phylogenies using graphs. In Lipo, C., O’Brien, M. J., Collard, M., and Shennan, S. J., editors, *Mapping our ancestors: Phylogenetic approaches in anthropology and prehistory*. Transaction Publishers.
- Lipo, C. and Madsen, M. 2000. Neutrality, ”style,” and drift: Building methods for studying cul-

- tural transmission in the archaeological record. In Hurt, T. D. and Rakita, G. F. M., editors, *Style and Function: Conceptual Issues in Evolutionary Archaeology*, pages 91–118. Bergin and Garvey, Westport, Connecticut.
- Lipo, C., Madsen, M., Dunnell, R., and Hunt, T. 1997a. Population structure, cultural transmission, and frequency seriation. *Journal of Anthropological Archaeology*, 16(4):33.
- Lipo, C. P. 2001a. Community structures among late mississippian populations of the central mississippi river valley. In Hunt, T., Lipo, C. P., and Sterling, S., editors, *Posing Questions for a Scientific Archaeology*, pages 175–216. Bergin and Garvey, Westport.
- Lipo, C. P. 2001b. *Science, Style and the Study of Community Structure: An Example from the Central Mississippi River Valley*. British Archaeological Reports, International Series, no. 918, Oxford.
- Lipo, C. P. 2001c. *Science, Style and the Study of Community Structure: An Example from the Central Mississippi River Valley*. British Archaeological Reports, International Series, no. 918, Oxford.
- Lipo, C. P. and Eerkens, J. W. 2008. Culture history, cultural transmission, and explanation of seriation in the southeastern united states. In *Cultural Transmission and Archaeology: Issues and Case Studies*, pages 120–131. Society for American Archaeology Press, Washington, DC.
- Lipo, C. P. and Madsen, M. E. 1997. The method seriation: Explaining the variability in the frequencies of types. In *62nd Annual Meeting for the Society for American Archaeology*.
- Lipo, C. P. and Madsen, M. E. 2001. Neutrality, "style," and drift: building methods for studying cultural transmission in the archaeological record. In Hurt, T. D. and Rakita, G. F. M., editors, *Style and Function: Conceptual Issues in Evolutionary Archaeology*, pages 91–118. Bergin and Garvey, Westport, Connecticut.
- Lipo, C. P., Madsen, M. E., and Dunnell, R. C. 2015. A theoretically-sufficient and computationally-practical technique for deterministic frequency seriation. *PLoS ONE*, 10(4):e0124942.
- Lipo, C. P., Madsen, M. E., Dunnell, R. C., and Hunt, T. 1997b. Population structure, cultural transmission, and frequency seriation. *Journal of Anthropological Archaeology*, 16(4):301 – 333.

- Loizou, G. and Maybank, S. J. 1987. The Nearest Neighbor and the Bayes Error Rates. *Pattern Analysis and Machine Intelligence, IEEE Transactions on*, PAMI-9(2):254–262.
- Lyman, R. 2003. The influence of time averaging and space averaging on the application of foraging theory in zooarchaeology. *Journal of Archaeological Science*, 30(5):595–610.
- Lyman, R., O'Brien, M., and Dunnell, R. 1997. *The rise and fall of culture history*. Springer.
- Lyman, R. L. 2008. Cultural transmission in north american anthropology and archaeology, ca. 1895–1965. *Cultural transmission and archaeology: Issues and case studies*, ed. MJ O'Brien. Society for American Archaeology.
- Lyman, R. L. and O'Brien, M. 2006. *Measuring Time with Artifacts*. University of Nebraska, Lincoln.
- MacArthur, B. D., Sánchez-García, R. J., and Anderson, J. W. 2008. Symmetry in complex networks. *Discrete Applied Mathematics*, 156(18):3525–3531.
- Madsen, M. and Lipo, C. P. 2015. An approach to fitting transmission models to seriations for regional-scale analysis. In *Paper presented at the 80th Annual Meeting of the Society for American Archaeology, San Francisco, CA*.
- Madsen, M. E. 2012a. Unbiased cultural transmission in time-averaged archaeological assemblages. *ArXiv e-prints*, 1204.2043.
- Madsen, M. E. 2012b. Unbiased cultural transmission in time-averaged archaeological assemblages. *ArXiv e-prints*, 1204.2043.
- Madsen, M. E. and Lipo, C. P. 2014. Combinatorial structure of the deterministic seriation method with multiple subset solutions. <http://arxiv.org/abs/1412.6060>.
- Madsen, M. E., Lipo, C. P., and Bentley, R. A. 2008. Explaining seriation patterns through network-structured cultural transmission models. In *Poster presented at the 73rd Annual Meeting of the Society for American Archaeology*.
- Marean, C. W., Spencer, L. M., Blumenschine, R. J., and Capaldo, S. D. 1992. Captive hyaena bone choice and destruction, the Schlepp effect and olduvai archaeofaunas. *Journal of Archaeological*

- Science*, 19(1):101–121.
- Marin, J.-M., Pudlo, P., Robert, C. P., and Ryder, R. J. 2012. Approximate bayesian computational methods. *Statistics and Computing*, 22(6):1167–1180.
- Marquardt, W. H. 1978. Advances in archaeological seriation. *Advances in Archaeological Seriation*, 1:257–314.
- Matthews, J. 1963. Application of matrix analysis to archaeological problems. *Nature*, 198:930–934.
- Mayer-Oakes, W. J. 1955. *Prehistory of the Upper Ohio Valley: A Introductory Study*. Carnegie Museum, Annals Vo. 34, Pittsburgh.
- McBrearty, S. 2007. Down with the revolution. *Rethinking the human revolution*. Cambridge: MacDonald Institute for Archaeological Research Monographs, pages 133–152.
- McBrearty, S. and Brooks, A. S. 2000. The revolution that wasn't: a new interpretation of the origin of modern human behavior. *Journal of human evolution*, 39(5):453–563.
- McKay, B. D. and Piperno, A. 2014. Practical graph isomorphism, {II}. *Journal of Symbolic Computation*, 60(0):94 – 112.
- McLachlan, G. J. 1975. Confidence Intervals for the Conditional Probability of Misallocation in Discriminant Analysis. *Biometrics*, 31(1):161.
- Meggers, B. J. and Evans, C. 1957. *Archaeological investigation in the mouth of the Amazon*. Bureau of American Ethnology, Bulletin 167, Washington.
- Mesoudi, A. 2014. Experimental studies of modern human social and individual learning in an archaeological context: People behave adaptively, but within limits. In *Dynamics of Learning in Neanderthals and Modern Humans Volume 2*, pages 65–76. Springer.
- Mesoudi, A. and Lycett, S. J. 2009. Random copying, frequency-dependent copying and culture change. *Evolution and Human Behavior*, 30:41–48.
- Mesoudi, A., Whiten, A., Mesoudi, A., and Whiten, A. 2008. The multiple roles of cultural transmission experiments in understanding human cultural evolution. *Philosophical Transactions of the*

- Royal Society of London. Series B: Biological Sciences*, 363:3489–3501.
- Moore, M. W. 2010. “grammars of action” and stone flaking design space. In Nowell, A. and Davidson, I., editors, *Stone tools and the evolution of human cognition*, pages 13–43. University of Colorado Press, Boulder.
- Moran, P. 1958. Random processes in genetics. In *Mathematical Proceedings of the Cambridge Philosophical Society*, volume 54, pages 60–71. Cambridge Univ Press.
- Moran, P. 1962. *The statistical processes of evolutionary theory*. Clarendon Press; Oxford University Press.
- Muthukrishna, M., Shulman, B. W., Vasilescu, V., and Henrich, J. 2014. Sociality influences cultural complexity. *Proceedings of the Royal Society B: Biological Sciences*, 281(1774):20132511.
- Nakahashi, W. 2013. Cultural evolution and learning strategies in hominids. In Akazawa, T., Nishiaki, Y., and Aoki, K., editors, *Dynamics of Learning in Neanderthals and Modern Humans Volume 1*, Replacement of Neanderthals by Modern Humans Series, pages 245–254. Springer Japan.
- Neff, H. 1992. Ceramics and evolution. *Archaeological Method and Theory*, 4:141–193.
- Neiman, F. 1995. Stylistic variation in evolutionary perspective: Inferences from decorative diversity and *American Antiquity*.
- Neiman, F. D. 1990. *An Evolutionary Approach to Archaeological Inference: Aspects of Architectural Variation in the 17th Century Chesapeake*. PhD thesis, Yale University.
- Nelson, N. C. 1916. Chronology of the tanos ruins, new mexico. *American Anthropologist*, 18:159–180.
- Nickel, M., Tresp, V., and Kriegel, H.-P. 2011. A three-way model for collective learning on multi-relational data. In Getoor, L. and Scheffer, T., editors, *Proceedings of the 28th International Conference on Machine Learning (ICML-11)*, ICML ’11, pages 809–816, New York, NY, USA. ACM.
- Nishiaki, Y., Aoki, K., and Akazawa, T. 2013. Introduction. In Akazawa, T., Nishiaki, Y., and Aoki, K., editors, *Dynamics of Learning in Neanderthals and Modern Humans Volume 1*, Replacement of

- Neanderthals by Modern Humans Series, pages 1–3. Springer Japan.
- O'Brien, M. and Lyman, R. 1998. *James A. Ford and the growth of Americanist archaeology*. Univ of Missouri Pr.
- O'Brien, M., Lyman, R., Mesoudi, A., and VanPool, T. 2010. Cultural traits as units of analysis. *Philosophical Transactions of the Royal Society B: Biological Sciences*, 365(1559):3797–3806.
- O'Brien, M. J., Boulanger, M. T., Buchanan, B., Bentley, R. A., Lyman, R. L., Lipo, C. P., Madsen, M. E., and Eren, M. I. 2015. Design space and cultural transmission: Case studies from paleoindian eastern north america. *Journal of Archaeological Method and Theory*, pages 1–49.
- O'Brien, M. J. and Lyman, R. L. 1999. *Seriation, Stratigraphy, and Index Fossils. The Backbone of Archaeological Dating*. Kluwer Academic/Plenum, New York.
- O'Brien, M. J. and Lyman, R. L. 2000. *Applying evolutionary archaeology: A systematic approach*. Springer.
- O'Brien, M. J. and Shennan, S. 2010. *Innovation in cultural systems: Contributions from evolutionary anthropology*. MIT Press.
- Olszewski, T. 2011. Remembrance of things past: modelling the relationship between species' abundances in living communities and death assemblages. *Biology Letters*, 8(1):131–134.
- Osgood, C. 1951. Culture: Its empirical and non-empirical character. *Southwestern Journal of Anthropology*, 7:202–214.
- Otter, R. 1948. The number of trees. *The Annals of Mathematics*, 49(3):583–599.
- Peng, B. and Kimmel, M. 2005. simupop: a forward-time population genetics simulation environment. *Bioinformatics*, 21(18):3686–3687.
- Peng, B., Kimmel, M., and Amos, C. 2012. *Forward-Time Population Genetics Simulations: Methods, Implementation, and Applications*. Hoboken, Wiley-Blackwell.
- Perreault, C. and Brantingham, P. 2011. Mobility-driven cultural transmission along the forager-collector continuum. *Journal of Anthropological Archaeology*, 30:62–68.

- Petrie, F. W. M. 1899. Sequences in prehistoric remains. *Journal of the Anthropological Institute*, 29:295–301.
- Phillips, P., Ford, J. A., and Griffin, J. B. 1951. *Archaeological Survey in the Lower Mississippi Alluvial Valley, 1940-1947*, volume 25. Peabody Museum, Harvard University, Cambridge.
- Plutinski, A. 2004. Interview with Warren Ewens.
- Porčić, M. 2014. Exploring the effects of assemblage accumulation on diversity and innovation rate estimates in neutral, conformist, and anti-conformist models of cultural transmission. *Journal of Archaeological Method and Theory*, pages 1–22.
- Premo, L. 2012. Local extinctions, connectedness, and cultural evolution in structured populations. *Advances in Complex Systems*, 15(01n02).
- Premo, L. and Scholnick, J. 2011. The spatial scale of social learning affects cultural diversity. *American Antiquity*, 76(1):163–176.
- Premo, L. S. 2014a. Cultural Transmission and Diversity in Time-Averaged Assemblages. *Current Anthropology*, 55(1):105–114.
- Premo, L. S. 2014b. Cultural Transmission and Diversity in Time-Averaged Assemblages. *Current Anthropology*, 55(1):105–114.
- Provine, W. 1989. *Sewall Wright and Evolutionary Biology*. Chicago, University of Chicago Press.
- Provine, W. 2001. *The Origins of Theoretical Population Genetics*. Chicago, University of Chicago Press.
- Ridgeway, G. 1999. The state of boosting. *Computing Science and Statistics*, pages 172–181.
- Robinson, W. S. 1951. A method for chronologically ordering archaeological deposits. *American Antiquity*, 16(4):293–301.
- Rogers, A. R. 2000. On Equifinality in Faunal Analysis. *American Antiquity*, 65(4):709–723.
- Rogers, E. 2003. *The Diffusion of Innovations*, 5th edition. Free Press, New York.
- Rorabaugh, A. N. 2014. Impacts of drift and population bottlenecks on the cultural transmission of

- a neutral continuous trait: an agent based model. *Journal of Archaeological Science*, 49:255–264.
- Rothman, K., Greenland, S., and Lash, T. 2008. *Modern epidemiology*. Lippincott Williams & Wilkins.
- Rotman, J. J. 1995. An introduction to the theory of groups, volume 148 of graduate texts in mathematics.
- Rouse, I. 1967. Seriation in archaeology. In Riley, C. and Taylor, W., editors, *American Historical Anthropology*, pages 153–195. Southern Illinois University Press.
- Rouse, I. B. 1939. *Prehistory in Haiti: A Study in Method*. Yale University Publications in Anthropology, No. 21, New Haven.
- Rowe, J. H. 1959. Archaeological dating and cultural process. *Southwestern Journal of Anthropology*, pages 317–324.
- Savenije, H. H. G. 2001. Equifinality, a blessing in disguise? *Hydrological Processes*, 15(14):2835–2838.
- Schank, R. C. and Abelson, R. P. 1977. Scripts, plans, goals, and understanding: An inquiry into human knowledge structures (artificial intelligence series).
- Schapire, R. E. and Freund, Y. 2012. *Boosting: Foundations and algorithms*. MIT Press.
- Schiffer, M. 1987. *Formation Processes of the Archaeological Record*. University of New Mexico Press, Albuquerque.
- Schiffer, M. B. and Skibo, J. M. 1987. Theory and experiment in the study of technological change. *Current Anthropology*, 28(5):595–622.
- Schillinger, K., Mesoudi, A., and Lycett, S. J. 2014. Copying error and the cultural evolution of additive vs. reductive material traditions: an experimental assessment. *American Antiquity*, 79(1):128–143.
- Scholnick, J. 2010. *Apprenticeship, Cultural Transmission and the Evolution of Cultural Traditions in Historic New England Gravestones*. PhD thesis, University of Arizona.
- Scholnick, J. B. 2012. The spatial and temporal diffusion of stylistic innovations in material culture. *Advances in Complex Systems*, 15(01n02).

- Shennan, S. 2000. Population, culture history, and the dynamics of culture change. *Current Anthropology*, 41(5):811–835.
- Shennan, S. 2001. Demography and cultural innovation: a model and its implications for the emergence of modern human culture. *Cambridge Archaeological Journal*, 11(01):5–16.
- Shennan, S. 2011. Descent with modification and the archaeological record. *Philosophical Transactions of the Royal Society B: Biological Sciences*, 366(1567):1070–1079.
- Shennan, S. and Wilkinson, J. 2001. Ceramic style change and neutral evolution: A case study from neolithic europe. *American Antiquity*, 66(4):577–593.
- Shepardson, B. L. 2006. *Explaining Spatial and Temporal Patterns of Energy Investment In The Pre-historic Statuary of Rapa Nui (Easter Island)*. PhD thesis, University of Hawai'i.
- Slatkin, M. 1994. An exact test for neutrality based on the ewens sampling distribution. *Genetical Research*, 64(01):71–74.
- Slatkin, M. 1996. A correction to the exact test based on the ewens sampling distribution. *Genetical research*, 68(03):259–260.
- Smilkov, D. and Kocarev, L. 2012. Influence of the network topology on epidemic spreading. *Physical Review E*, 85(1):016114.
- Smith, C. S. 1950. *The archaeology of coastal New York*. American Museum of Natural History, Anthropological Papers 43(2), New York.
- Smith, K. and Neiman, F. D. 2005. Frequency seriation, correspondence analysis, and woodland period ceramic assemblage variation in the deep south. *Southeastern Archaeology*, 26:49–72.
- Spier, L. 1917. An outline for a chronology of zuni ruins. *Anthropological Papers of the American Museum of Natural History*, 18:209–331.
- Steele, J., Glatz, C., and Kandler, A. 2010. Ceramic diversity, random copying, and tests for selectivity in ceramic production. *Journal of Archaeological Science*, 37(6):1348–1358.
- Stein, J. 1987. Deposits for archaeologists. *Advances in archaeological method and theory*, 11:337–395.

- Sterelny, K. 2012. *The evolved apprentice*. MIT Press.
- Stout, D. 2002. Skill and cognition in stone tool production: An ethnographic case study from irian jaya 1. *Current Anthropology*, 43(5):693–722.
- Stout, D. 2011. Stone toolmaking and the evolution of human culture and cognition. *Philosophical Transactions of the Royal Society B: Biological Sciences*, 366(1567):1050–1059.
- Straus, L. G. 2005. A mosaic of change: the middle–upper paleolithic transition as viewed from new mexico and iberia. *Quaternary international*, 137(1):47–67.
- Tajima, F. 1989. Statistical method for testing the neutral mutation hypothesis by dna polymorphism. *Genetics*, 123(3):585–595.
- Teltser, P. A. 1995. Culture history, evolutionary theory, and frequency seriation. In Teltser, P. A., editor, *Evolutionary Archaeology: Methodological Issues*, pages 51–68. University of Arizona Press, Tucson.
- Terashima, H. 2013. The evolutionary development of learning and teaching strategies in human societies. In Akazawa, T., Nishiaki, Y., and Aoki, K., editors, *Dynamics of Learning in Neanderthals and Modern Humans Volume 1*, Replacement of Neanderthals by Modern Humans Series, pages 141–150. Springer Japan.
- Tomašových, A. and Kidwell, S. 2010a. The effects of temporal resolution on species turnover and on testing metacommunity models. *The American Naturalist*, 175(5):587–606.
- Tomašových, A. and Kidwell, S. 2010b. Predicting the effects of increasing temporal scale on species composition, diversity, and rank-abundance distributions. *Paleobiology*, 36(4):672–695.
- Tostevin, G. B. 2012. *Seeing lithics: a middle-range theory for testing for cultural transmission in the pleistocene*. Oxford: Oxbow Books.
- Tostevin, G. B. 2019. Content matters. *Beyond the Meme: Development and Structure in Cultural Evolution*, 22.
- Tumer, K. and Ghosh, J. 2003. Bayes error rate estimation using classifier ensembles. *International*

- Journal of Smart Engineering System Design*, 5(2):95–109.
- Villa, P. and Roebroeks, W. 2014. Neandertal Demise: An Archaeological Analysis of the Modern Human Superiority Complex. *PLoS ONE*, 9(4):e96424.
- von Bertalanffy, L. 1949. Problems of organic growth. *Nature*, 163(4135):156–158.
- Wakano, J. Y. and Aoki, K. 2007. Do social learning and conformist bias coevolve? Henrich and Boyd revisited. *Theoretical Population Biology*, 72(4):504–512.
- Wakeley, J. 2008. *Coalescent Theory*. Cambridge, Harvard University Press.
- Watkins, J. 2010. Convergence time to the ewens sampling formula. *Journal of Mathematical Biology*, 60:189–206.
- Watterson, G. 1975. On the number of segregating sites in genetical models without recombination. *Theoretical population biology*, 7(2):256–276.
- Watterson, G. 1976. The stationary distribution of the infinitely-many neutral alleles diffusion model. *Journal of Applied Probability*, 13:639–651.
- Whitlam, R. G. 1981. Problems in ceramic classification and chronology: An example from the mobile bay area, alabama. *Midcontinental Journal of Archaeology*, 6(2):179–206.
- Wilcox, A. 1973. Indices of qualitative variation and political measurement. *The Western Political Quarterly*, 26(2):325–343.
- Wilder, B. and Kandler, A. 2015. Inference of cultural transmission modes based on incomplete information. Forthcoming.
- Wimsatt, W. C. 2007. *Re-engineering philosophy for limited beings: Piecewise approximations to reality*. Harvard University Press.
- Wimsatt, W. C. and Griesemer, J. R. 2007. Reproducing entrenchments to scaffold culture: The central role of development in cultural evolution. *Integrating evolution and development: From theory to practice*, pages 227–323.
- Wissler, C. 1916. The application of statistical methods to the data on the trenton argillite culture.

American Anthropologist, 18(2):190–197.

Wolpert, D. H. 2002. The supervised learning no-free-lunch theorems. In *Soft Computing and Industry*, pages 25–42. Springer.

Wolpert, D. H. and Macready, W. G. 1997. No free lunch theorems for optimization. *Evolutionary Computation, IEEE Transactions on*, 1(1):67–82.

Wright, S. 1931. Evolution in mendelian populations. *Genetics*, 16(2):97–159.